1969

Fourier Transforms for System Identification.

Carlos Ray Dollar
Louisiana State University and Agricultural & Mechanical College

FOURIER TRANSFORMS FOR SYSTEM IDENTIFICATION

A Dissertation

Submitted to the Graduate Faculty of the
Louisiana State University and
Agricultural and Mechanical College
in partial fulfillment of the
requirements for the degree of
Doctor of Philosophy

in

The Department of Chemical Engineering

by
Carlos Ray Dollar
B.S., University of Mississippi, 1965
M.S., Louisiana State University, 1967
August, 1969

ACKNOWLEDGEMENT

This research was conducted under the guidance of Dr. Paul W. Murrill, Professor and Head of the Department of Chemical Engineering and Dr. Cecil L. Smith, Assistant Professor of Chemical Engineering at Louisiana State University. To both, the author extends his sincere appreciation for their assistance, interest, and encouragement throughout this project.

The author also wishes to express his appreciation for the support of this work provided by Project THEMIS Contract No. F44620-68-C-0021 administered for the U.S. Department of Defense by the U.S. Air Force Office of Scientific Research. Thanks are also due to the National Science Foundation for financial support of the author and to the Computer Research Center for the use of their facilities.

Sincere thanks are extended to Mrs. Pat Mills for her assistance with the preparation of the manuscript. The author also wishes to thank the Dr. Charles E. Coates Memorial Fund, donated by George H. Coates, for financial assistance in the preparation of this manuscript.

TABLE OF CONTENTS

LIST OF TABLES

LIST OF FIGURES

ABSTRACT

The use of pulse testing for system identification has achieved wide acceptance in recent years. This dissertation presents a quanitative treatment, wherever possible, of the factors which influence the maximum recoverable frequency obtainable from the Fourier analysis of pulse test data. As a tool for performing the study, an error criterion for mathematically defining the maximum recoverable frequency is selected and justified from among twelve proposed criteria.

The criterion is applied to noiseless systems and a correlation is developed between sampling frequency and the maximum recoverable frequency for first and second order systems. This establishes the sampling frequency constraint on the maximum recoverable frequency.

Noise proved to have a considerable influence on the maximum recoverable frequency. Graphs are presented which correlate the maximum recoverable frequency and the root-mean-square (RMS) value of noise for various sampling frequencies and input pulses. For a given sampling frequency a correlating equation is developed for the noise RMS value and the frequency content of the output pulse and graphs are presented showing this relationship for several different sampling frequencies. This relationship defines the noise constraint on the maximum recoverable frequency. The noise

constraint is applied in conjunction with the sampling frequency constraint to four cases and the constraints are shown to be adequate for predicting the maximum recoverable frequency.

The use of filtering to improve information recovery is investigated and pre-sample filtering (filtering of the continuous signal) is shown to significantly improve the recovery, even with no noise present. Upper and lower constraints for the filter time constant of the first order lag filter used in the study are defined.

The effect of data significant figures and computer significant figures on the maximum recoverable frequency is explored and graphs are presented showing the effects. The number of data significant figures is related to the RMS value of normal process noise by an equation.

A calculation method utilizing the real-valued Fast Fourier Transform is presented and shown to be superior to conventional techniques in accuracy as well as speed.

CHAPTER 1

INTRODUCTION

The explicit evaluation of a system transfer function and its parameters is referred to as system identification, a problem with which control engineers are constantly concerned. The frequency domain has proven a fruitful region in which to solve this problem. Pulse testing has received considerable acclaim because potentially a complete set of frequency response data can be obtained from a single test. Since it is via the Fourier transform that the pulse test data is converted to frequency response data, the Fourier transform assumes an important role in this approach to system identification. Given data for the input pulse, $x(t)$, and the output pulse, $y(t)$, of a system, the frequency response data is obtained from the ratio of Fourier transforms

$$G(j\omega) = \frac{\int_0^\infty y(t)\, e^{-j\omega t}\, dt}{\int_0^\infty x(t)\, e^{-j\omega t}\, dt}$$

Although the method appears simple to apply several problems arise in the practical computation of the Fourier integrals. A few general guidelines for collecting and processing pulse test data have been offered, but the effects of the various sources of

error are poorly understood. What is needed is quantitative information on the effects of the various errors so that the limiting errors for a given situation can be pinpointed and corrective or compensating action taken. Selection of the input pulse is very important in obtaining useful information from the Fourier transform. The problem is complicated by the fact that a good pulse for one situation may be a poor one for another situation. Very little information has been provided to distinguish between the various situations. Clements (3) presents a very informative graph which compares the normalized frequency contents of several pulse shapes and should be very helpful in selecting a pulse shape. His contention is that frequency content is extremely important in determining the maximum recoverable frequency and he suggests 0.2 as the minimum value of normalized frequency content of the input pulse for which frequency response data should be accepted. However, this value is given without regard to noise level or sampling frequency, which may have a significant effect on the maximum recoverable frequency. The interrelation between these various factors in determining the maximum recoverable frequency will be investigated in this study.

A serious problem encountered in Fourier transform computation in the "blow-up" phenomenon caused by folding of the high frequency components onto the low frequency components as a result of sampling. (The sampling referred to is the collecting of the discrete data points of the input pulse, $x(t)$, and the output pulse, $y(t)$, for use in the Fourier transform calculation.) Shannon's Sampling Theorem, which is strictly applicable only to band-limited

functions, can be used to place an upper bound on the frequency region in which results are accurate. Functions describing physical systems are rarely band-limited so that the blow-up frequency is normally much less than the upper bound defined by the Sampling Theorem. Lees (4) indicates that ten times as many data points are needed as the minimum required by the Sampling Theorem. Work in Chapter 3 was directed toward obtaining a better estimate of the "blow-up" frequency and a correlation between the maximum recoverable frequency and the sampling frequency was developed.

Noise definitely is an important factor in determining the maximum recoverable frequency but no correlation of its effect on the maximum recoverable frequency has yet been offered in the literature. Closely allied with the noise entering through the process is the error introduced by the limited accuracy of the recording equipment to be contributing more noise than disturbances entering the process. The number of significant figures carried in the computer performing the Fourier transform calculation directly affects the accuracy of the calculation and is of special concern in special purpose computers where accuracy is frequently sacrificed for economy. Correlations of the effects of process noise, data significant figures and computer significant figures are developed in Chapters 4 and 5.

Although there is some disagreement, reportedly the integration technique used to evaluate the Fourier integral influences the accuracy of the computation significantly. In Chapters 3 and 6

an investigation was made into the relative merits of some simple and sophisticated techniques which have been proposed. In Chapter 6 the real-valued Fast Fourier Transform is applied to the system identification problem and comparisons are made between it and other techniques.

What would seem to be a promising area for improving the Fourier transform results is filtering. Intuitively it would appear that the fold-over effect would be very susceptible to this treatment and this was investigated in Chapter 5. Pre-sample filtering was demonstrated to be very beneficial and constraints were set up for choosing first order lag filter time constants.

The goal of this study was to correlate with the maximum recoverable frequency the factors which influence the accuracy of Fourier analysis. By presenting a quantitative treatment of these factors wherever possible, new insight into the pulse testing technique should be provided and a more efficient application made possible. The digital computer presents outstanding advantages in a study of this kind because of the feasibility and simplicity of treating these factors individually when desired.

LITERATURE CITED

1. Bergland, G. D., "A Fast Fourier Transform Algorithm for Real-Valued Series," Communications of the A. C. M., Vol. 11, no. 10, pp. 703-710, October, 1968.

2. Blackman, R. B. Data Smoothing and Prediction. Dallas: Addison-Wesley Publishing Company, Inc., 1965.

3. Clements, William C. Jr., "Pulse Testing for Dynamic Analysis," Ph.D. Dissertation, Vanderbilt University, 1963.

4. Lees, Sidney and Ray C. Dougherty, "Refinement of the Pulse Testing Procedure Computer Limitations," October, 1964.

5. Ryker, C. E., P. S. Buckley, and others. "Dynamic Response Testing of Process Control Instrumentation," Instrument Society of America, October, 1968.

6. Shannon. "The Philosophy of P. C. M.," Proceedings of I. R. E., November, 1948.

CHAPTER 2

CRITERIA FOR EVALUATING FOURIER TRANSFORM COMPUTATIONAL RESULTS

The Fourier transform is a powerful computational tool for such seemingly diverse studies as digital analysis, filter simulation, and determination of frequency response data from pulse testing data. The latter case is extremely useful in determining transfer functions of components, plants, etc., and this latter application has been the thrust for performing this study.

The classical approach to pulse testing requires collecting input and output time domain data for a system. This data is transformed to the frequency domain via the Fourier transform to construct a Bode plot or its equivalent from which the system model or transfer function can be extracted. The frequency response data is determined by:

$$G(j\omega) = \frac{F[y(t)]}{F[x(t)]} = \frac{\int_0^\infty y(t)e^{-j\omega t}dt}{\int_0^\infty x(t)e^{-j\omega t}dt} \qquad 2.1$$

where $x(t)$ is the input, $y(t)$ is the output, and $F[\ ]$ denotes Fourier transform. For the Fourier integrals in the above equation to converge, $x(t)$ and $y(t)$ must both be closed pulses, i.e. pulses which return to their starting value.

2.1 Shannon's Sampling Theorem

A problem arises because discrete, sampled, points are used to represent the continuous functions $y(t)$ and $x(t)$. In 1948 C. E. Shannon in what has become known as Shannon's Sampling Theorem, proved that it is possible to represent all the information in a continuous signal with sampled data. He proved mathematically that if a continuous function is sampled at a frequency of at least twice the highest frequency in the function, then the continuous function can be recovered from the sampled points. The useful information of most physical systems is at relatively low frequencies; however, these systems do contain some extremely high frequency components so that to completely recover the continuous function would require an infinite rate of sampling. This is not practical. Sampling at a slower rate produces distortion by what is known as the "fold-over" effect as the high frequency components aliase themselves onto lower frequencies. This distortion causes the Bode plot to blow up at the higher frequencies. However, as the sampling rate is increased, the highest recoverable frequency increases.

2.2 Blow-up Definition

There is a need for developing a correlation to determine the maximum recoverable frequency for Fourier analysis. Before this can be done a criterion must be developed to define the blow-up frequency on the Bode plot. Visual determination of the blow-up point by comparing the true analytical plot with the plot calculated by Fourier analysis is not desirable. Results obtained by this method

would be open to question since they would depend on human judgement with no definite blow-up criterion. The blow-up point is somewhat arbitrary since the error may increase in a gradual manner so that the plot is unreliable before wild oscillation begins. What is needed is a mathematically definable criterion with uniform application to all cases.

2.3 Error Criteria

An absolute value of the error criterion would seem to be a workable criterion, but the particular error to be used must be considered. A Bode plot consists of a plot of the log of the magnitude ratio (magnitude of $G(j\omega)$) versus the log of the frequency and a plot of the phase angle (of $G(j\omega)$) versus the log of the frequency. Two errors to be considered are obvious: (1) the error in the log of the magnitude ratio and (2) the phase angle error. A third error for consideration is the complex point error. The value of the transfer function calculated by Fourier analysis is a complex point. The distance between this complex point and the true complex point calculated with an analytical expression is the complex point error. In addition a percentage error might be useful. The definition is straightforward for the complex point error - simply divide the complex point error by the magnitude of the true complex point. A percentage error is not desirable for the phase angle. If a system has dead time the value of the phase angle increases rapidly with frequency so that a fairly large phase angle error is a small percentage error. The actual phase angle error is much more

important than the percentage error. For the log magnitude a percentage error is not desirable either. When the magnitude ratio is 1.0 or near 1.0 the error would be divided by zero or an extremely small number producing misleading results. However, the log magnitude error is already a normalized quantity since

$$\log MR_c - \log MR_A = \log \frac{MR_c}{MR_A} \qquad 2.2$$

where MR_c = Magnitude ratio calculated by Fourier analysis

MR_A = True magnitude ratio calculated analytically

Another approach to the problem is to consider the error area, i.e. the area between the Fourier analysis curve and the true analytical curve, in determining a blow-up criterion. This area can be obtained by integrating the absolute value of the error along the log of the frequency axis. A natural extension of this is the integral of the squared error. This makes a total of twelve different criteria to consider.

1. $|e_{LMR}|$
2. $|e_\theta|$
3. $|e_{cp}|$
4. $\left|\frac{e_{cp}}{M_{cp}}\right|$
5. $\int |e_{LMR}| dL\omega$
6. $\int |e_\theta| dL\omega$

7. $\int |e_{cp}| dL\omega$

8. $\int \left| \frac{e_{cp}}{M_{cp}} \right| dL\omega$

9. $\int e_{LMR}^2 dL\omega$

10. $\int e_{\theta}^2 dL\omega$

11. $\int e_{cp}{}^2 dL\omega$

12. $\int \left(\frac{e_{cp}}{M_{cp}}\right)^2 dL\omega$

where e = error

LMR = log of the magnitude ratio

$L\omega = \log_{10}$ of the frequency

θ = phase angle

cp = complex point

2.4 Systems and Input for Criteria Evaluation

In order to select a criterion some Bode plots must be calculated and the criteria applied and evaluated. The systems selected for the tests were

1. first order lag
2. first order lag plus dead time
3. second order lag
4. second order lag plus dead time

These should encompass the majority of process type applications.

The input used for all these systems was a pulse. The pulse was a ramp, dropping to zero from its highest point, put through

a first order lag. This should be physically realizable. The frequency content of this pulse was desirable since no zeroes were encountered. The frequency content of a pulse is very important as discussed by Clements (2), but good results were obtained below the 0.2 minimum normalized frequency content recommended by Clements. This may have been due to the use of a noiseless system. However, when the frequency content of the input was zero, the results were meaningless. This occurred when a triangular pulse input was tried since it had several zeroes in the frequency range investigated. These points would have wreaked havoc with an error criterion, hence the desirableness of the pulse used.

2.5 Transform Technique

As noted in the first paragraph, the standard procedure for transforming pulse response time domain data to the frequency domain is Fourier analysis. The particular method of evaluating the Fourier integral in this investigation was as follows. A straight line approximation was used for both the output curve $y(t)$ and the input curve $x(t)$ between sampling points.

$$y(t) = a + bt \qquad\qquad x(t) = c + dt$$

The substitution

$$e^{-j\omega t} = \cos \omega t - j \sin \omega t \qquad 2.3$$

was made in the Fourier integral, along with the approximations for $y(t)$ and $x(t)$, and the integration was performed analytically. The total integral was then approximated by a summation of integrals, each over a sampling interval. This gives the evaluation procedure

for Equation 2.1 as

$$G(j\omega) = \frac{\frac{1}{\omega^2}\sum_{i=1}^{N}(SY)(DCO) - j\sum_{i=1}^{N}(SY)(DSI)}{\frac{1}{\omega^2}\sum_{i=1}^{N}(SX)(DCO) - j\sum_{i=1}^{N}(SX)(DSI)} \qquad 2.4$$

where N = number of output or input data points

Δt = time increment between data points

$$SY = \frac{y[(i+1)\Delta t] - y[i\Delta t]}{\Delta t}$$

$$SX = \frac{x[(i+1)\Delta t] - x(i\Delta t)}{\Delta t}$$

$$DCO = \cos[\omega(i+1)\Delta t) - \cos[\omega i\Delta t]$$

$$DSI = \sin[\omega(i+1)\Delta t] - \sin[\omega i\Delta t] \quad .$$

To increase the computation speed the following trigonometric substitutions were made for DCO and DSI

$$DCO = 2. \quad \sin[\frac{\omega\Delta t}{2}] \sin[\frac{\omega((i+1)\Delta t + i\Delta t)}{2}]$$

$$DSI = 2. \quad \sin[\frac{\omega\Delta t}{2}] \cos[\frac{\omega((i+1)\Delta t + i\Delta t)}{2}]$$

This integration procedure was used for all work in this chapter and succeeding chapters except where another integration routine is specifically specified.

2.6 Criteria Evaluation

Figures 2-2 through 2-8 show these 12 criteria applied to a specific case. Figure 2-1 is the Bode plot for that case. In Figures 2-7 and 2-8 the integral criteria were normalized and plotted together to compare curve shapes. It is desirable that the value of the criterion increase very rapidly around the blow-up frequency so that a sharp definition of the blow-up point is given. Otherwise, consistent results may not be obtained from case to case since for a slowly increasing value of the error criterion, a small change in its value would give a large change in the frequency.

If an integral criterion will give a satisfactory definition of the blow-up frequency, then it would be preferable to an absolute value of the error criterion since the absolute value of the error criterion would suffer from the fault of prematurely predicting the blow-up when one bad point is surrounded by many good points. After examining the figures presented here and many others, it was seen that several of the integral criteria appear suitable. The squared error integrals give the best curve shapes for defining the blow-up point since they turn up sharper. They weight the large errors heavier than the small errors which is desirable since the larger errors indicate the rapid approach of the blow-up point.

Calculation of many cases revealed that neither the log magnitude nor the phase angle plot always deteriorates first. Consequently, both plots have to be taken into account. For this reason a complex point error criterion would be preferable, otherwise two criteria would have to be used requiring a blow-up value

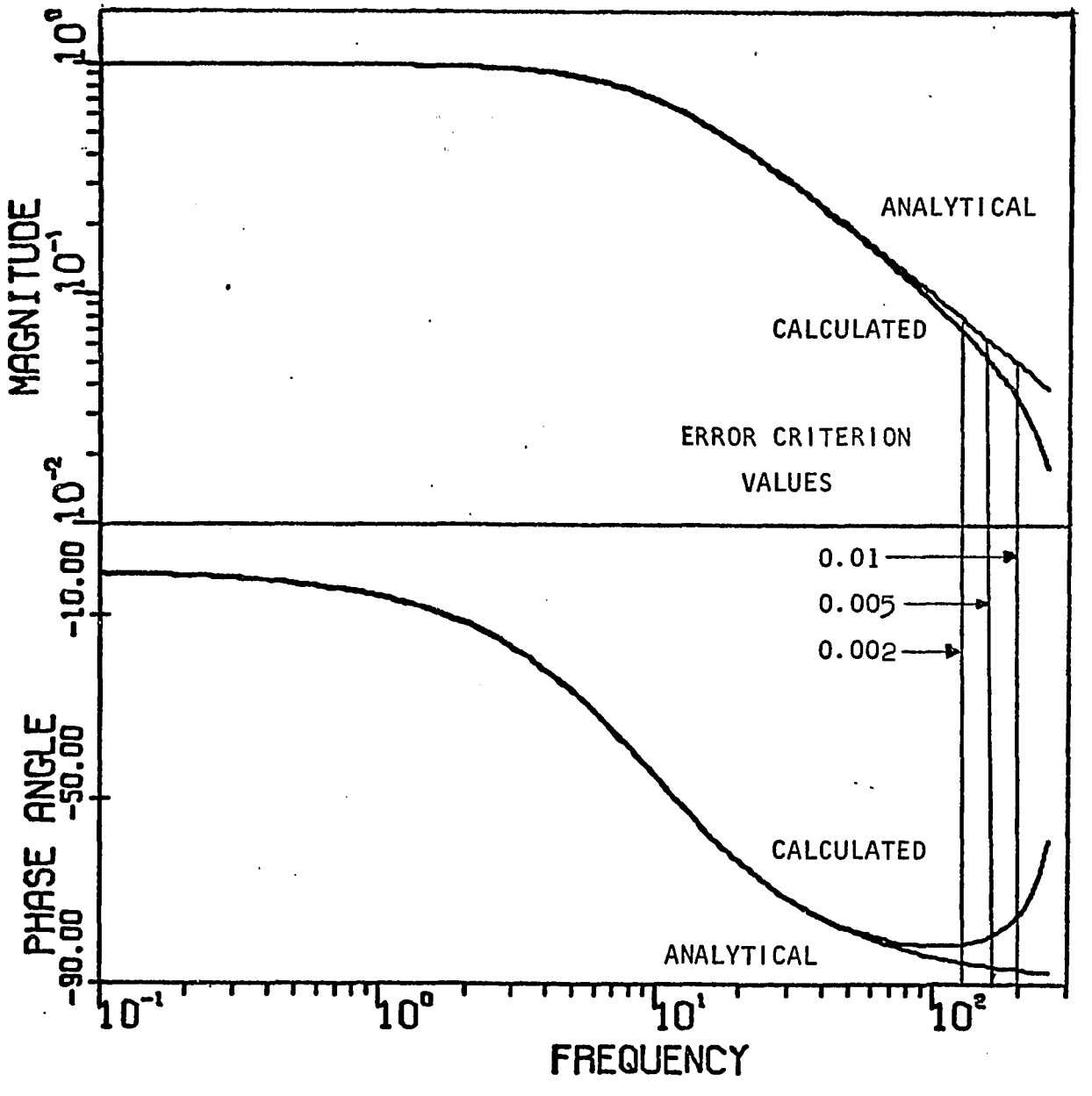

FIGURE 2-1. Bode Plot with the Blow-Up Frequency Marked as Defined by Three Values of the Error Criterion

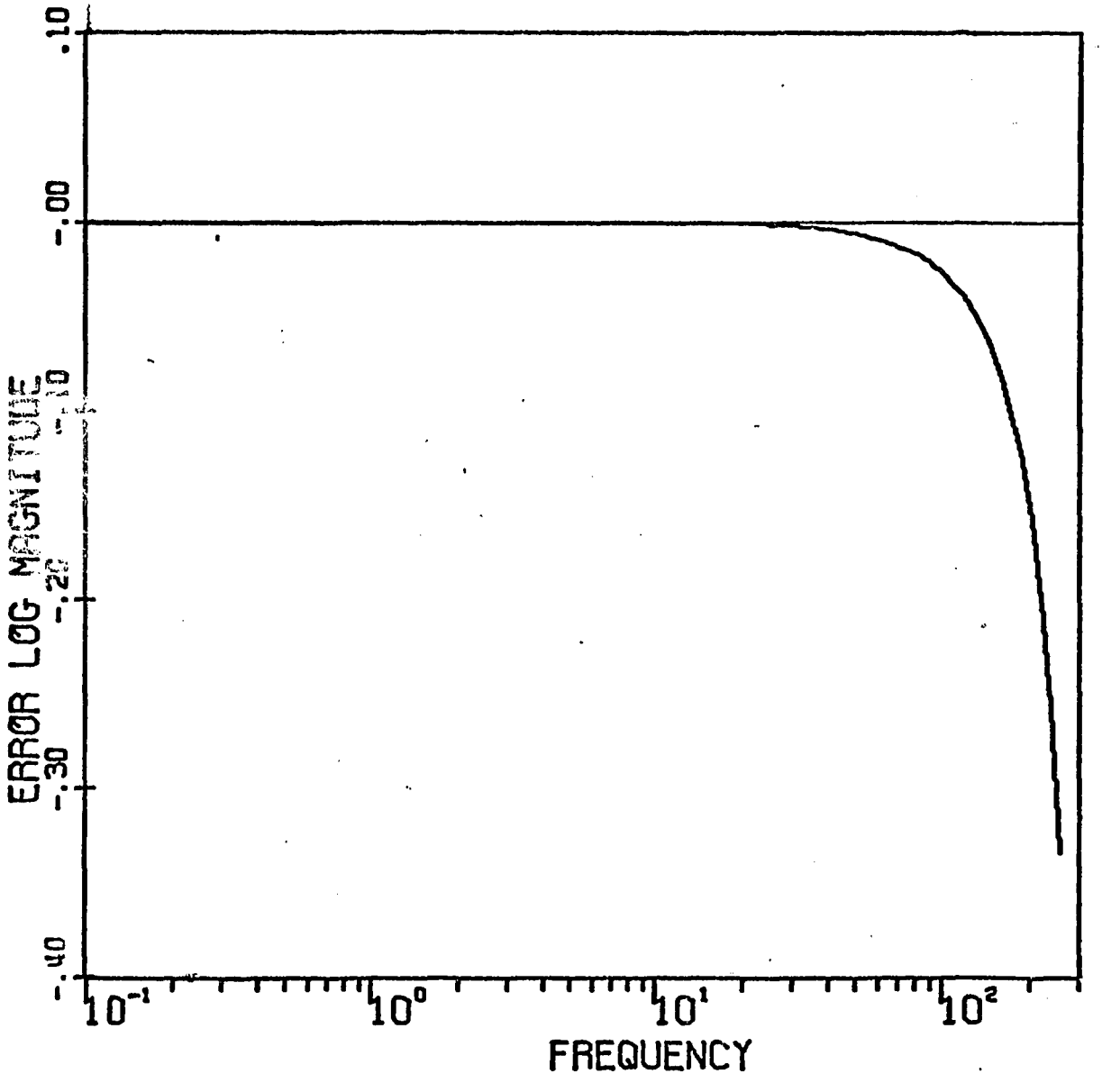

FIGURE 2-2. Error in the Log of the Magnitude Ratio Versus Frequency

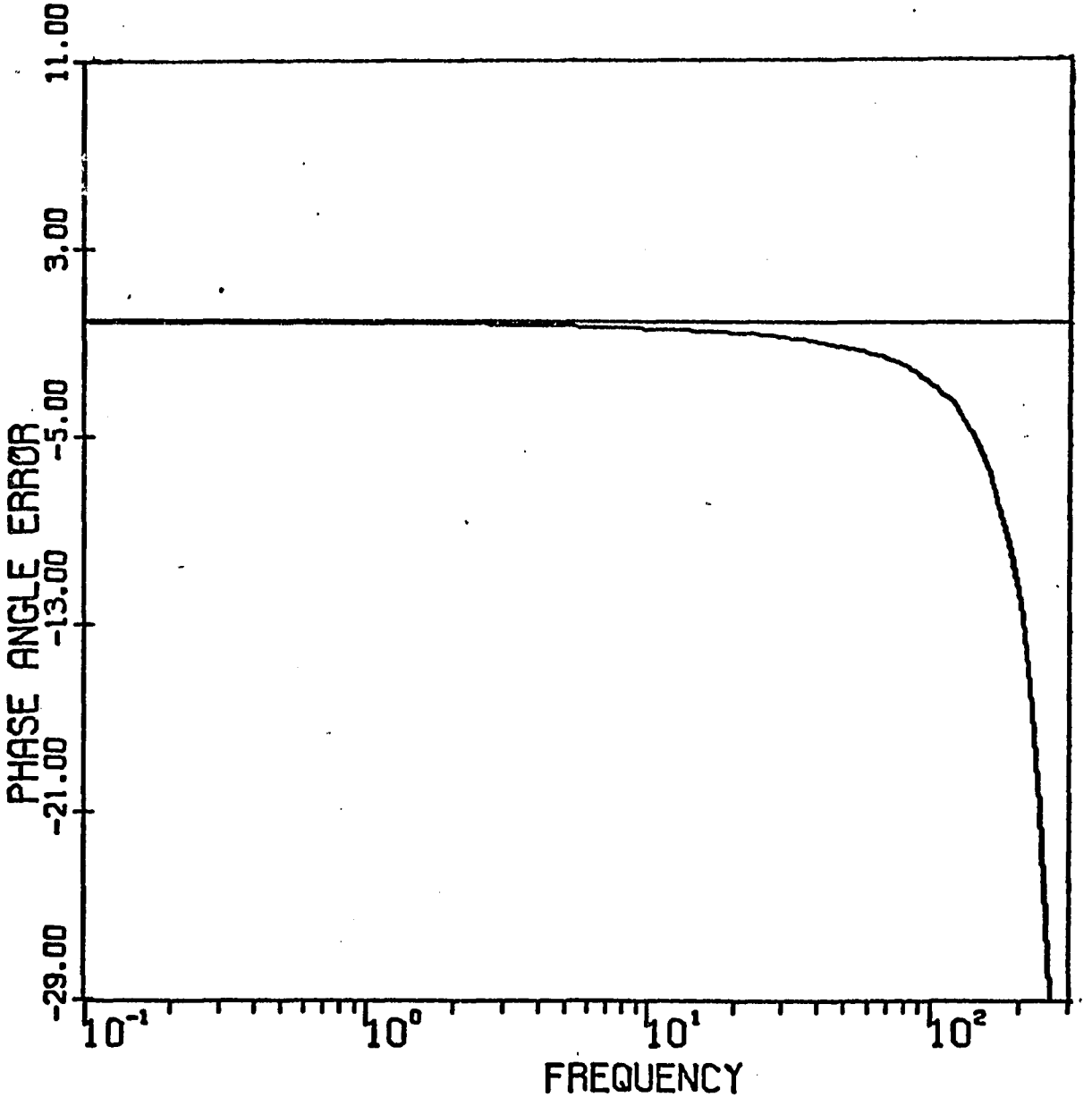

FIGURE 2-3. Phase Angle Error versus Frequency

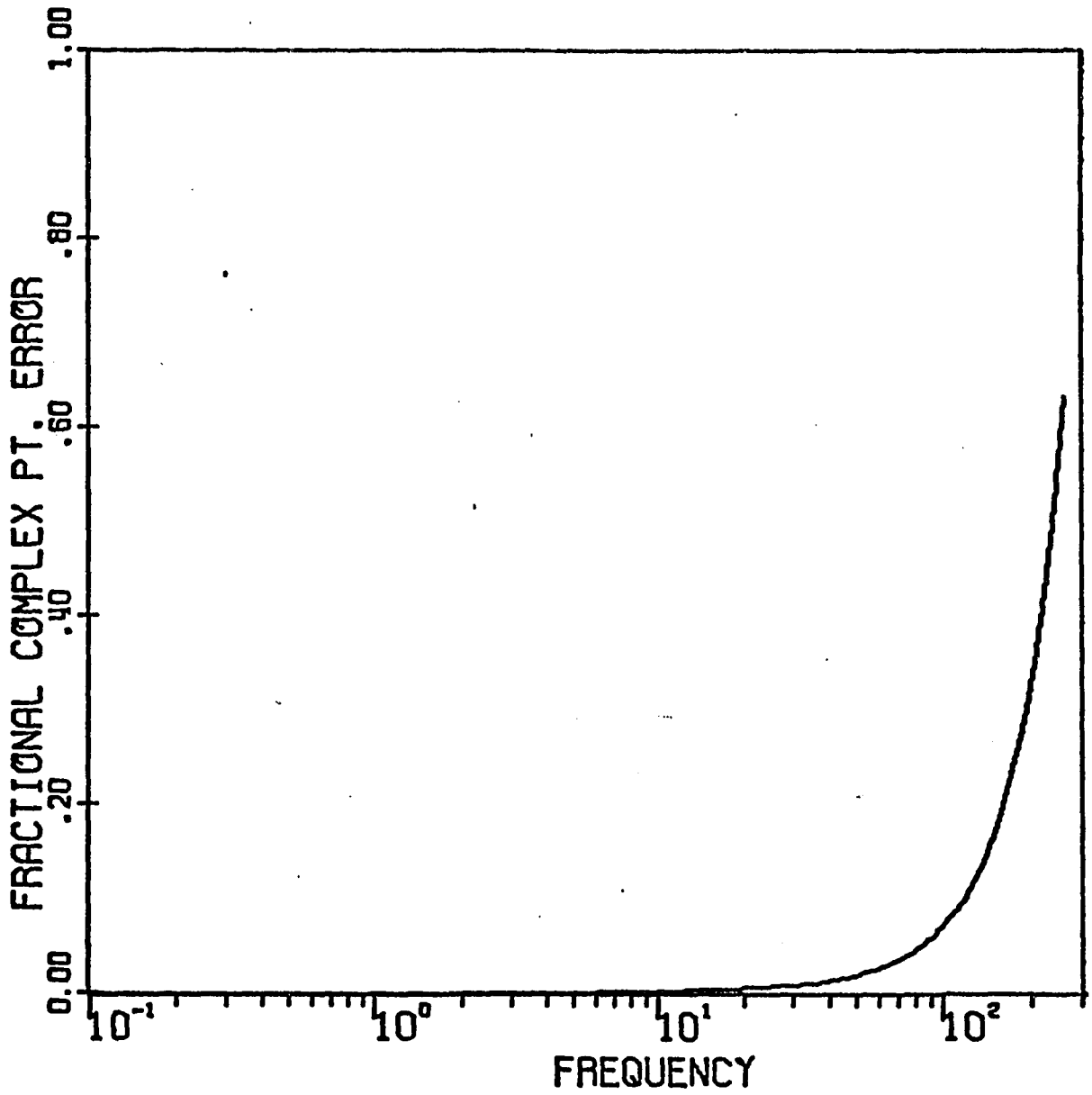

FIGURE 2-4. Error in the Complex Point versus Frequency

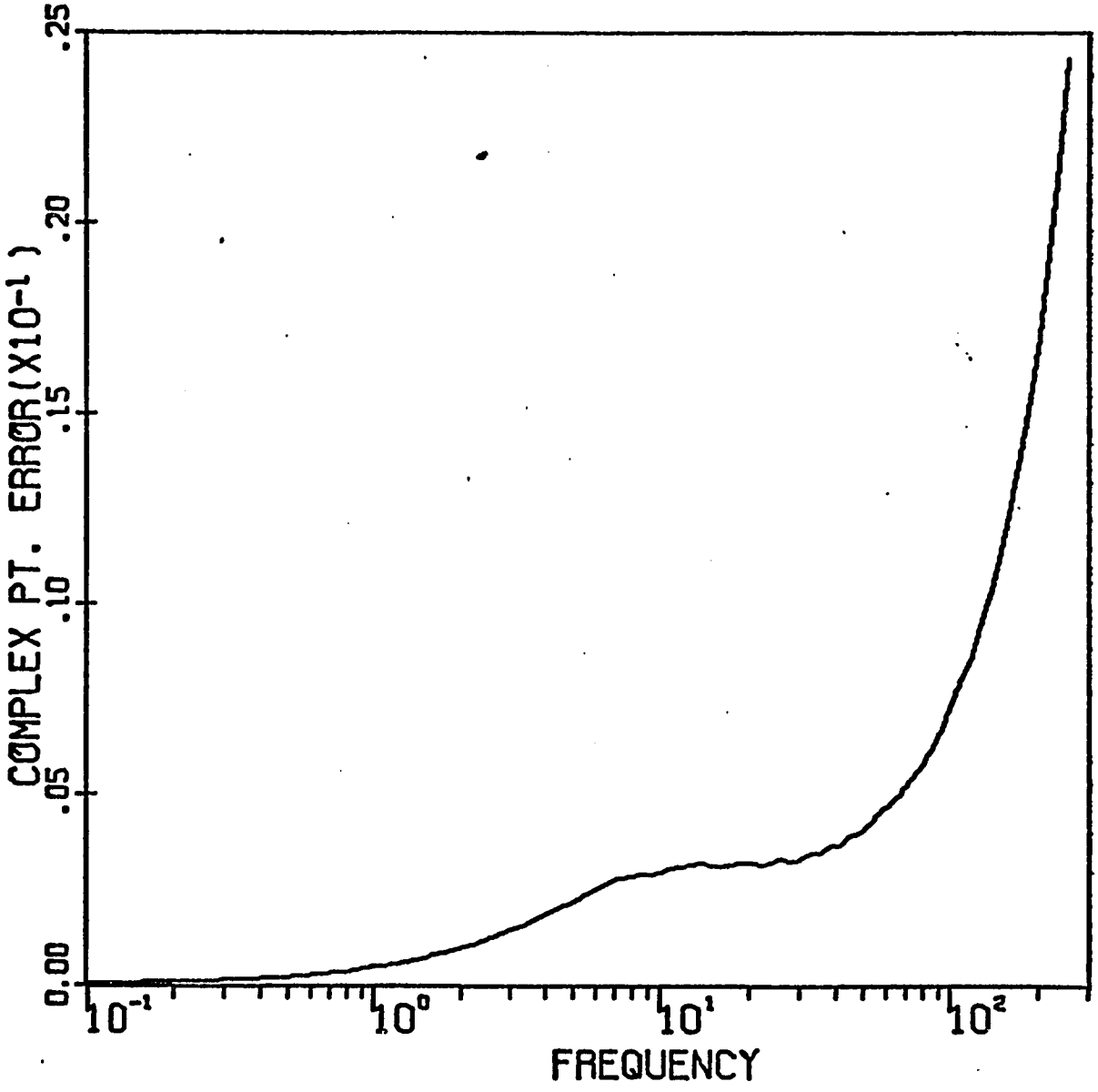

FIGURE 2-5. Fractional Complex Point Error versus Frequency

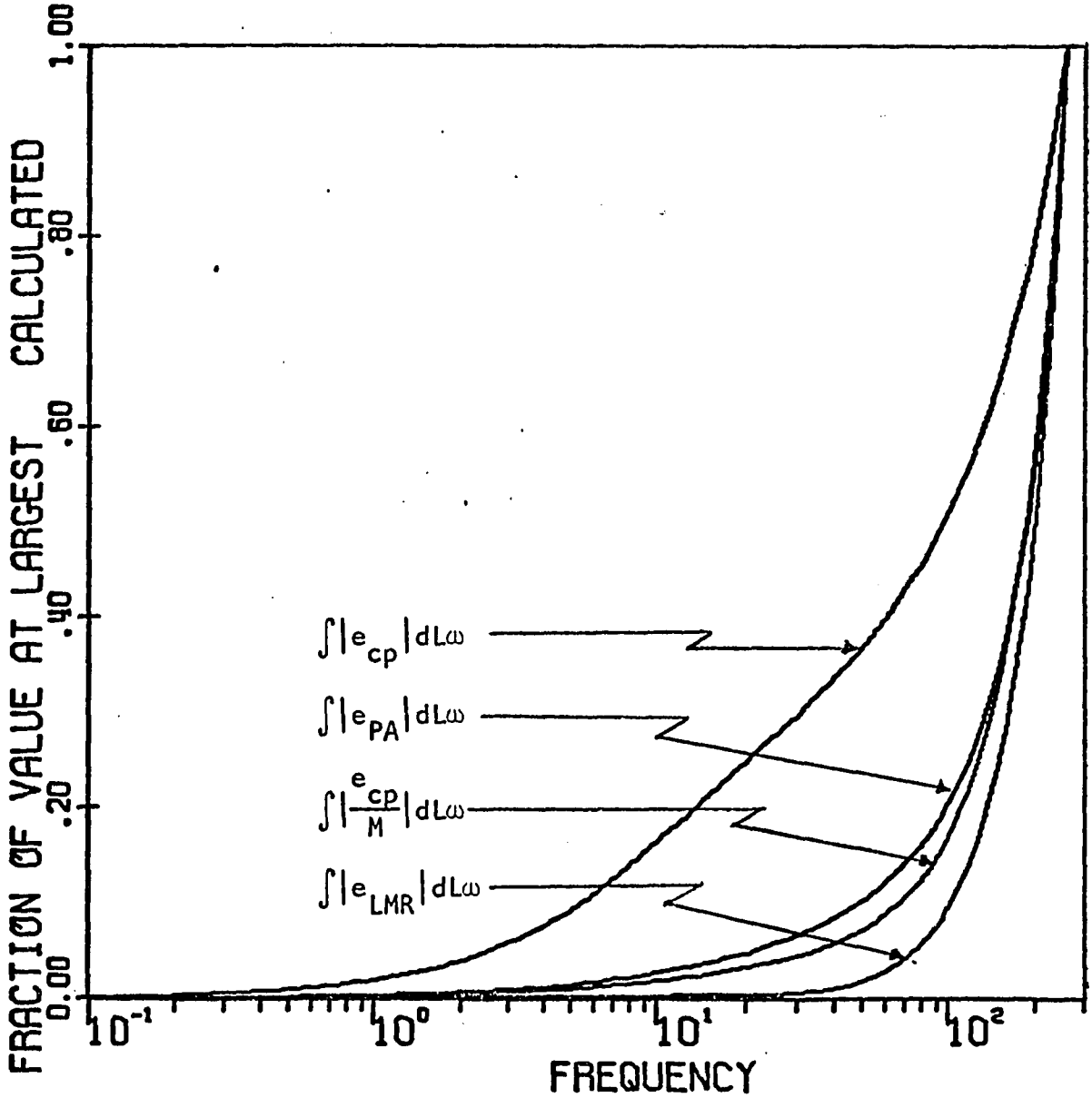

FIGURE 2-6. Comparison of Curve Shapes of the Four Integral of the Absolute Error Criteria

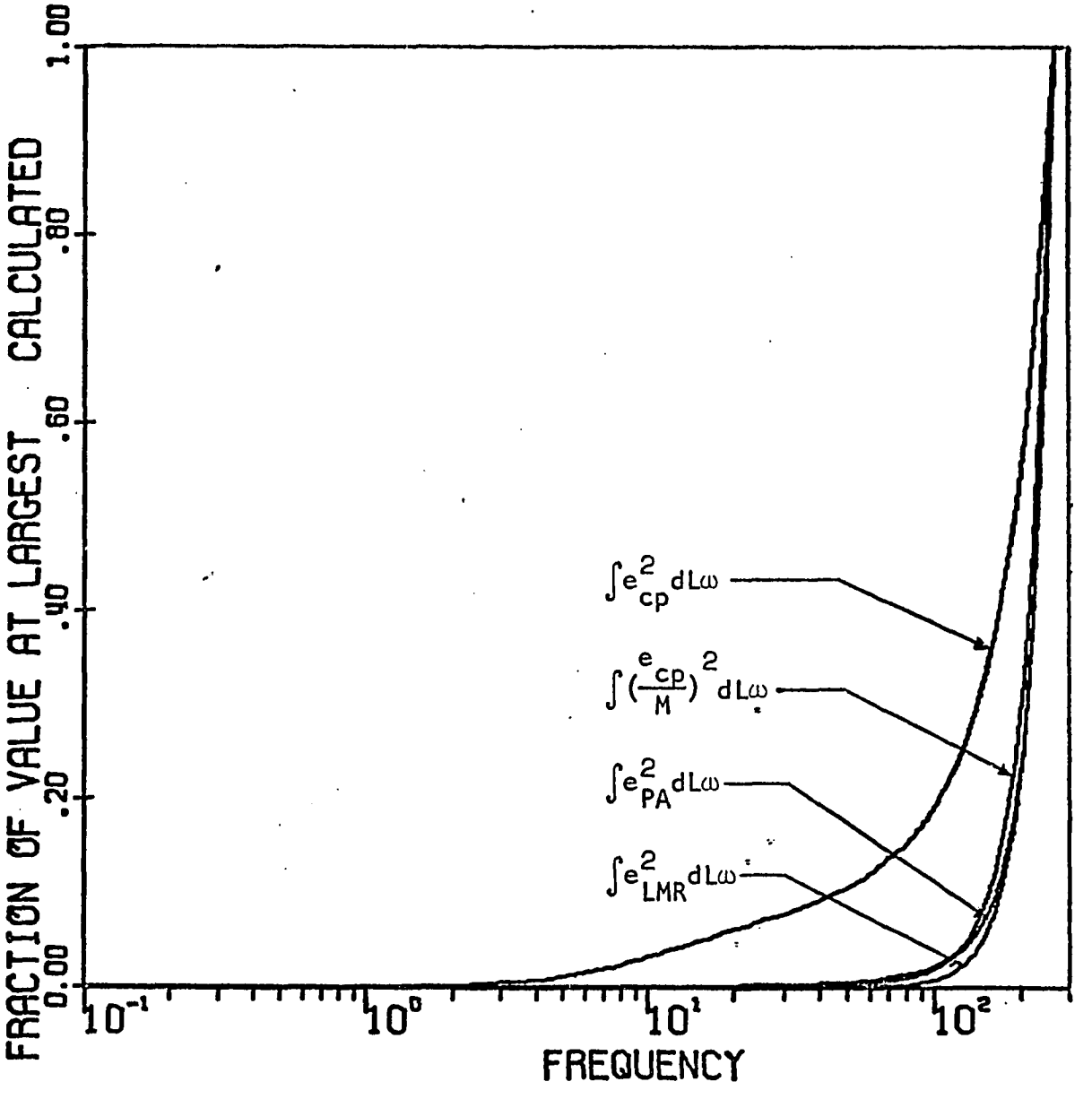

FIGURE 2-7. Comparison of Curve Shapes of the Four Integral of the Squared Error Criteria

for each criterion. Since these values are arbitrary, this would considerably complicate the problem. In searching for an error to use in frequency domain least squares curve fitting for mathematical models, Schnelle (6) also settled on the complex point error rather than either the log magnitude or phase angle error: He showed that both the log magnitude and phase angle errors are required and that the phase angle error should be weighted. Hence, it is easier to use the complex point error. Examination of Figure 2-7 shows that the squared fractional complex point error integral should be used instead of the squared complex point error integral because it has a much better curve shape. Since it uses a percentage error value, this criterion is also less dependent on the point of the plot at which blow-up occurs.

Although the integral of the squared fractional complex point error criterion appears to be the preferred one because of its ease of application coupled with its desirable curve shape, an evaluation of its performance must be made. To make this evaluation the matrix of systems and sampling times shown in Table 2-1 was prepared. It tabulates values of the integral of the squared fractional complex point error, error of the log magnitude ratio, and the phase angle error corresponding to a frequency of half the "theoretical" Shannon maximum recoverable frequency. (This "theoretical" value assumes that there are no frequency components higher than half the sampling frequency.) As can be seen, at this frequency the calculated values of the Bode plots show noticeable

TABLE 2-1

Error Criterion Evaluation

τ	Z	ω_n	Dead Time	Sampling Time	$\int (\frac{e_{cp}}{M})^2 dL\omega$	e_{pA}	e_{LM}
0.1				0.005	0.004462	-0.91	-.0506
0.1				0.010	0.003795	-5.31	-.0775
0.1				0.020	0.004168	-4.67	-.0899
0.1				0.040	0.004904	-5.37	-.0936
	1	10		0.005	0.006894	-12.20	-.0587
	1	10		0.010	0.003749	-5.54	-.0593
	1	10	0.02	0.010	0.003749	-5.54	-.0593

deviation from the theoretical values. To be a good criterion the complex point criterion should be sensitive to changes in both the log magnitude and the phase angle errors. Table 2-1 shows that it is sensitive to changes in either type error. For the first order system at sampling times of 0.01 and 0.04 the phase angle errors are approximately equal but the log magnitude error is greater for the sampling time of 0.04. The complex error criterion shows a significant increase in response to this increase in log magnitude error. To observe the effect of phase angle errors compare the second order system at sampling times of 0.005 and 0.01. Here the log magnitude errors are approximately equal but the phase angle errors are quite different. Accordingly the complex error criterion shows a significant increase with the increase in phase angle error. Thus it was concluded that the integral of the squared fractional complex point error is the most suitable criterion.

2.7 Selecting the Cut-Off Point

To set a value for the error criterion several Bode plots were constructed along with graphs of the selected error criterion plotted against the log of the frequency. By examining these plots some values of the error criterion could be picked off which gave a reasonable blow-up point. Since this point is arbitrary several values were chosen (0.01, 0.005, 0.002). Figure 2-1 shows how each of these values defines the blow-up point for a particular, representative case.

2.8 Conclusion

The need for mathematically defining the blow-up frequency of Fourier transforms was pointed out and several criteria for defining the blow-up were proposed and evaluated. Following this evaluation the integral of the squared fractional complex point error was selected as the best criterion. The selected criterion should prove extremely useful in such applications as evaluating the effects of sampling frequency, random noise, integration technique, and filtering on recoverable frequency.

LITERATURE CITED

1. Carroll, S. N. and W. L. McDaniel, Jr., "Use of Convolution Integral in Sampled Data Theory," I.E.E.E. Transactions on Automatic Control, April, 1966.

2. Clements, William C. Jr., "Pulse Testing for Dynamic Analysis," Ph.D. Dissertation, Vanderbilt University, 1963.

3. Lees, Sidney and Ray C. Dougherty, "Refinement of the Pulse Testing Procedure Computer Limitations," October, 1964.

4. Murrill, Paul W. Automatic Control of Processes. Scranton, Pennsylvania: International Textbook Company, 1967.

5. Papoulis, Athanasios. The Fourier Integral and Its Applications. New York: McGraw-Hill Book Company, Inc., 1962.

6. Schnelle, Karl B., Jr., "Experiments to Illustrate the Dynamic Testing of Chemical Process Systems," Report supported by Grant Number G-22952 of the Science Teaching Equipment Development Program, Course Content Improvement Section, Division of Scientific Personnel and Education of the National Science Foundation, 1965.

7. Shannon. "The Philosophy of P. C. M.," Proceedings of I. R. E., November, 1948.

CHAPTER 3

SAMPLING EFFECTS IN FOURIER ANALYSIS

The determination of system mathematical models from Bode plots hinges on the accurate calculation of the Bode plot over the frequencies of interest. It is a well-known phenomenon that as the Bode plot is extended to higher and higher frequencies, a frequency is reached beyond which the plot degenerates rapidly. Since a Bode plot is composed of the ratio of Fourier transforms at various frequencies, the primary problem is evaluating the Fourier transform. Assuming that the system input has a frequency content at the frequencies of interest, then the two major sources of error in calculating Fourier transforms are (1) fold-over arising from sampling effects and (2) noise in the data. This chapter will be devoted to sampling effects with treatment of noise effects being deferred to a later chapter.

3.1 Fold-Over

The need for sampling arises because discrete data points are frequently used to represent the input and output functions when evaluating the Fourier transforms. Plotting the frequency spectra of continuous and sampled functions gives a graphic illustration of the fold-over effect resulting from sampling. Shown in Figure 3-1(a) is the frequency spectrum of a continuous function $x(t)$ band-limited to ω_B (i.e. no frequency components higher than ω_B). Sampling this

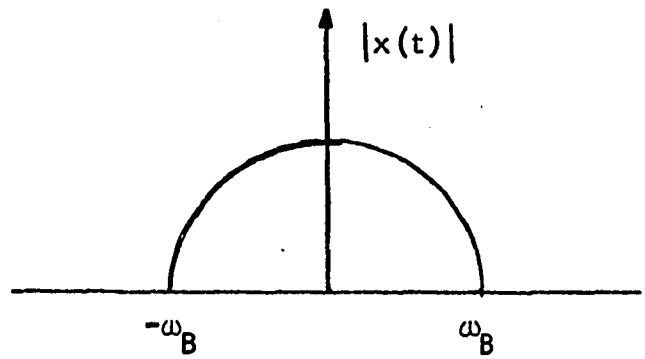

a) Frequency Spectrum of a Band-Limited, Continuous Signal

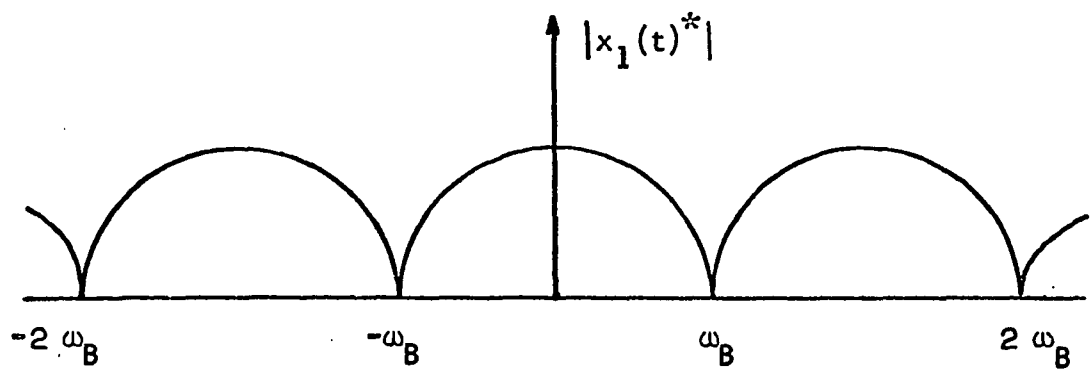

b) Frequency Spectrum of Signal in a) Sampled at a Frequency of $2\omega_B$

FIGURE 3-1

function $x(t)$ at a frequency of $\omega_{s1} = 2\,\omega_B$ (this is the minimum Shannon sampling frequency for complete information recovery) produces the sampled function $x(t)_1^*$ with the frequency spectrum shown in Figure 3-1(b). Note that the spectrum for the original signal is repeated and centered around multiples of the sampling frequency ω_{s1}. Now observe what happens if the sampling frequency is greater than $2\,\omega_B$. In Figure 3-2(a) the spectrum of $x(t)_2^*$ is shown for a sampling frequency of $\omega_{s2} = 3\,\omega_B$. The shape of the spectra is not altered but since they center around multiples of the sampling frequency their displacement along the frequency axis is increased. However if the sampling frequency is less than $2\,\omega_B$ the spectra will fold over, as shown in Figure 3-2(b), and produce distortion in the higher frequency components of the signal. Normally this is what happens since real systems are seldom band-limited and consequently would require an impractical, infinite rate of sampling to avoid all distortion. From an examination of Figure 3-2 it seems probable that increasing the sampling frequency to increase the displacement of the spectra will reduce the distortion of non-band-limited signals.

3.2 Correlating Sampling Frequency and Recoverable Frequency

Verifying this last statement should not be difficult. Using a noiseless system (to isolate the fold-over effect) a pulse input can be introduced and then various sampling rates used to record data from the input and output curves, i.e., a different sampling rate for each set of curves. Applying the error criterion developed

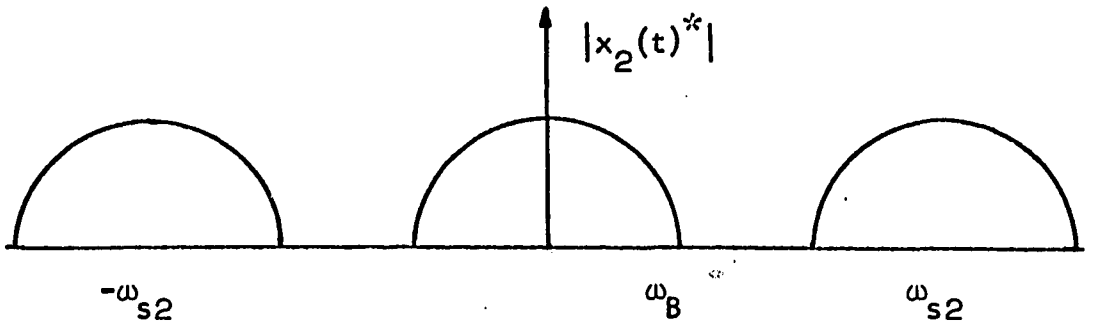

a) Frequency Spectrum of Signal 3-1 a) Sampled at a Frequency of 3 ω_B

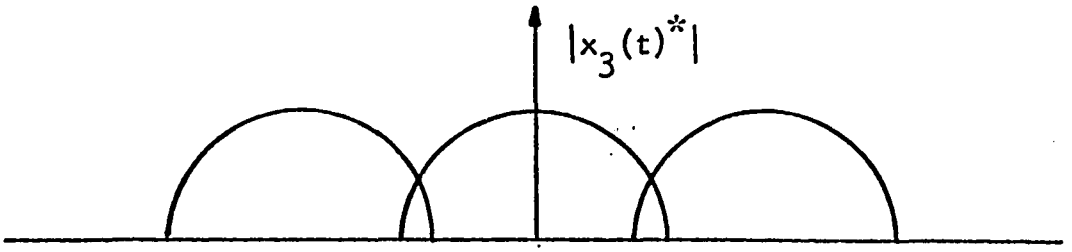

b) Frequency Spectrum of Signal 3-1 a) Sampled at a Frequency Less than 2 ω_B

FIGURE 3-2

in Chapter 2,

$$\int \left(\frac{e_{cp}}{M_{cp}}\right)^2 dL\omega \qquad 3.1$$

where e_{cp} = complex point error

M_{cp} = magnitude of complex point

$L\omega$ = $\log_{10}$ of the frequency

a maximum recoverable frequency, ω_R, can be found for each sampling rate or frequency and the effect of sampling frequency should be apparent. This was done using three error criterion values of 0.01, 0.005, and 0.002. The input was a ramp pulse put through a first order lag and the system was a first order lag as shown in Figure 3-3. The results indicated that the recoverable frequency definitely is a function of the sampling frequency for a noiseless system. Defining the "theoretical" maximum recoverable frequency, ω_M, to be 1/2 the sampling frequency, the results were correlated in terms of a percentage of this theoretical maximum. As Figures 3-4, 3-5, and 3-6 show, the <u>percentage</u> of the theoretical maximum frequency does not appear to be a function of the sampling frequency although there is some scatter in the data. The average percentage recoveries for the various error criterion values are 65.8% for 0.01, 59.1% for 0.005, and 49.6% for 0.002. The minimum percentage recoveries are 60% for 0.01, 50% for 0.005, and 38% for 0.002. Introduction of a dead time into the system does not affect the correlation. Reference to the last two entries in Table 2-1 of Chapter 2 will show that dead time has no effect on error values.

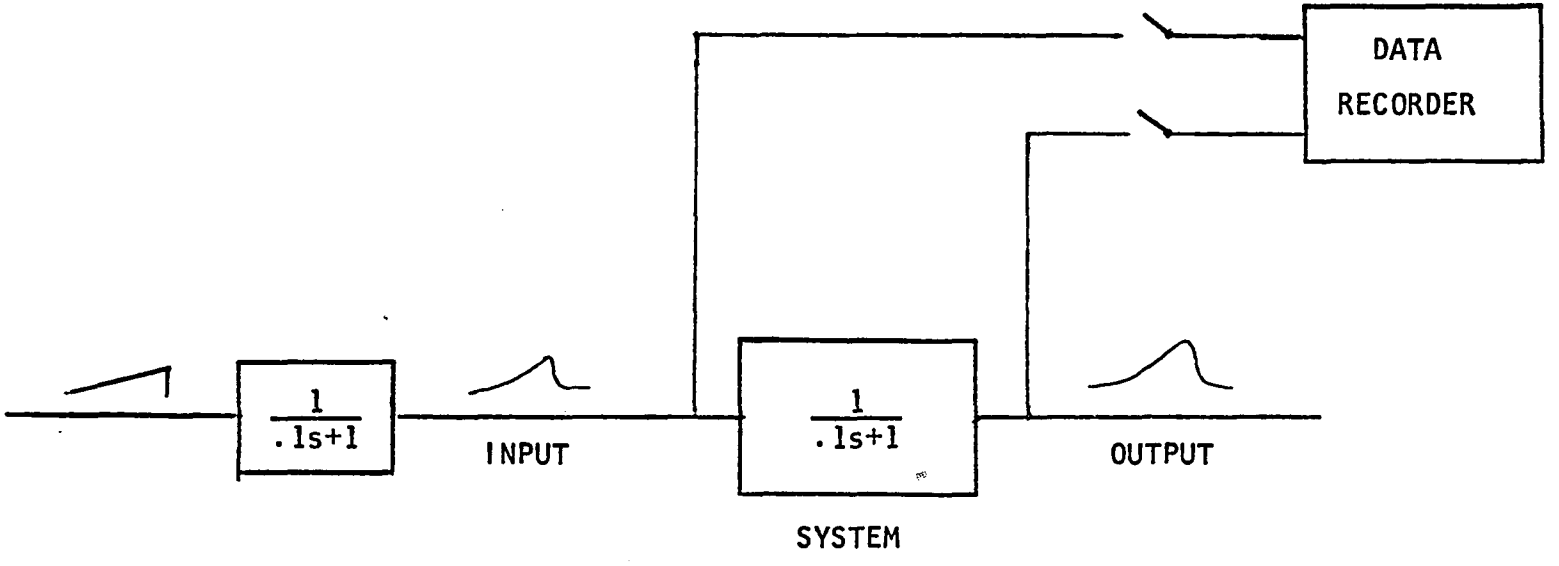

FIGURE 3-3. System and Input

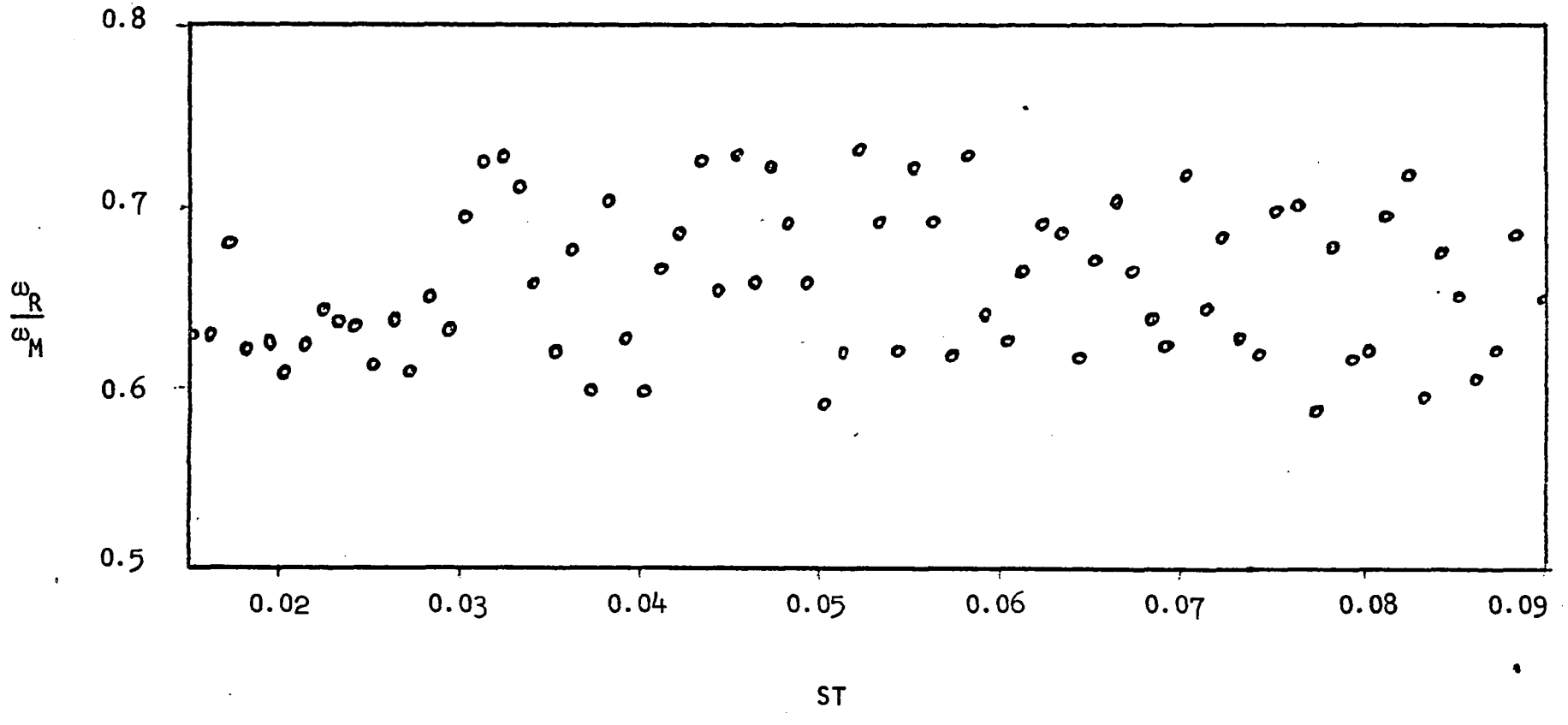

FIGURE 3-4. Recoverable Fraction of Shannon Frequency versus Sampling Time (2π/sampling frequency). Error Criterion Value of 0.01.

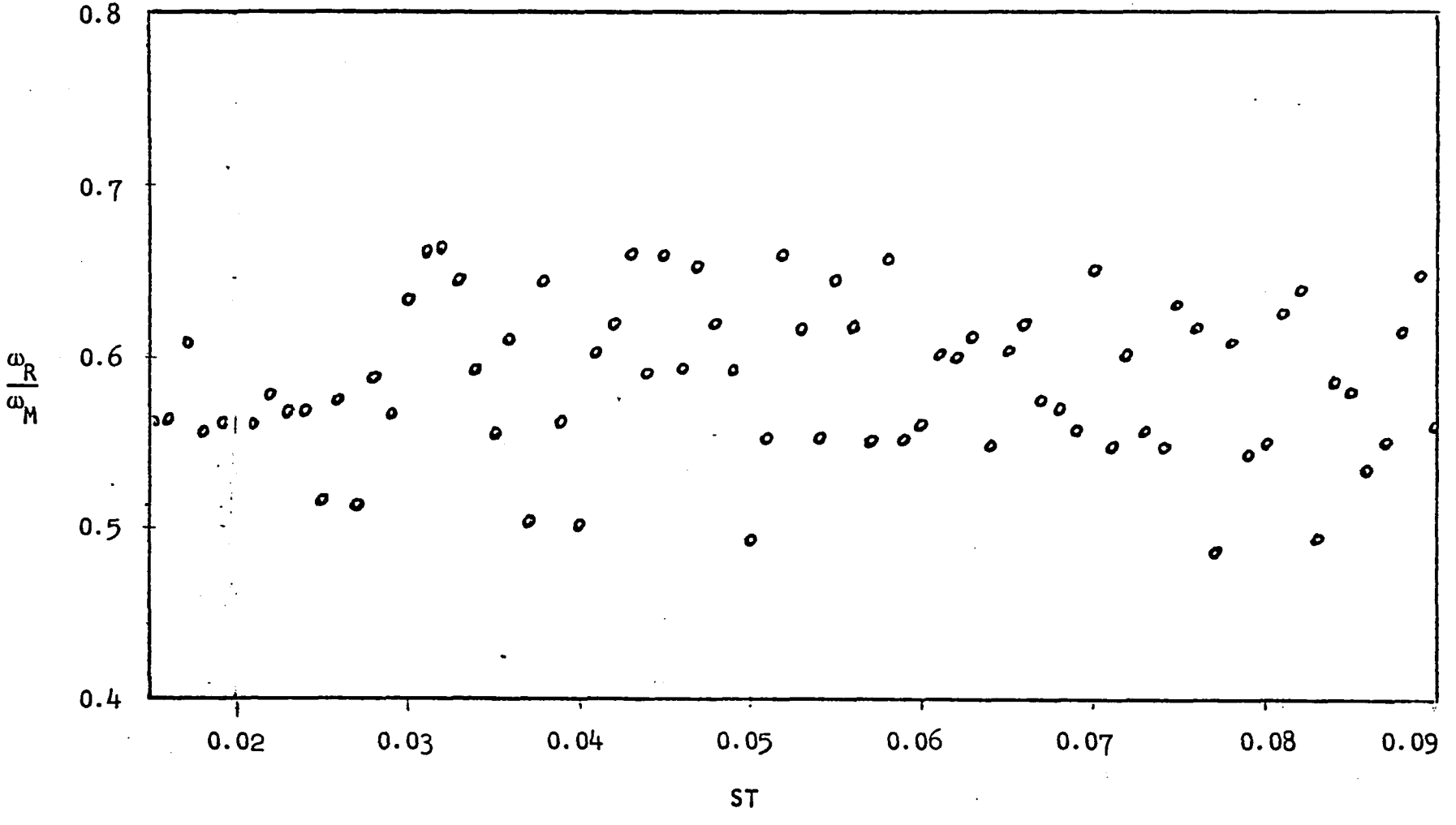

FIGURE 3-5. Recoverable Fraction of Shannon Frequency versus Sampling Time (2π/sampling frequency). Error Criterion Value of 0.005.

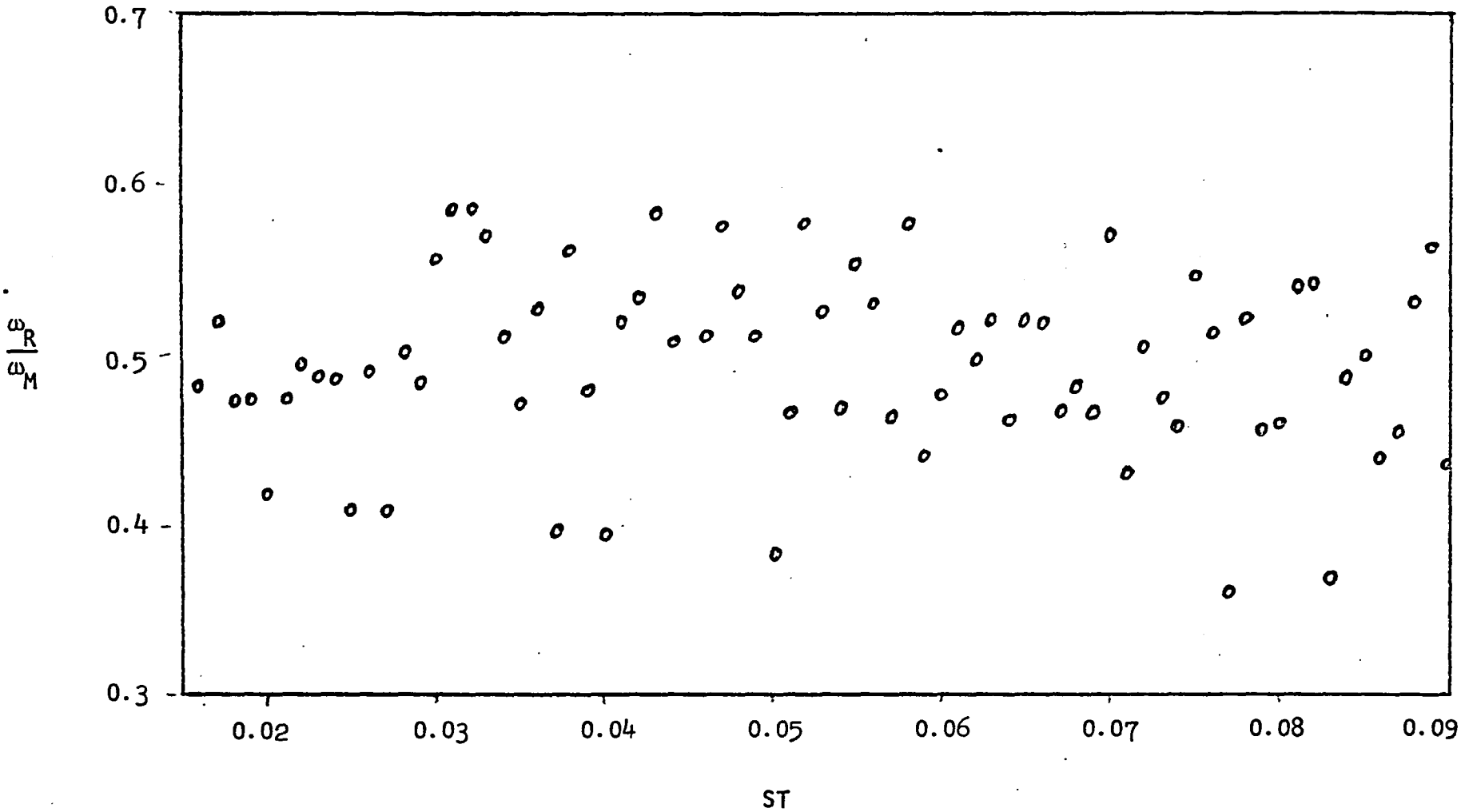

FIGURE 3-6. Recoverable Fraction of Shannon Frequency versus Sampling Time (2π/sampling frequency). Error Criterion Value of 0.002.

Higher percentage recoveries were found for a second order system. This might have been expected since a second order system attenuates the input sharper than a first order system, and therefore, it reduces the fold-over effect in the output transform. Figure 3-7 shows the average recoverable fraction of the theoretical maximum recoverable frequency plotted versus ratios of second order system time constants for 0.01 error criterion value. Note that as the time constant ratio decreases (meaning that the system is approaching a first order system) the recoverable fraction decreases, approaching the recoverable fraction of a first order system. Hence, for the noiseless system, a first order lag is the conservative case. If 0.01 is taken as a reasonable value of the error criterion, recovery of no more than 66% of the theoretical maximum recoverable frequency should be expected.

3.3 Frequency Content

As frequency content is important in pulse testing, a precise definition will now be given to facilitate understanding of much of the presentation to follow. The frequency content of a non-periodic pulse $x(t)$ occurring over a time interval T_P is defined as:

$$\text{Frequency content} = \int_0^{T_P} x(t)\, e^{-j\omega t}\, dt \qquad 3.2$$

Clements (2) provides an excellent development which shows that the frequency content of non-periodic functions varies continuously with frequency while the frequency content of periodic functions has values only at discrete frequencies corresponding to integral multiples of the fundamental frequency. Note that the definition

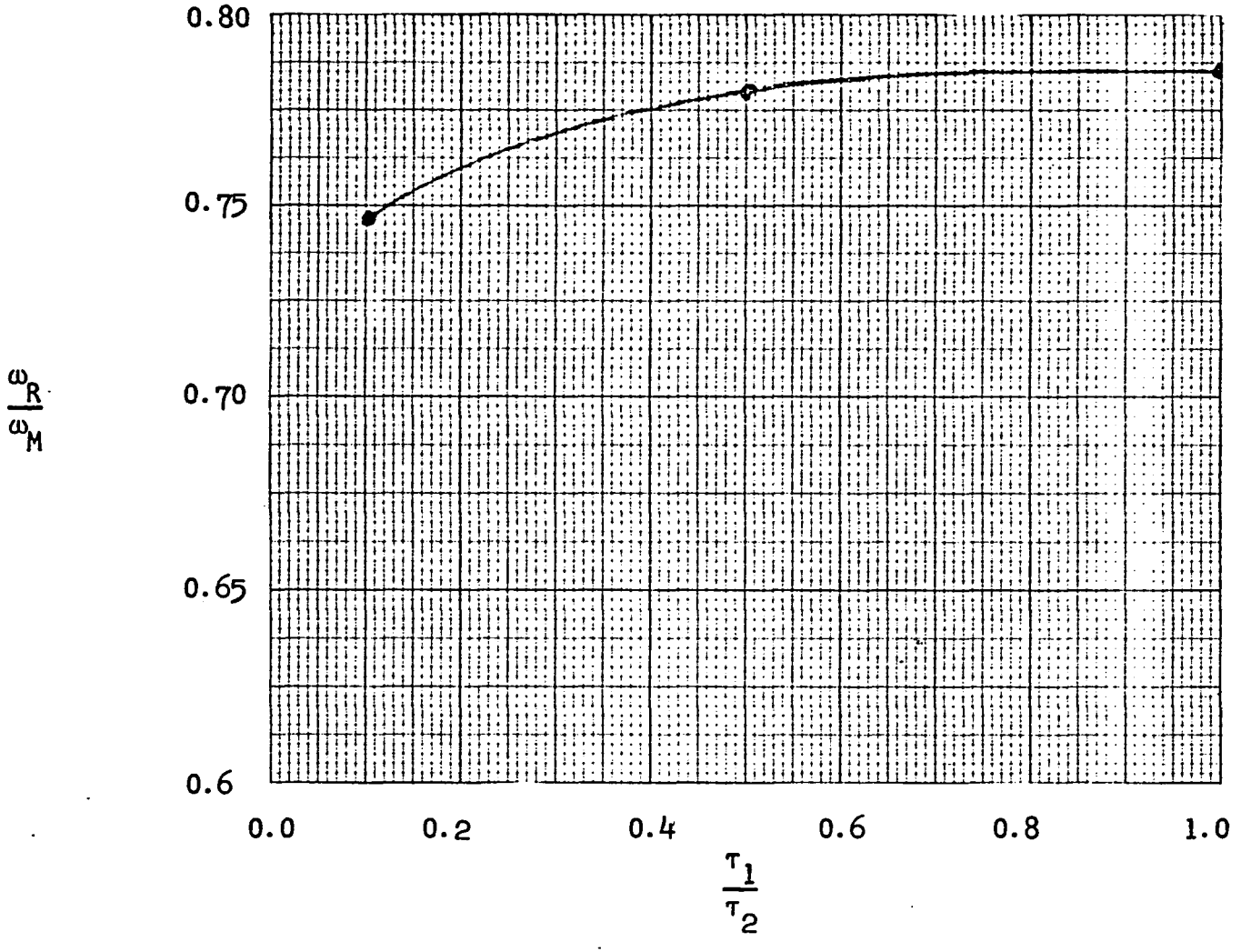

FIGURE 3-7. Average Recoverable Fraction of Shannon Recoverable Frequency versus Ratios of Second Order System Time Constants. Error Criterion Value of 0.01.

of frequency content for a non-periodic pulse corresponds to the definition of the Fourier transform of the input or output. Therefore, for a non-periodic pulse input, the Fourier transforms of the input and output have values at all frequencies. One well-chosen non-periodic pulse input, i.e., one with a significant value of frequency content at all of the frequencies of interest, will yield sufficient data to construct the entire Bode plot, while many sinusoidal input tests would be required to construct the same plot. This is the basis for the popularity of the pulse testing technique. As frequency content is a complex number it possesses both a magnitude and a phase angle, however all plots and values given will refer only to its magnitude.

3.4 Severe Fold-Over in the Input

It is often desirable to increase the frequency content of an input at high frequencies, and this can be accomplished by shortening the input pulse duration. For a noiseless system this had little effect until the ratio of pulse duration, T_p, to sampling interval, ST, fell below 5; then the results degenerated badly as shown in Table 3-1. In several instances the magnitude ratio was offset by a constant amount. A very plausible explanation for this behavior at low pulse duration to sampling interval ratios is severe fold-over in the input (the output is filtered by the system). Apparently, as the sampling interval is lengthened, decreasing the sampling frequency, the spectra are displaced less and the fold-over increases for a given pulse. Figure 3-8 shows a comparison of the input and output transforms with their analytic values for an example where the pulse time to sampling interval ratio is below five. The

TABLE 3-1

Effect of Pulse Duration to Sampling Time Ratio on the Recoverable Fraction

ST	T_P	$\frac{T_P}{ST}$	$\frac{\omega_R}{\omega_M}$
0.03	0.5	16.7	.67
0.06	1.0	16.7	.68
0.09	1.0	11.1	.62
0.03	.25	8.3	.71
0.06	.5	8.3	.71
0.09	.5	5.6	.69
0.03	.125	4.2	.05
0.06	.25	4.2	.10
0.09	.25	2.8	.04

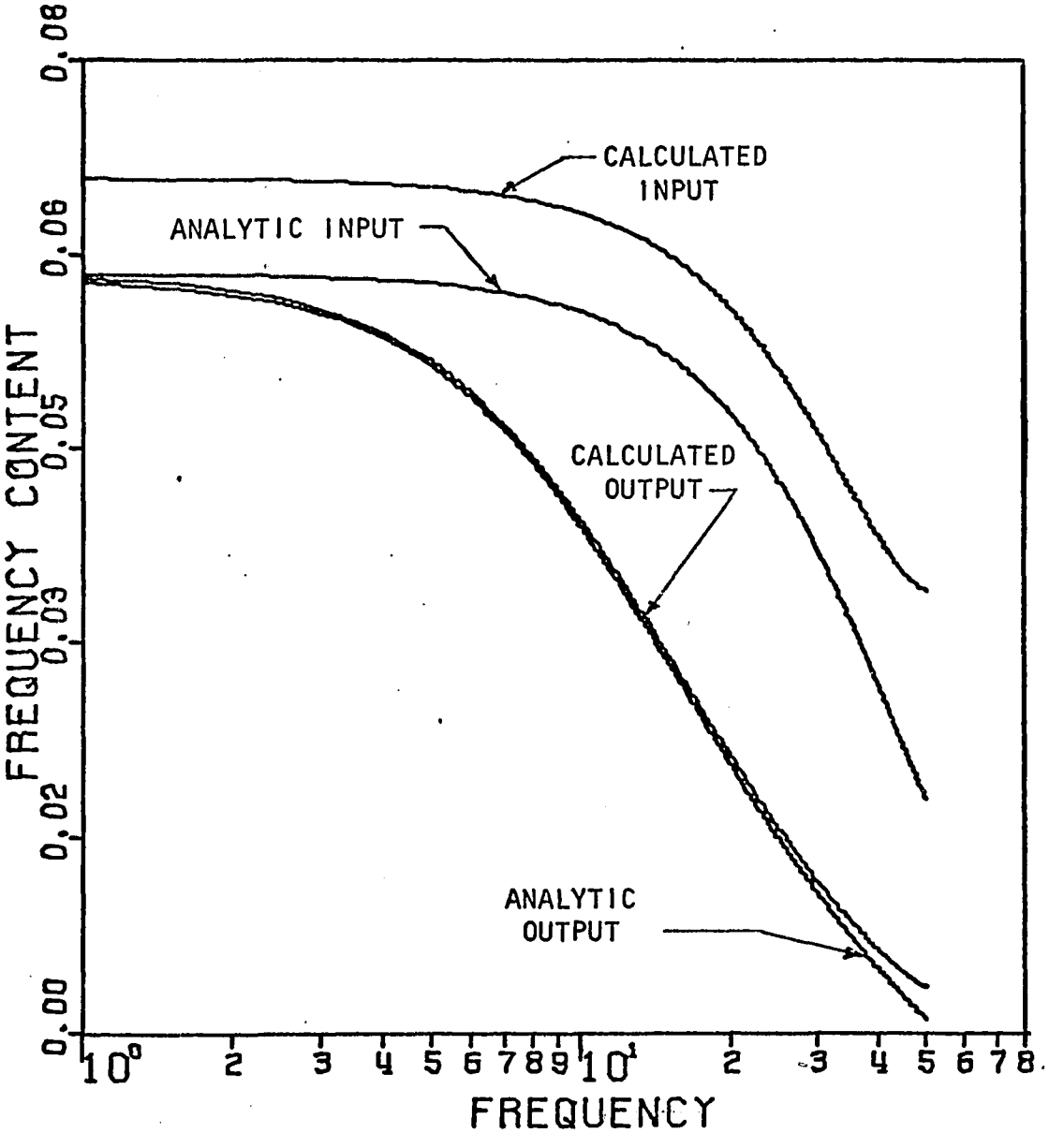

FIGURE 3-8. Comparison of Analytic and Calculated Input and Output Transforms. Pulse Time to Sampling Time Ratio Below Five.

number 5 is probably specific to the pulse type, which had the equations

$$x(t) = 8\left(\frac{t}{T_P}\right)^3 \qquad 0 \le t \le \frac{T_P}{2} \qquad 3.3$$

$$x(t) = 8\left(1 - \frac{t}{T_P}\right)^3 \qquad \frac{T_P}{2} < t \le T_P \qquad 3.4$$

but the same result is to be expected from other pulse types at low pulse duration to sampling time ratios.

3.5 Integration Technique

There has been considerable discussion and some disagreement over what integration technique should be used in the Fourier transform calculations and both numerical and "analytic" approaches have been offered.

The basic equation to evaluate is

$$G(j\omega) = \frac{\int_0^{T_y} y(t)e^{-j\omega t}\,dt}{\int_0^{T_x} x(t)e^{-j\omega t}\,dt} \qquad 3.5$$

Normally the Euler substitution

$$e^{-j\omega t} = \cos(\omega t) - j\,\sin(\omega t) \qquad 3.6$$

is made to facilitate the actual calculation, but this will not be necessary for the present purposes. Frequent comment is made

in the literature that the direct application of a quadrature formula such as the trapezoid rule or Simpson's rule to the evaluation of the integrals is unsatisfactory because at high frequencies the rapid oscillation of the product curves, such as $y(t)\cos(\omega t)$, will cause the approximation to degenerate seriously. To overcome this difficulty a number of people have advocated approximating the curves $x(t)$ and $y(t)$ over a small increment of time, substituting this approximation into the integral and analytically performing the integration. The total integral is obtained by summing all of the small integrals necessary to span the entire pulse time. It is quite interesting to note the resulting equations produced when various degrees of sophistication in approximating function for the curves $x(t)$ and $y(t)$ are used.

The simplest approximation for the curves is to assume a constant value over the time increment, a stepped curve approximation. Substituting this approximation and analytically integrating gives for the ratio of output to input transforms

$$G(j\omega) = \frac{\Delta t_y \dfrac{\sin(\omega\Delta t_y/2)}{\omega\Delta t_y/2} \displaystyle\sum_{k=1}^{n} y(k\Delta t_y)\, e^{-j\omega k\Delta t_y}}{\Delta t_x \dfrac{\sin(\omega\Delta t_x/2)}{\omega\Delta t_x/2} \displaystyle\sum_{i=1}^{m} x(i\Delta t_x)\, e^{-j\omega i\Delta t_x}} \qquad 3.7$$

If the more sophisticated approximation of a straight line between points on the curves is used even better results should be obtained. Proceeding as before the following result is

obtained

$$G(j\omega) = \frac{\Delta t_y \left[\frac{\sin(\omega\Delta t_y/2)}{\omega\Delta t_y/2}\right]^2 \sum_{k=1}^{n} y(k\Delta t_y)\, e^{-j\omega k\Delta t_y}}{\Delta t_x \left[\frac{\sin(\omega\Delta t_x/2)}{\omega\Delta t_x/2}\right]^2 \sum_{i=1}^{m} x(i\Delta t_x)\, e^{-j\omega i\Delta t_x}} \qquad 3.8$$

Note the similarity of this result to the previous one. In both cases the same summation term is multiplied by a correction factor. Lees (4) has shown that this holds true as the sophistication of the approximation is increased further. As pointed out by both Lees (4) and Clements (2), if Δt_y equals Δt_x then the correction factors cancel leaving simply the ratio of summation terms. This is the same result which would be obtained by one of the crudest of approximations for evaluating integrals - simply assuming the integral can be represented by a summation of rectangles. Therefore, if the time increments for taking data from the input and output curves are equal, then the integration technique is of no consequence and a sophisticated approximation is unnecessary. This result removes all doubts about the accuracy of the integration technique employed in the Fast Fourier Transform to be discussed in Chapter 6.

It might be argued that smaller time increments are necessary for approximating the input curve since it necessarily will have a shorter time base than the output curve. To determine the effect of using different sampling time increments for approximating the curves and, also to compare analytical versus numerical

integration techniques, several test cases were calculated for a first order lag system with a 0.1 time constant and a pulse input described by equations 3-1 and 3-2. The results presented in Table 3-2 show a definite trend of a decrease in the recoverable frequency with an increase in the sampling time increment of either the input or output curve, but the results are evenly divided as to which curve affected the results most with a decrease in its sampling time. These results are for noise-free data. When noise is present, it will almost invariably be at a higher level in the output than in the input, causing the output transform to deteriorate at a lower frequency than the input. Therefore if two different sampling frequencies are to be used, a good case could be made for using the higher sampling frequency on the output rather than the input.

The question of "analytical" versus numerical integration technique is also treated in Table 3-2 as stated previously. The "analytical" technique uses a straight line approximation between data points which is substituted into the Fourier transform integral and integrated analytically. The numerical technique simply evaluates the integration formula:

$$G(j\omega) = \frac{\sum_{k=1}^{n} y(k\Delta t_y)\, e^{-j\omega k\Delta t_y}}{\sum_{i=1}^{m} x(i\Delta t_x)\, e^{-j\omega i\Delta t_x}} \qquad 3.9$$

TABLE 3-2

Effect of Sampling Time and Integration Technique on Recoverable Frequency

INPUT SAMPLING TIME INCREMENT	OUTPUT SAMPLING TIME INCREMENT	PULSE DURATION	INTEGRATION TECHNIQUE	
			ANALYTICAL	NUMERICAL
			ω_R	ω_R
.030	.030	0.25	73.92	73.92
.030	.030	0.50	70.33	70.33
.030	.030	1.00	68.42	68.42
.030	.030	2.00	72.00	72.02
.030	.030	2.00	72.00	72.02
.035	.030	2.00	53.79	60.95
.040	.030	2.00	70.31	51.51
.050	.030	2.00	70.32	40.88
.030	.035	2.00	77.22	68.40
.030	.040	2.00	64.86	73.72
.030	.050	2.00	45.92	57.39
.030	.025	2.00	73.67	87.65
.025	.030	2.00	69.50	83.64

The table confirms the analytical prediction that the results will be identical for the different integration techniques when $\Delta t_x = \Delta t_y$. When Δt_x is not equal to Δt_y there is considerable variation in the recoverable frequency between the two techniques, but there appears to be no justification for saying that one technique is better than the other. In the range of practical variations of the two sampling frequencies, the ratio of the correction factors for the output and input integrals does not appear to be a significant factor in the results.

When unequal sampling rates are used for the input and output, specifying an integration technique to obtain the best results and choosing the sampling rates to recover the desired frequencies becomes a difficult task. Neither the optimum sampling rates nor the best integration technique can be chosen with any certainty because of inconsistent variations exhibited by both. Since results obtained using equal sampling rates for input and output are not dependent on the integration technique and have been found to be much more predictable than results for unequal rates, equal sampling rates are recommended for Fourier analysis.

3.6 Conclusions

The fold-over effect from sampling proved to have a considerable influence on the maximum recoverable frequency. As a result, for a noiseless system the maximum recoverable frequency was found to be a function of the sampling frequency, where the sampling frequencies for the input and output were equal. Defining a

"theoretical" maximum recoverable frequency as 1/2 the sampling frequency, the percentage recovery of this theoretical value was found to be approximately constant for a wide range of sampling frequencies and equal to 66% for first order systems and an error criterion value of 0.01. Noiseless second order systems allowed higher percentage recoveries than first order systems. At very low pulse duration to sampling time ratios (5 or less for the pulse used in the study) fold-over in the input caused a sudden and drastic deterioration in the recoverable frequency.

Simple numerical integration techniques were found to be equal to more sophisticated "analytical" integration techniques for calculating the ratio of Fourier transforms necessary to convert time domain pulse response data to frequency response data, even when the input and output sampling times were unequal. However, for unequal sampling times, considerable and unpredictable variation was found between the results of the analytical and numerical techniques. Because of this and because the results using unequal sampling rates were unpredictable even for a single integration technique, equal sampling rates are recommended for input and output. Results from equal sampling rates are not dependent upon the integration technique and proved much more predictable.

LITERATURE CITED

1. Black, Harold S. Modulation Theory. New York: D. Van Nostrand Company, Inc., 1953.

2. Clements, William C., Jr., "Pulse Testing for Dynamic Analysis," Ph.D. Dissertation, Vanderbilt University, 1963.

3. Dreifke, G. E., "Effects of Input Pulse Shape and Width on Accuracy of Dynamic System Analysis from Experimental Pulse Data," Sc.D. Thesis, Washington University, 1961.

4. Lees, Sidney and Ray C. Dougherty, "Refinement of the Pulse Testing Procedure Computer Limitations," October, 1964.

5. Lindorff, David P. Theory of Sampled-Data Control Systems. New York: John Wiley and Sons, Inc., 1965.

6. Papoulis, Athanasios. The Fourier Integral and Its Application. New York: McGraw-Hill Book Company, Inc., 1962.

7. Ragazzini, J. R. and G. F. Franklin. Sampled-Data Control Systems, McGraw-Hill Book Co., 1958.

8. Shannon. "The Philosophy of P. C. M.," Proceedings of I. R. E., November, 1948.

CHAPTER 4

NOISE EFFECTS IN FOURIER ANALYSIS

The two major sources of error in calculating Fourier transforms are (1) fold-over from sampling and (2) noise in the data. Chapter 4 will be devoted to the second problem - noise in the data. Noise enters the calculation through the input, $x(t)$, and the output, $y(t)$, which are included in the ratio of Fourier integrals used to calculate $G(j\omega)$, the system Fourier transform.

$$G(j\omega) = \frac{\int y(t)\ e^{-j\omega t}\ dt}{\int x(t)\ e^{-j\omega t}\ dt} \qquad 4.1$$

4.1 Defining the Maximum Recoverable Frequency

In order to make comparisons and correlations describing the effects of noise it was necessary to define the maximum recoverable frequency. This was achieved by applying the error criterion developed in Chapter 2 and using a value of 0.01.

$$\int_0^{T_P} \left(\frac{e_{cp}}{M_{cp}}\right)^2 dL\omega = 0.01 \qquad 4.2$$

where T_P = pulse duration

e_{cp} = difference in magnitude between calculated and true complex point

M_{cp} = magnitude of true complex point

$L\omega = \log_{10}$ of the frequency

This 0.01 value applies not only to the work done in this chapter but also to the results from other chapters that are applied in this chapter.

4.2 Noise Introduction and Characterization

By introducing a known amount of white noise into a system it should be possible to determine the effects of noise on the maximum recoverable frequency. In most cases the input will be relatively noise-free compared to the output, indicating most of the noise is picked up in the process. To simulate process conditions the approach taken was to add the noise to the output as diagrammed in Figure 4-1. Another point in favor of adding the noise to the output is that the output is attenuated by the process so that the same level of noise will have a much greater effect on the output than on the input.

A commonly used criterion for characterizing noise is its root-mean-square (RMS) value as defined in the following equation:

$$RMS = \sqrt{\frac{\sum_{i=1}^{N} (e_i^2)}{N}} \qquad 4.3$$

where e_i = the i^{th} value of noise

N = total number of noise values

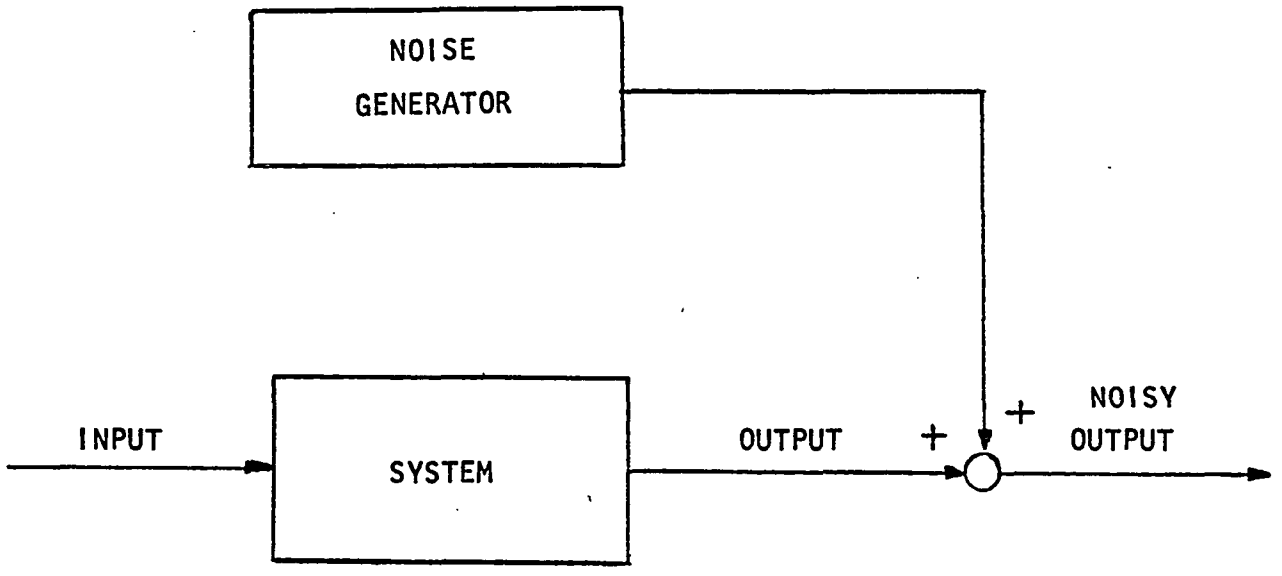

FIGURE 4-1. Addition of Noise to the System

This criterion was adopted and both positive and negative deviations were allowed. To see if the noise should be characterized by a time constant in addition to its RMS value, a test was made in which the noise was put through a first order lag before measuring its RMS value. The results are presented in Figure 4-2 where the recoverable frequency, ω_R, is plotted versus noise RMS value with the first order lag time constants of the noise as parameters. For a constant RMS value the recovery increases as the time constant increases, but the increase is not significant except for very large time constants at low noise levels. Furthermore, a time constant of zero was the most conservative case so that the RMS value alone appears to be a good criterion for measuring the noise.

4.3 The Effect of Noise

The system chosen for testing the effect of random noise was a first order lag (time constant = 0.1) because a first order lag plus dead time is a good approximation to many real systems and dead time does not affect the results. The input pulse was a ramp filtered by a first order lag and is shown in Figure 4-3. The results of the test are presented in Figure 4-4 where the fraction recovered - the ratio of the maximum recoverable frequency (as defined by the error criterion) to the theoretical maximum recoverable frequency (defined as one-half the sampling frequency) - is plotted versus noise RMS with sampling time as a parameter. The percentage recovery is very high at an RMS of zero (noise free system) where, as shown in Chapter 3 Section 3.2, the recovery

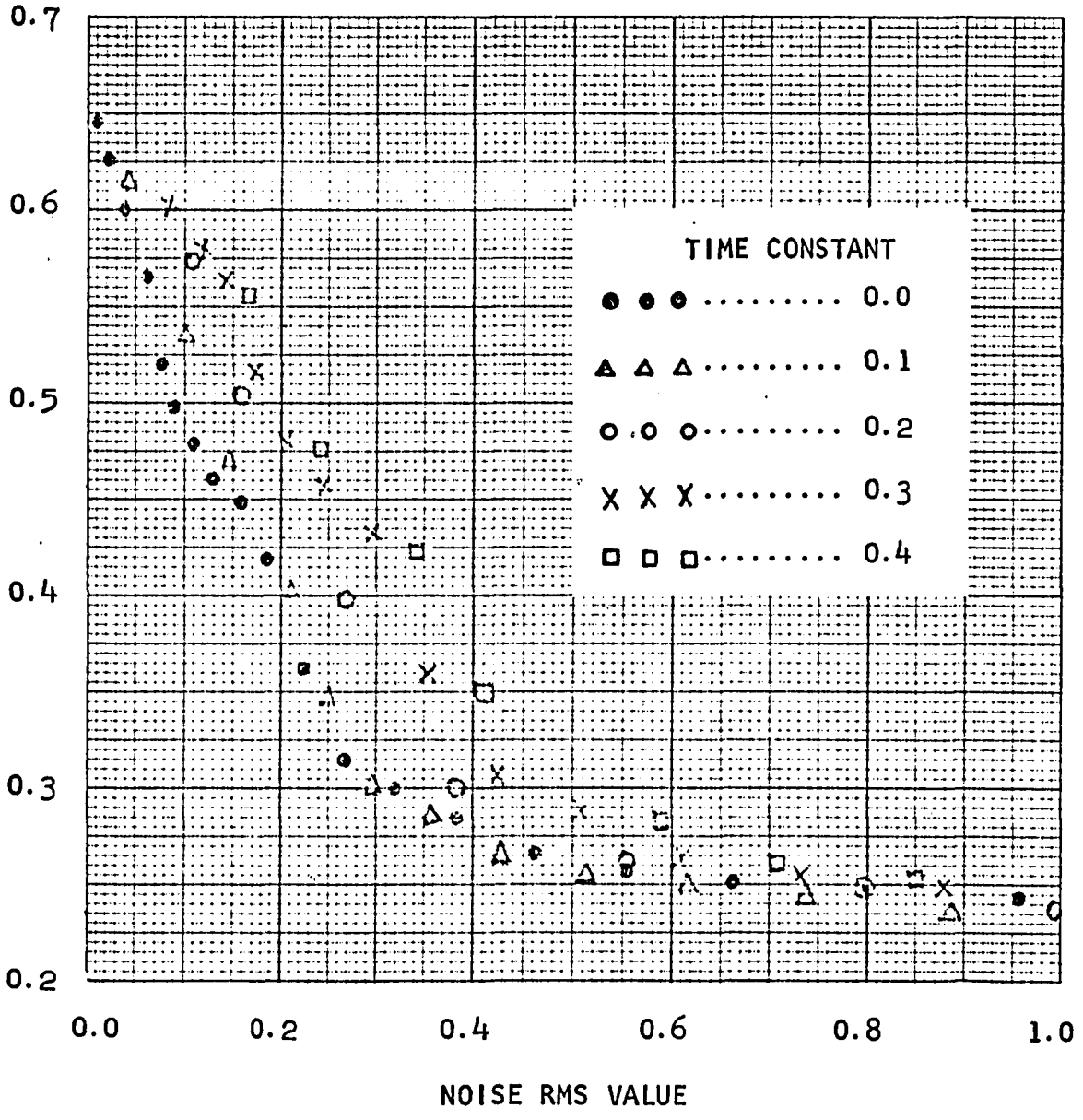

FIGURE 4-2. Comparison of the Effect of Filtered Noise on $\frac{\omega_R}{\omega_M}$ for Various Filter Time Constants. RMS Value Calculated after Filtering.

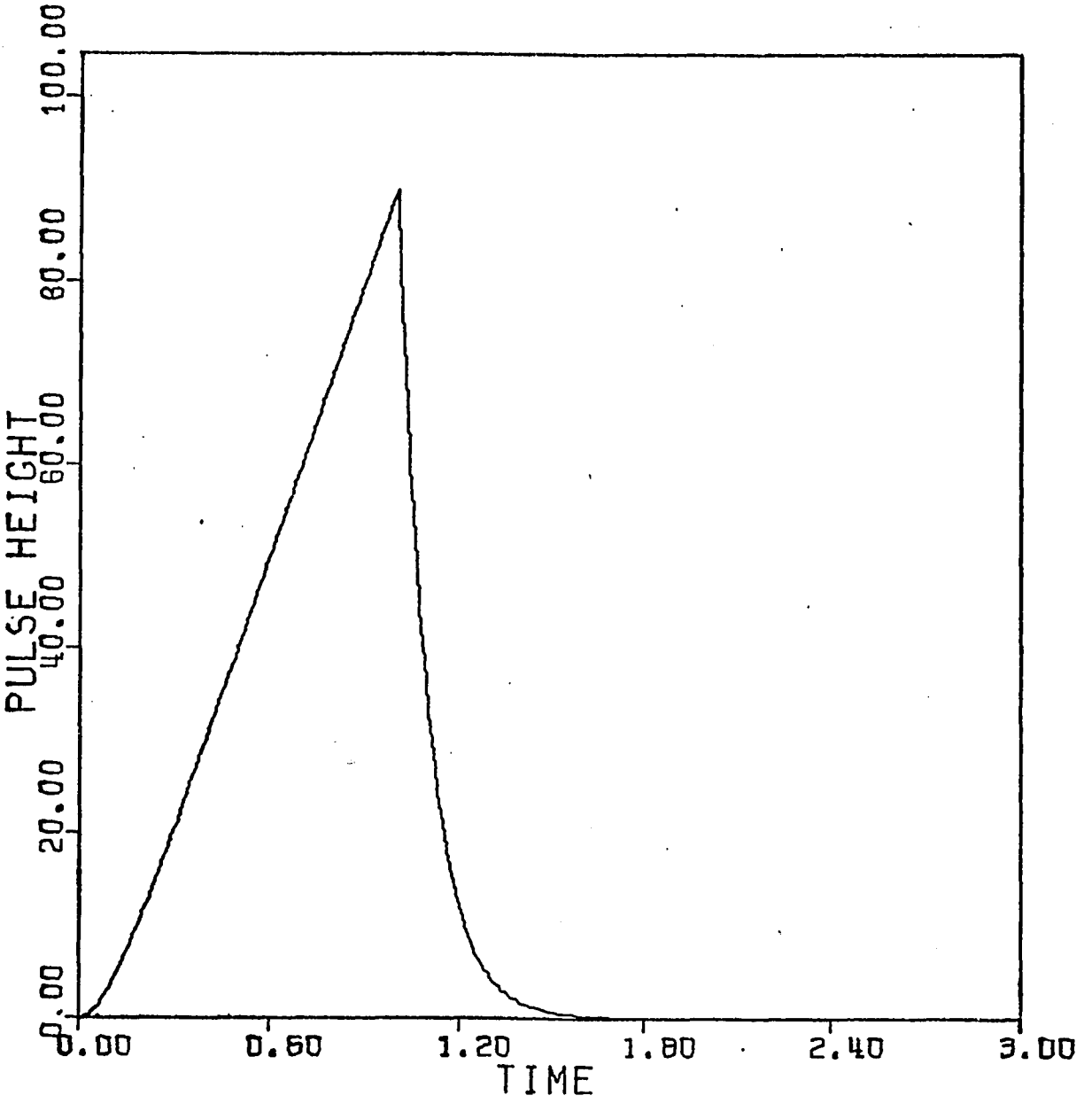

FIGURE 4-3. Ramp Pulse Filtered by a First Order Lag

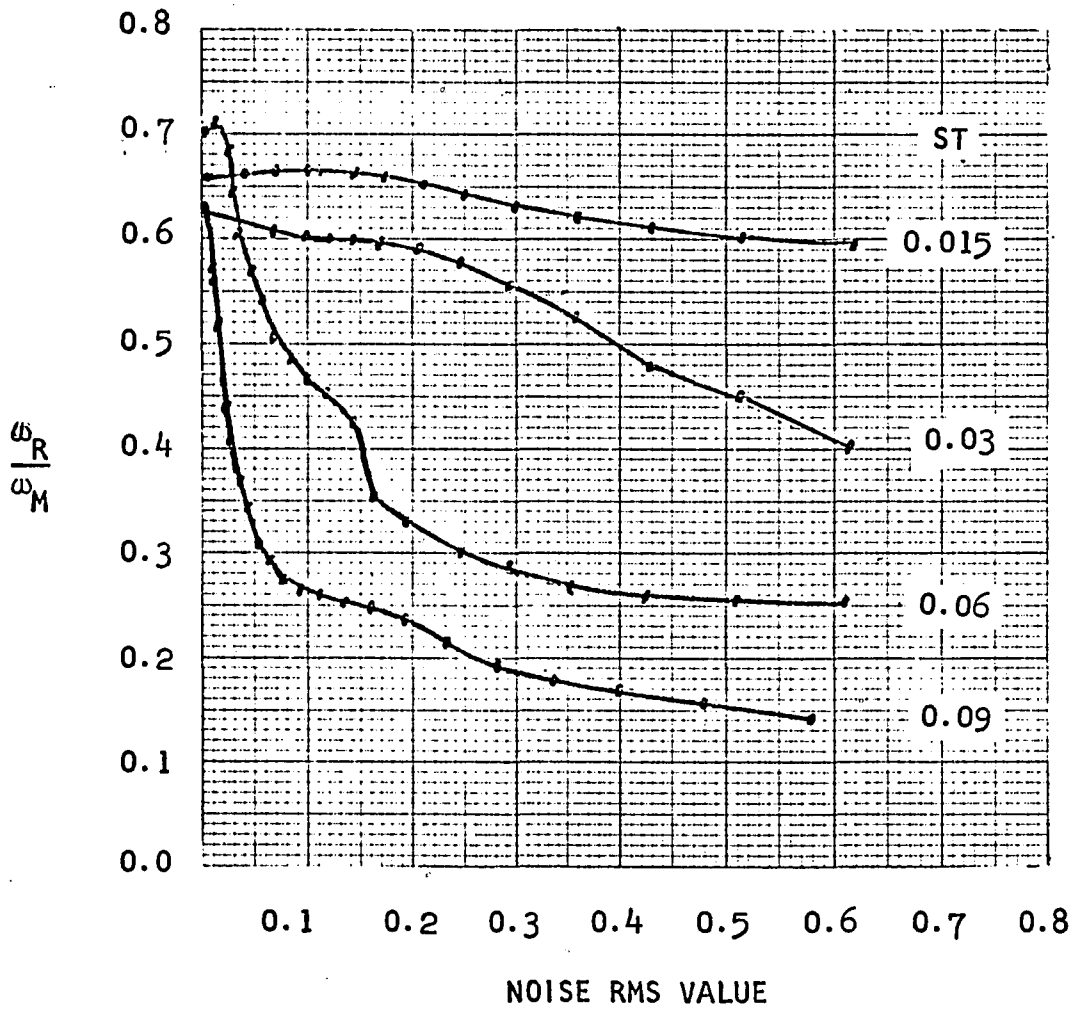

FIGURE 4-4. Effect of Noise on the Recoverable Fraction of the Theoretical Maximum Recoverable Frequency for Various Sampling Times.

averages 66%, a much higher figure than the 10% quoted by other investigators without regard to noise level. But as the noise RMS value increases there is a sharp decline in the recovery percentage for the faster sampling rates and, surprisingly, very little change at the slow sampling rates. It is clear that with the introduction of more than small levels of noise there is no longer a constant percentage recovery independent of sampling frequency.

4.4 Explaining the Noise Effects

Plotting recoverable frequency versus noise RMS value in Figure 4-5 provides more insight into the noise - sampling effect relationship. At low noise levels there is a considerable difference in the recoverable frequency for the various sampling frequencies, but as the noise level increases, the difference becomes much smaller. The obvious conclusion is that at low noise levels the fold-over effect from sampling is the controlling factor but as the noise level increases, noise soon becomes dominant. However, this does not fully explain why the fast sampling rates are affected so severely while the slow sampling rates are hardly affected. The key to this can be found in the plot of input pulse frequency content versus the log of the frequency, ω, given in Figure 4-6. Recall that the frequency content of the input pulse is the value of the input pulse Fourier transform.

$$\text{Frequency content} = \int_0^{T_P} x(t)\, e^{-j\omega t}\, dt \qquad 4.4$$

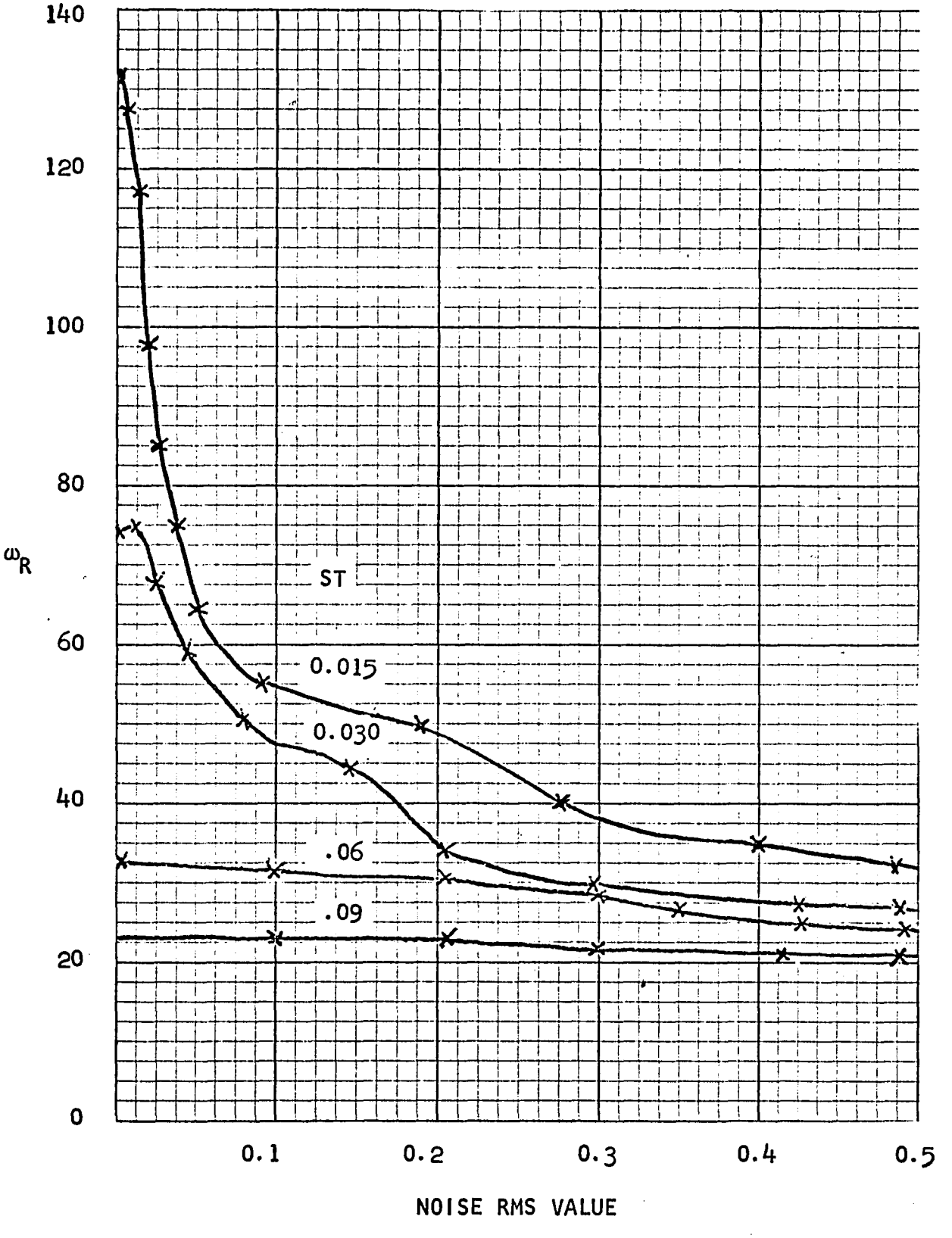

FIGURE 4-5. Effect of Noise on Maximum Recoverable Frequency for Various Sampling Times

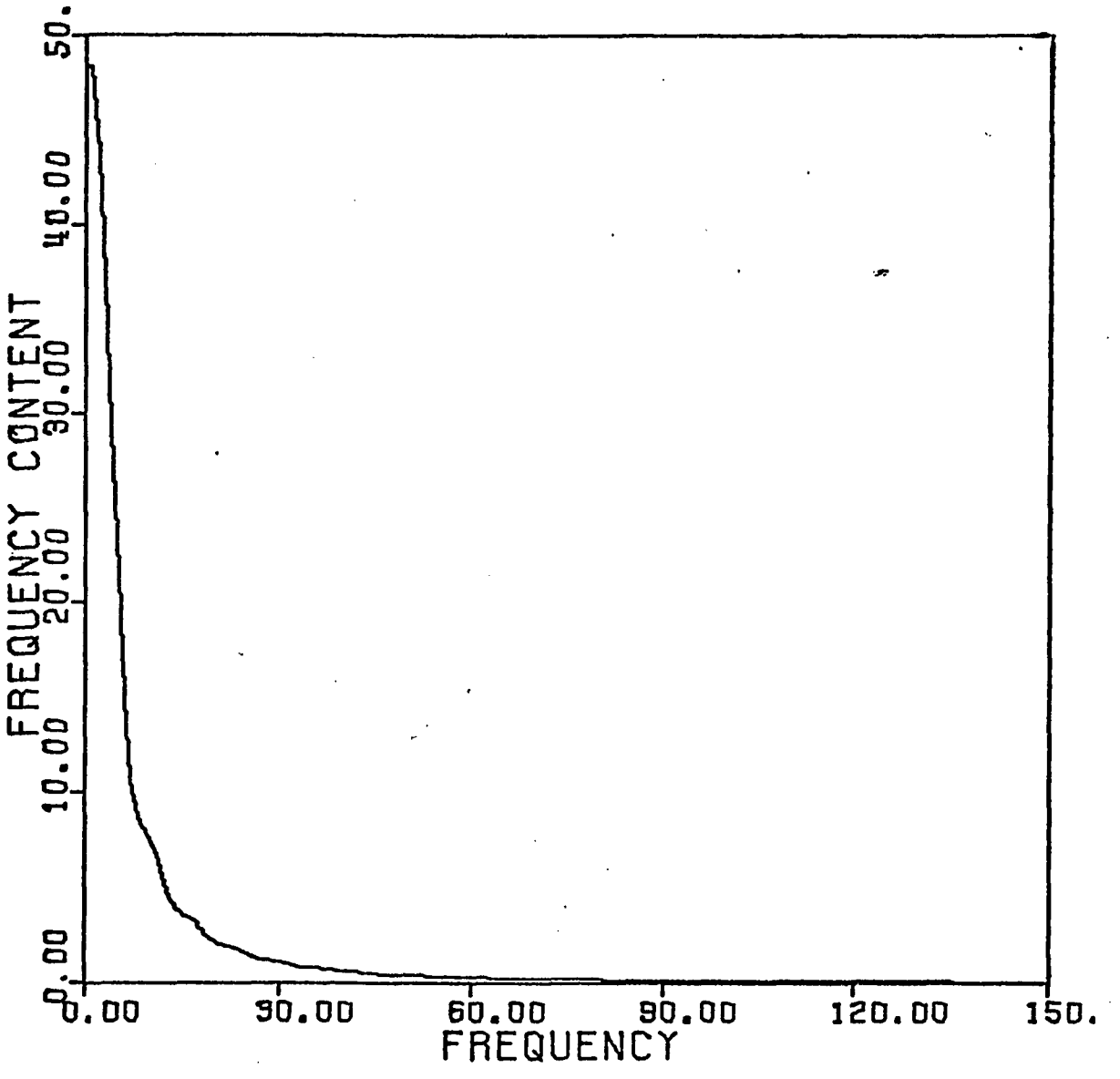

FIGURE 4-6. Input Pulse Frequency Content

With no noise the high sampling frequencies allowed recovery at high frequencies, where Figure 4-6 shows the frequency content curve has a small value and is relatively flat. Since the frequency content was low at the high frequencies, only a low level of noise was required to cause serious error in the Bode plot at high frequencies. This small frequency content value combined with the flatness of the curve permits low levels of noise to reduce the maximum recoverable frequency drastically. In contrast, the low sampling frequencies, even in the noise-free case, were recovering only low frequency information. Here, the input pulse frequency content is much higher and the frequency content curve has a much greater slope. As a result, the introduction of a small amount of noise did not seriously affect the recovery. This explanation assumes there is a relationship between noise level and frequency content at the blow-up frequency.

4.5 Correlating Noise RMS Value and Frequency Content

The existence of this relationship was proved by varying the frequency content of the input to give different recoverable frequency versus noise RMS plots at a given sampling frequency. The pulse chosen for the test was a cubed triangular pulse of unit height because this pulse shape has a frequency content which extends to high frequencies without encountering zeroes and the frequency content can be changed readily in a known manner. The equations for this pulse are given below and Figure 4-7 is a plot of the pulse for a unit height and a duration of 2 time units.

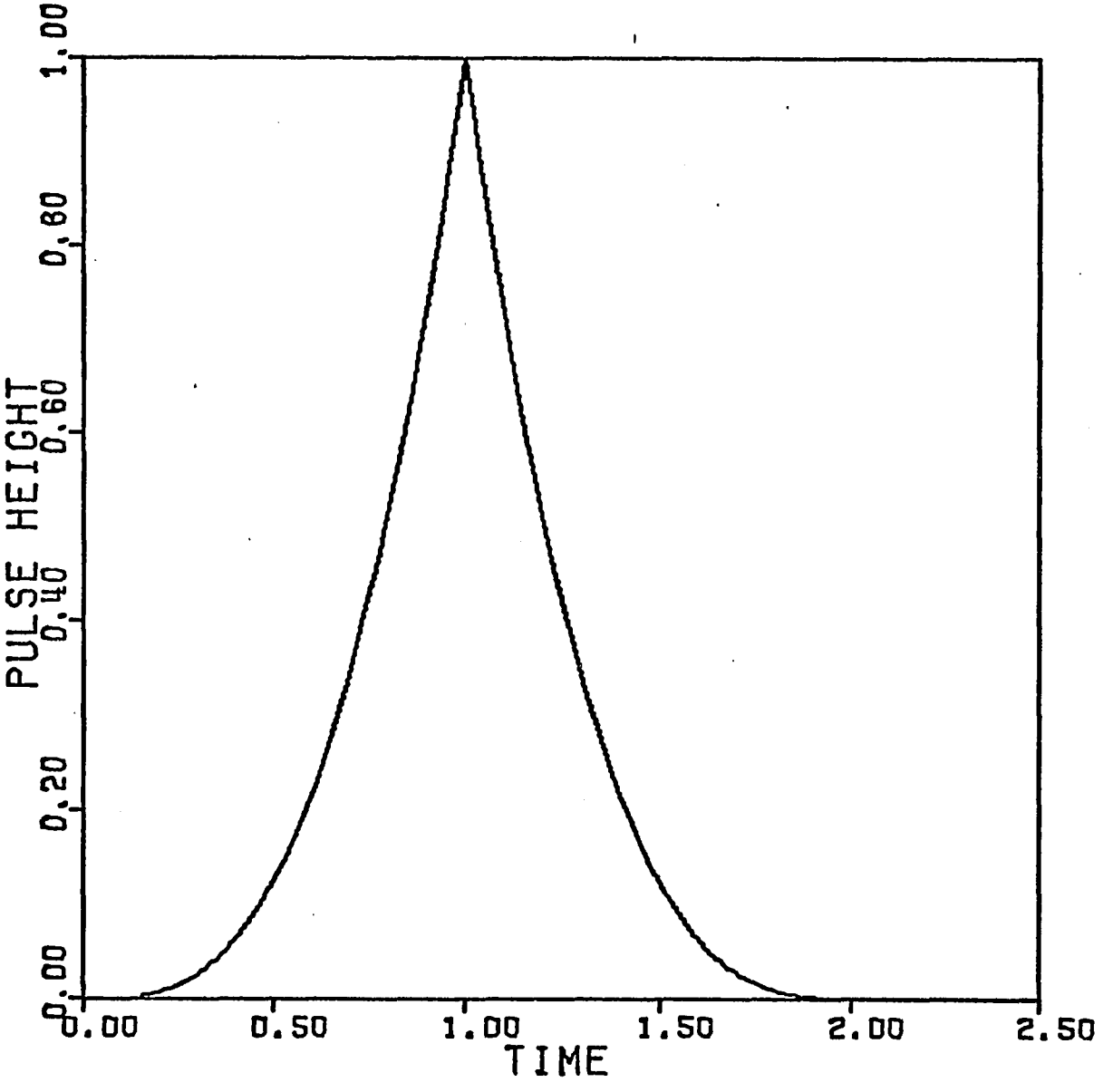

FIGURE 4-7. Cubed Triangular Pulse

$$x(t) = 8\,\frac{t^3}{T_P^3} \qquad 0 \le t \le \frac{T_P}{2} \qquad 4.5$$

$$x(t) = 8\,\left(1 - \frac{t}{T_P}\right)^3 \qquad \frac{T_P}{2} < t \le T_P \qquad 4.6$$

where T_P = pulse duration

The frequency content was varied by varying the pulse duration, T_P, and for most of the frequencies of interest, halving the pulse duration doubled the frequency content. To isolate the noise effect a high sampling frequency (1256 radians/sec) relative to the frequencies of interest ($\omega < 130$ radians/sec) was used to reduce the fold-over to a negligible point. The system used for the test was a first order lag with a time constant of 0.1.

Five different pulse durations were used in the test with the initial pulse duration equal to 2.0 time units and each succeeding pulse duration equal to 1/2 the preceeding duration. Thus the fifth pulse had a duration 1/16 as long as the first, giving the fifth pulse a frequency content 16 times as large as the first at the frequencies of interest. This provided a wide range of frequency content values at each frequency under consideration. Figure 4-8 reveals that there is a considerable change in the noise RMS versus recoverable frequency, ω_R, plot as the frequency content of the input changes. For a given noise level the recoverable frequency increased with increasing frequency content. As was to be expected since the noise was added to the

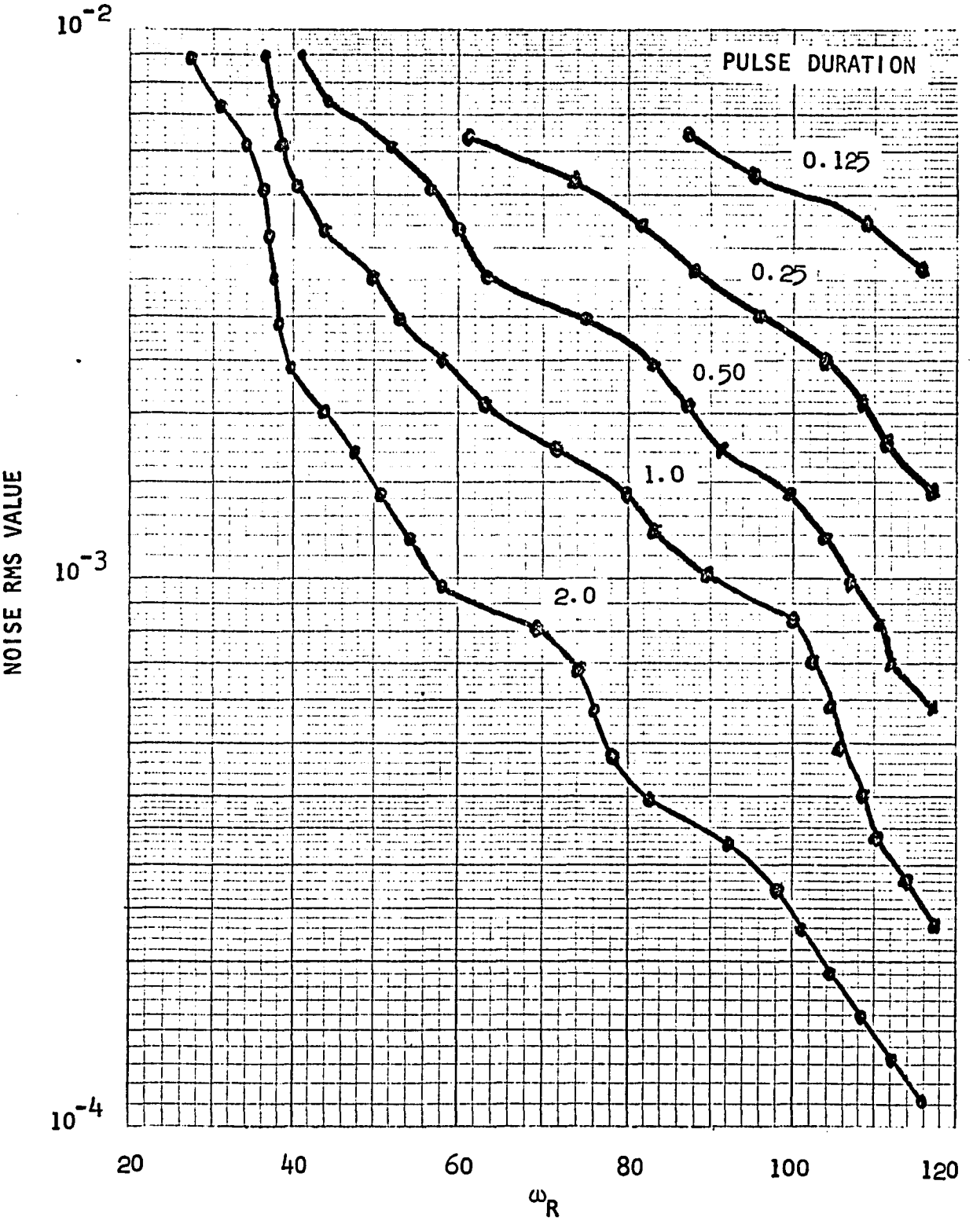

FIGURE 4-8. Effect on the Maximum Recoverable Frequency Versus Noise RMS Value Plot of Varying the Input Pulse Duration. Sampling Time of 0.005.

output (for the reasons given earlier in Section 4.2), the output transform always deteriorated at a lower frequency than the input transform. Consequently, the best correlation among recoverable frequency, noise level, and frequency content was found using the output frequency content. Plotting noise RMS versus the output frequency content of the maximum recoverable frequency (defined by the 0.01 error criterion value) on a log-log plot produced the correlation shown in Figure 4-9. This plot indicates that the relationship between noise RMS and frequency content is described by the equation:

$$\log \text{RMS} = b \log \text{FCO} + \log a \qquad 4.7$$

where FCO = frequency content of the output pulse at the maximum recoverable frequency, ω_R.

a,b = constants

Rearranging,

$$\frac{\log \frac{\text{RMS}}{a}}{\log \text{FCO}} = b \qquad 4.8$$

Since

$$\text{FCO} = |Y(j\omega_R| \qquad 4.9$$

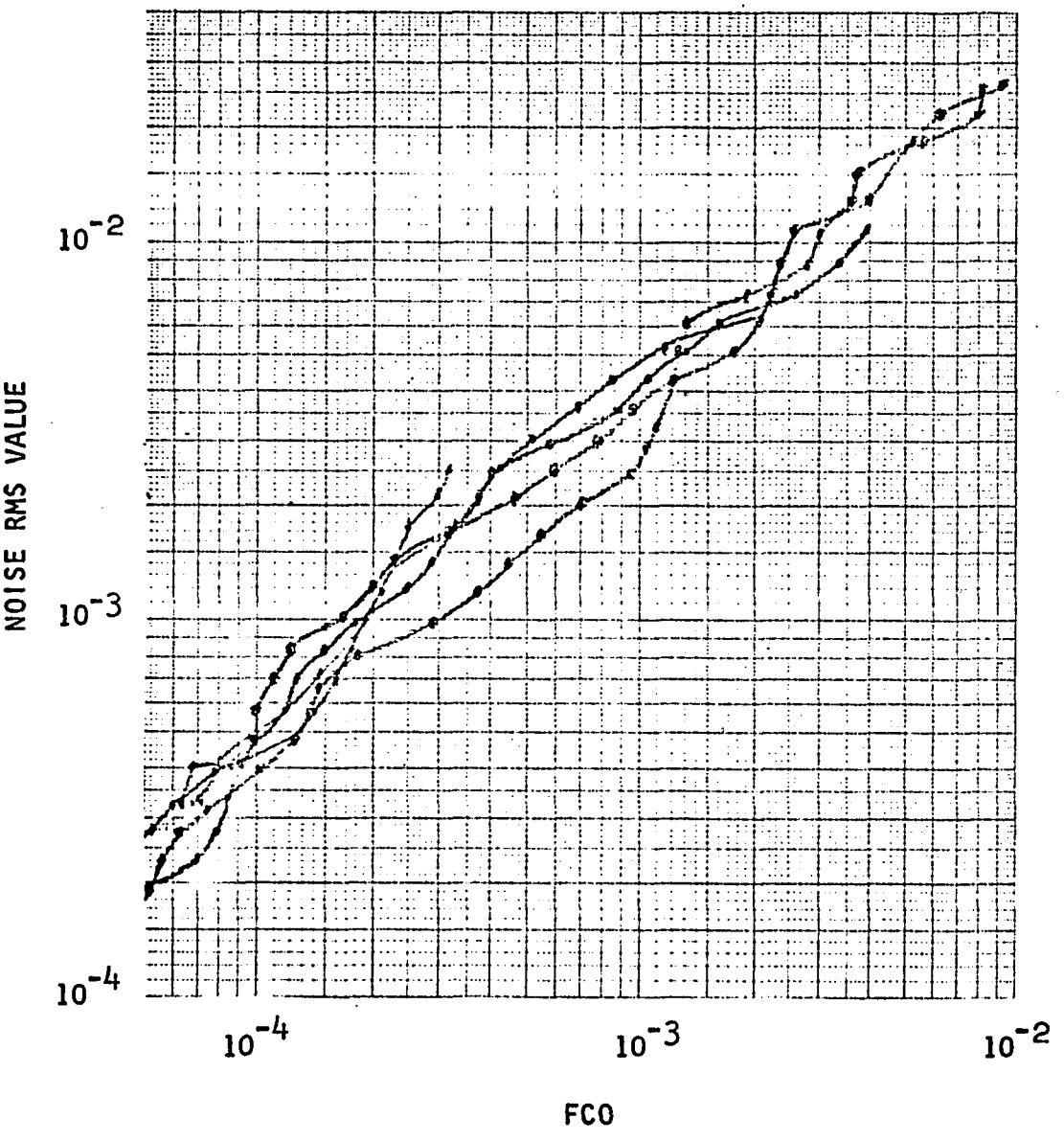

FIGURE 4-9. Noise RMS Value Versus the Frequency Content of the Output Pulse at the Maximum Recoverable Frequency. Sampling Time of 0.005.

Equation 4.8 can be written as

$$\frac{\log \frac{RMS}{a}}{\log |Y(j\omega_R)|} = b \qquad 4.10$$

Recalling that the LaPlace transform of the output, Y(S), is related to the LaPlace transform of the input, X(S), by the transfer function G(S) in the following manner

$$Y(S) = G(S)\ X(S) \qquad 4.11$$

Equation 4.10 can be written

$$\frac{\log RMS}{\log |G(j\omega_R)\ X(j\omega_R)|} = b \qquad 4.12$$

This shows the futility of attempting to correlate noise level with just the input frequency content because the effect of $G(j\omega_R)$ is considerable.

The correlation in Figure 4-9 is for a high sampling frequency which effectively removes the fold-over effect. To see how the correlation is affected when a lower, more practical sampling frequency is used, the test was repeated for sampling times of 0.015 time units (209 radians/time unit) and 0.03 time units (105 radians/time unit). (The corner frequency of the system is at 10 radians/time unit.) The shortest duration pulse (0.125 time units) was omitted because the pulse duration to sampling time

ratio was too low for the 0.03 sampling time and somewhat questionable for the 0.015 sampling time. Figures 4-10 and 4-11 show the results. Even with fold-over effects from sampling present, a straight line correlation between log RMS and log FCO is obtained in both cases; however, although the slopes are approximately equal there is an offset due to the sampling frequency. For a given noise level and frequency content, increasing the sampling frequency reduces the fold-over and increases the recoverable frequency. Figure 4-12 shows a comparison of the straight line approximations for the three cases (ST = 0.005, 0.015, 0.03). The frequency content values used are the analytical frequency content values at the maximum recoverable frequency. Because of the fold-over effect, frequency content values calculated numerically from the data points vary with sampling frequency for a given pulse. Figure 4-13 shows a comparison of output frequency content curves calculated numerically and analytically. For the output pulses derived from very short duration input pulses the frequency content curve calculated numerically deviates considerably from the true analytic curve. Using the true analytic value of frequency content for the correlation of RMS and FCO was more conservative than using the numerically calculated values because for the cases used here the numerically calculated values were lower. In most cases the discrepancy between numerical and analytic values will not be serious but the existence of the discrepancy should be noted.

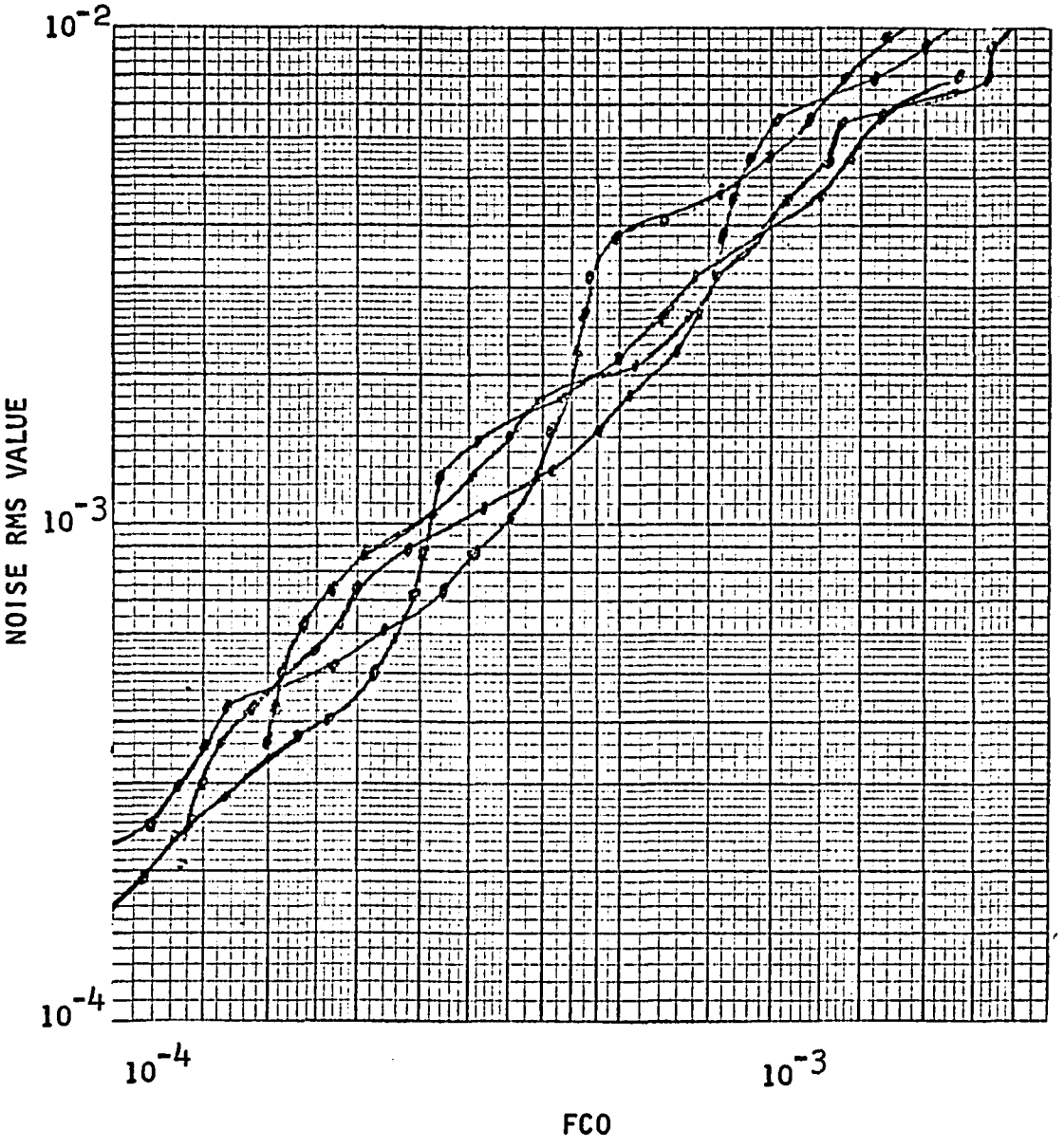

FIGURE 4-10. Noise RMS Value Versus the Frequency Content of the Output Pulse at the Maximum Recoverable Frequency. Sampling Time of 0.015.

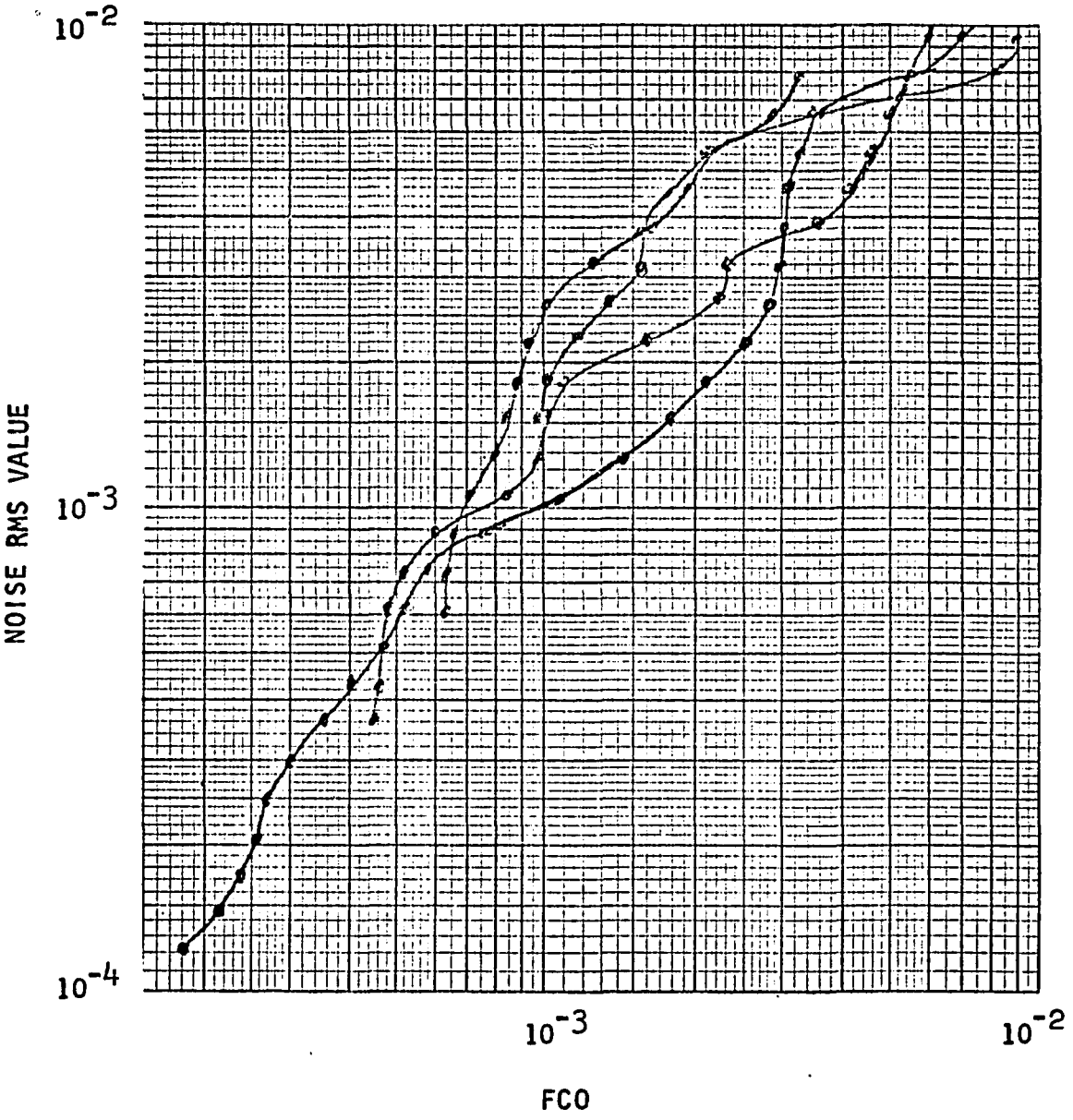

FIGURE 4-11. Noise RMS Value Versus the Frequency Content of the Output Pulse at the Maximum Recoverable Frequency. Sampling Time of 0.03.

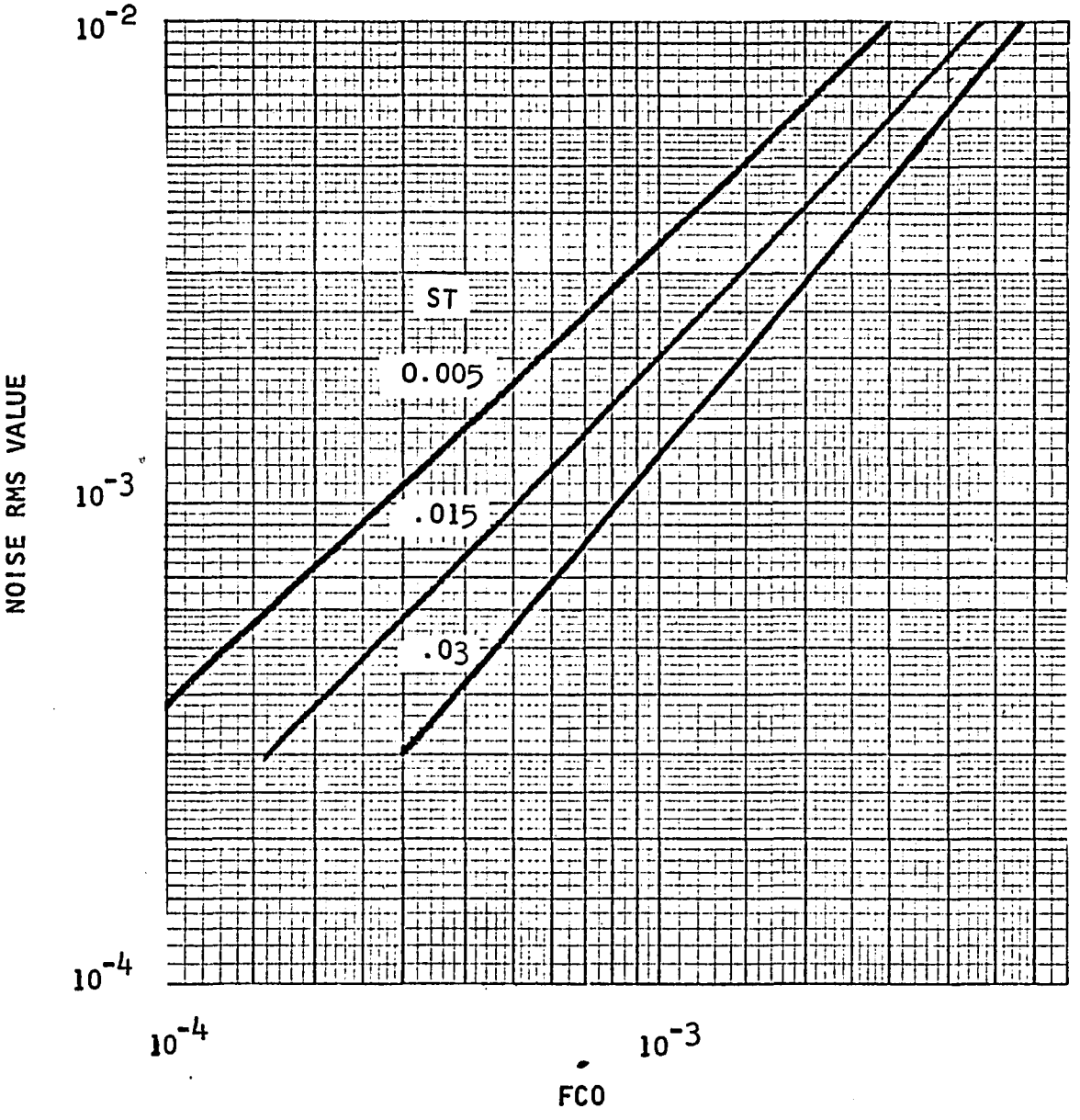

FIGURE 4-12. Comparison of the Straight Line Approximation to the Noise RMS Value Versus the Frequency Content of the Output Pulse at ω_R for Three Sampling Times.

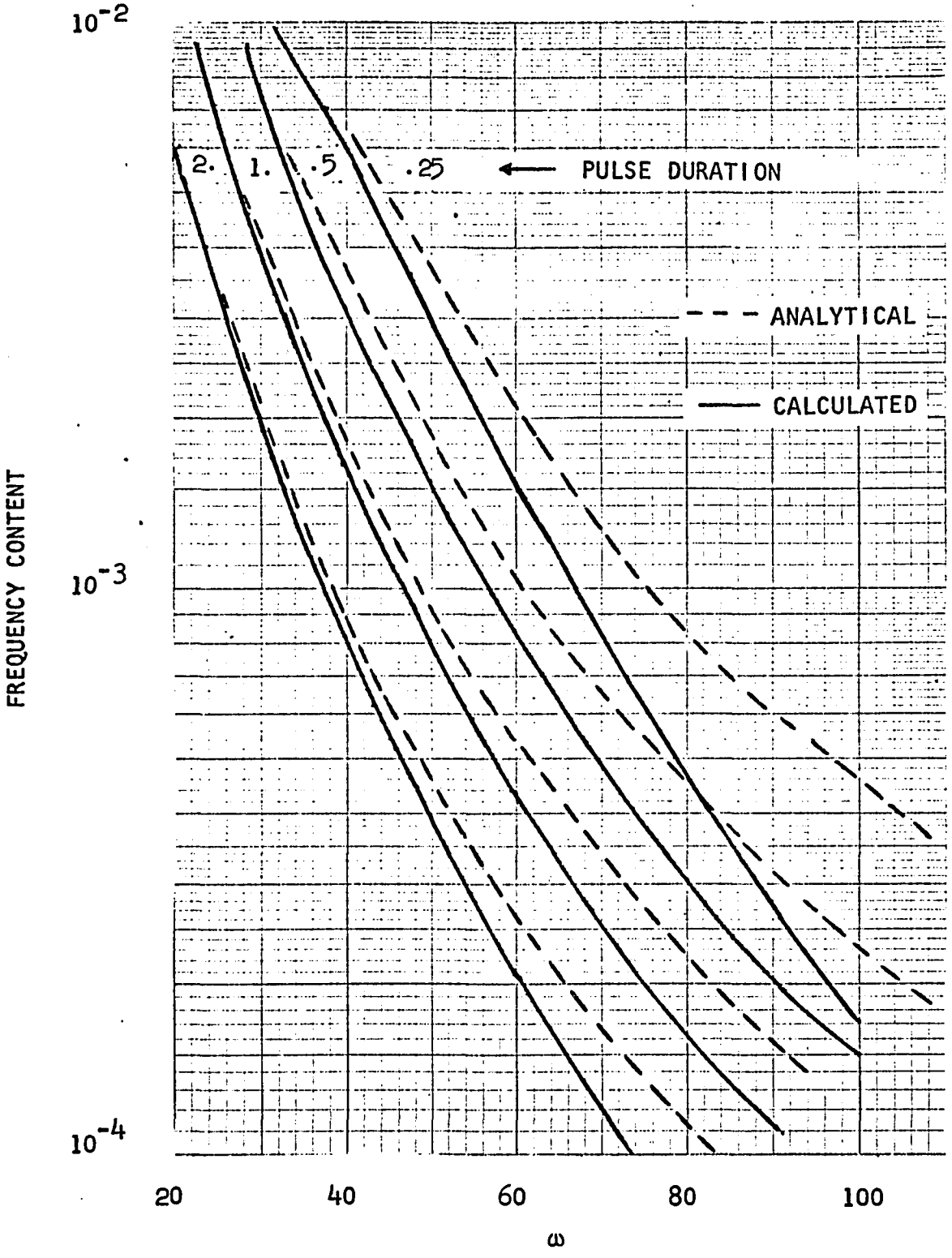

FIGURE 4-13. Comparison of Analytical with Calculated Frequency Content Curves for the Output Pulse. Sampling Time of 0.03.

4.6 Frequency Content

The importance of frequency content has been established and discussion in greater detail is warranted. Previously, the normalized frequency content has been considered by many people as perhaps the most important consideration in determining the maximum recoverable frequency, but the correllations of Figures 4-9, 4-10, and 4-11 show that the actual frequency content is the real quantity of interest and there is a difference. The normalized frequency content is the frequency content at any given frequency, ω, divided by the frequency content at $\omega = 0$, where the frequency content is a maximum. Thus the normalized frequency content begins at one. An example will vividly point out the difference between the two quantities. As stated earlier, one way to increase the frequency content of a pulse at its higher frequencies is to shorten the pulse duration. Using the pulse with Equations 4.5 and 4.6 the effect on the normalized frequency content of halving the pulse duration is shown by plotting the normalized frequency content for pulse durations of 1.0 and 0.5 in Figure 4-14. Note that both pulses begin at 1.0, but that the short duration pulse soon has a value much greater than the long duration pulse. Now observe the effect of halving the pulse duration when the same two pulses are used and the actual frequency content is plotted in Figure 4-15. While decreasing the pulse width increases the frequency content at high frequencies, the initial effect is to decrease the frequency content by the factor that the pulse width is decreased. If this

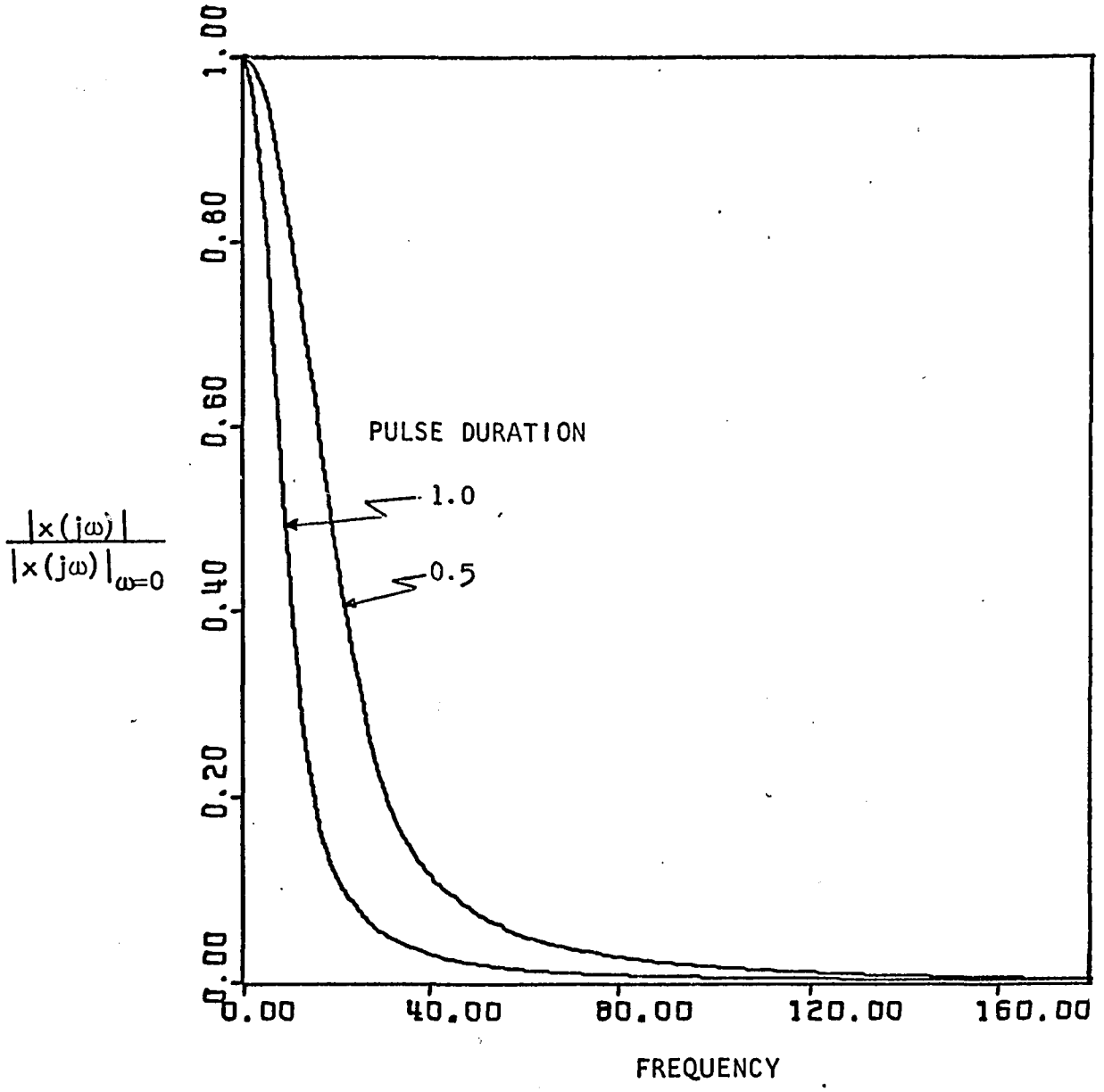

FIGURE 4-14. Effect on the Normalized Frequency Content of Halving the Pulse Duration

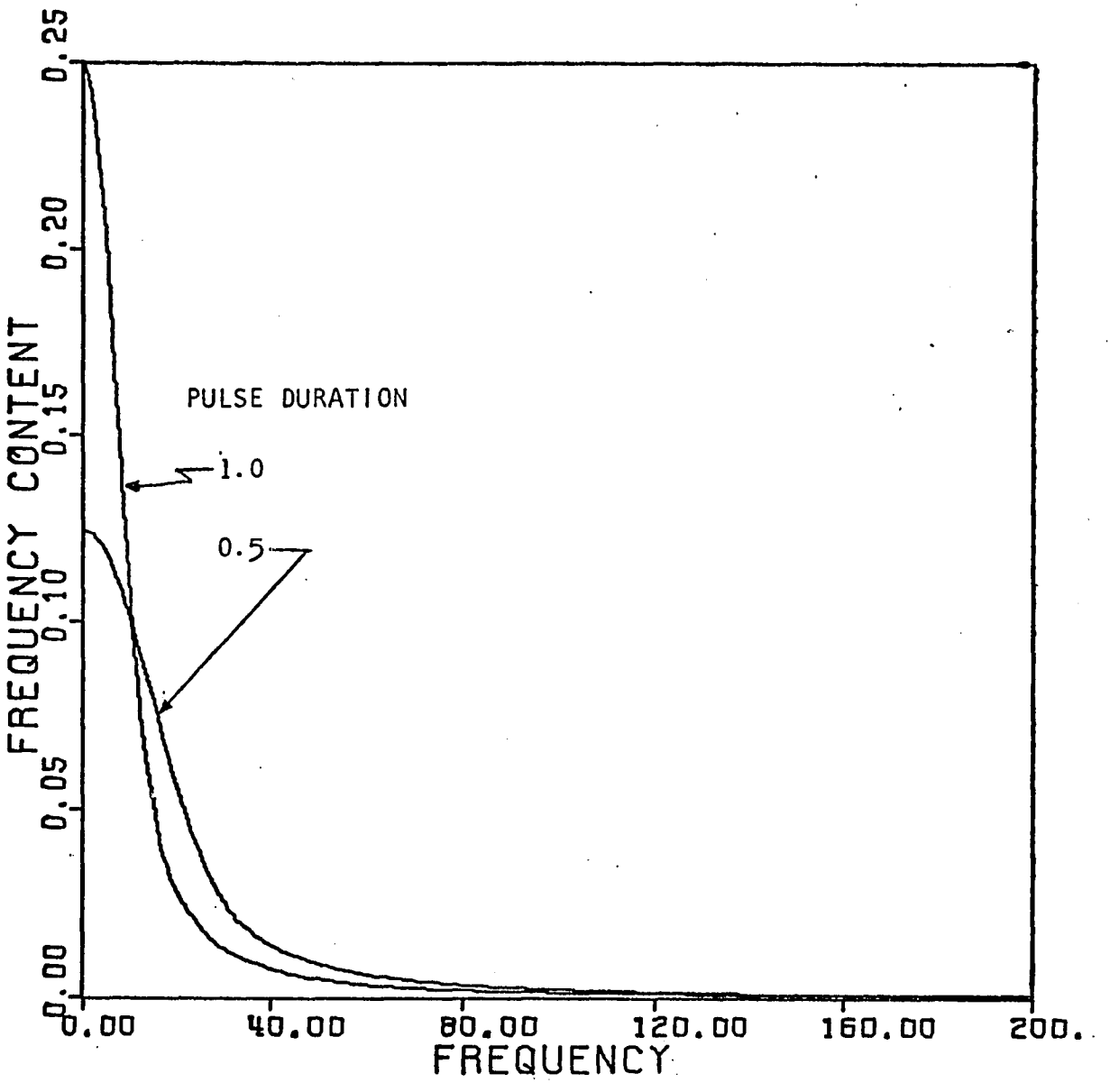

FIGURE 4-15. Effect on the Frequency Content of Halving the Pulse Duration

is carried to an extreme, the initial value of the frequency content could be below the value required by the noise level for information recovery so that no information could be recovered. A related observation was made in data calculated for this chapter. Apparently, at low frequencies (below the corner frequency), higher than normal frequency content to RMS ratios are required. For high noise levels the recovery was poor at low frequencies and much better at higher frequencies below the blow-up frequency. As the pulse duration decreased, the obscured frequencies persisted to higher and higher values. Although the shorter pulses helped the recovery at high frequencies, there was a harmful effect at low frequencies. This points out the danger that attempting to "overkill" with an extremely short pulse width may actually be detrimental at the frequencies of interest.

Besides pulse duration there are two other methods for increasing the frequency content. One is to increase the pulse height. The limitation here is that if too large a pulse height is used then the response of the system is not even approximately linear. The other method is to select a pulse shape with a larger frequency content at high frequencies. Clements (1) provides a plot showing the relative frequency contents of several pulse shapes.

4.7 Noise and Sampling Frequency Constraints

With Figure 4-12 and information developed in Chapter 3 on sampling effects, the constraints on recoverable frequency imposed

by noise and sampling frequency can be predicted. An example will provide a good illustration of how this works. For the example a given noise level and sampling frequency will be chosen and four input pulses, each with a different frequency content will be used. The pulses will be chosen so that both the noise and sampling frequency constraints will be explored. Equations 4.5 and 4.6 describe the input pulse and durations of 2.0, 1.0, 0.5, and 0.25 were used. The sampling time was 0.03, the noise level was RMS = 0.000515, and the system was a first order lag with a time constant of 0.1. Figure 4-12 predicts that for a noise level of RMS = 0.000515 and a sampling time of 0.03, a frequency content in the output pulse of 0.00047 is the minimum for information recovery. In Chapter 3 Section 3.2, for the noiseless case the average percentage recovery of the theoretical maximum recoverable frequency was found to be 66% (based on the 0.01 error criterion value adopted as the standard for this chapter). The predicted sampling frequency limit is, therefore,

$$0.66\ \left(\frac{\pi}{0.03}\right) = 69\ \frac{\text{radians}}{\text{time unit}} \qquad 4.13$$

The two constraints for information recovery are 1) the frequency content of the output must be at least 0.00047 and 2) the frequency cannot be greater than 69 radians/time unit. Figure 4-16 is a plot of the output frequency content for the 4 pulses and the two constraints are marked on the plot by dotted lines. The circles indicate the actual blow-up points on the output frequency content

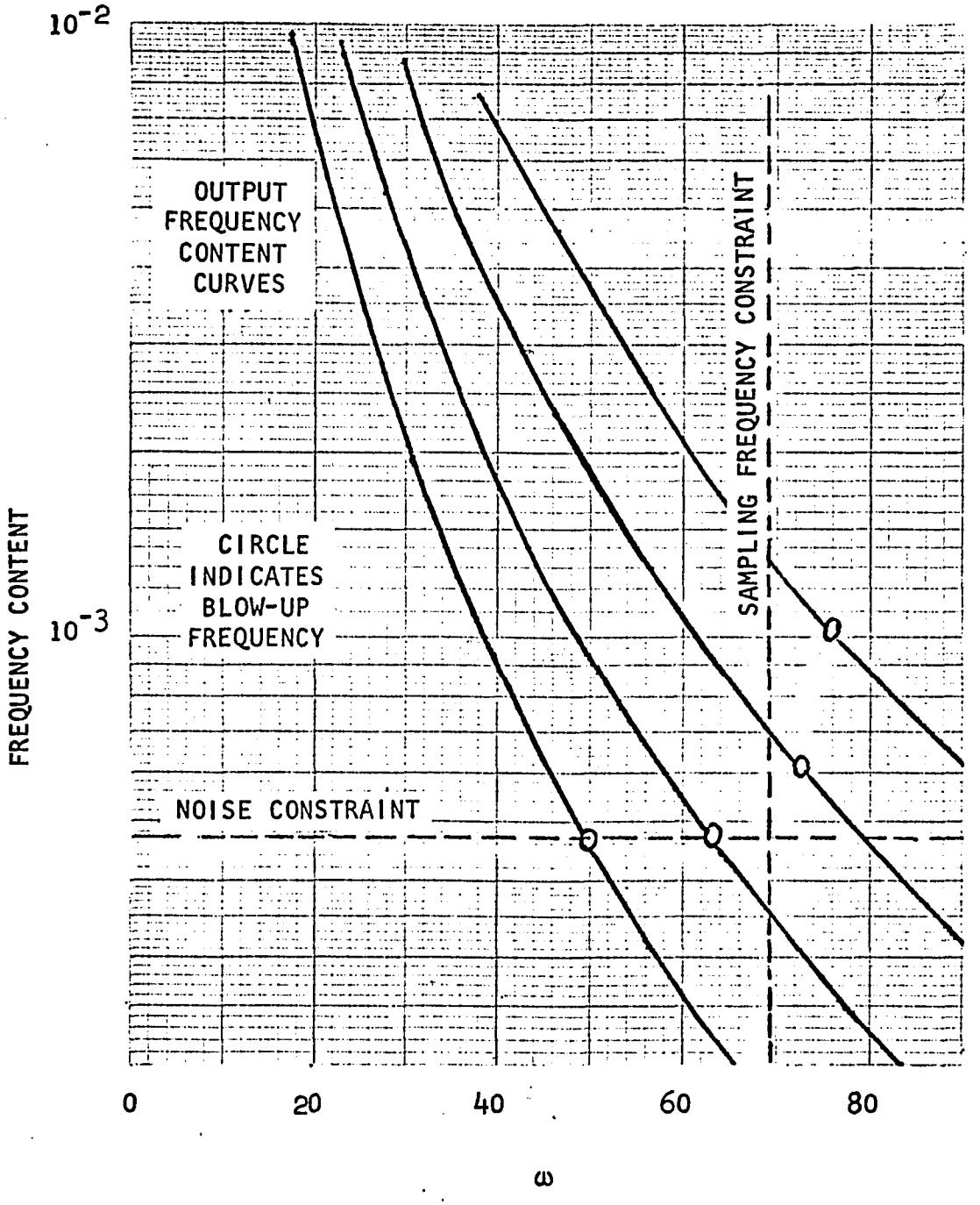

FIGURE 4-16. Use of Constraints to Predict Maximum Recoverable Frequency

curves and show that the constraints adequately predict the maximum recoverable frequency.

4.8 Conclusions

Noise was shown to cause significant reductions in the maximum recoverable frequency for high sampling frequencies and to have a much less severe effect on low sampling frequencies. This was explained by the shape of the frequency content curve and postulating the existence of a relationship between the noise level and the frequency content at the maximum recoverable frequency. The existence of this relationship was proved by the results presented in Figure 4-8 and graphs showing the relationship were plotted in Figures 4-9, 10, 11, and 12. It was shown that for a given sampling frequency the RMS value of the noise was related to the frequency content of the output pulse (FCO) by the following equation:

$$\log \text{RMS} = b \log \text{FCO} + \log a \qquad 4.14$$

The constant "a" was found to vary noticeably with sampling frequency while the constant "b" changed very little with sampling frequency. The noise constraint developed in this chapter coupled with the sampling frequency constraint developed in Chapter 3 adequately predicted the maximum recoverable frequency. It was shown how shortening the pulse duration to increase the frequency content could have the opposite effect at the frequencies of interest.

LITERATURE CITED

1. Clements, William C., Jr., "Pulse Testing for Dynamic Analysis," Ph.D. Dissertation, Vanderbilt University, 1963.

2. Dreifke, G. E., "Effects of Input Pulse Shape and Width on Accuracy of Dynamic System Analysis from Experimental Pulse Data," Sc.D. Thesis, Washington University, 1961.

3. Schnelle, Karl B., Jr., "Experiments to Illustrate the Dynamic Testing of Chemical Process Systems," Report supported by Grant Number G-22952 of the Science Teaching Equipment Development Program, Course Content Improvement Section, Division of Scientific Personnel and Education of the National Science Foundation, 1965.

4. Vincent, George C., "On the Dynamic Response of a Baffled Shell and Tube Heat Exchanger to Shell Flow Disturbances," Master's Thesis, St. Louis University, 1960.

CHAPTER 5

FILTERING AND SIGNIFICANT FIGURE EFFECTS IN FOURIER ANALYSIS

This chapter will be concerned with some practical aspects of computing Fourier transforms. The use of filtering, both pre- and post-sample, to improve information recovery will be examined, and the effect of significant figures, both in the data and in the computer, will be studied. The error criterion used to determine the maximum recoverable frequency is given by Equation 4.2.

5.1 Post-Sample Filtering

Figures 5-1 and 5-2 illustrate two ways to apply filtering: 1) filtering the continuous signal, i.e. pre-sample filtering; and 2) filtering the sampled data, i.e. post-sample filtering. In many instances the most convenient method would be post-sample filtering, and for some systems continuous filtering of certain variables would be virtually impossible (for example, composition determined via a chromatograph). Furthermore, post-sample filtering would allow the data to be collected without any special procedures or equipment. As this method is very appealing, tests were set up to evaluate it.

A first order lag system (time constant = 0.1), excited by the lagged ramp input pulse shown in Figure 5-3, was used for the evaluation test. To the discrete input and output data first order lag filters were applied with the time constant of the input filter

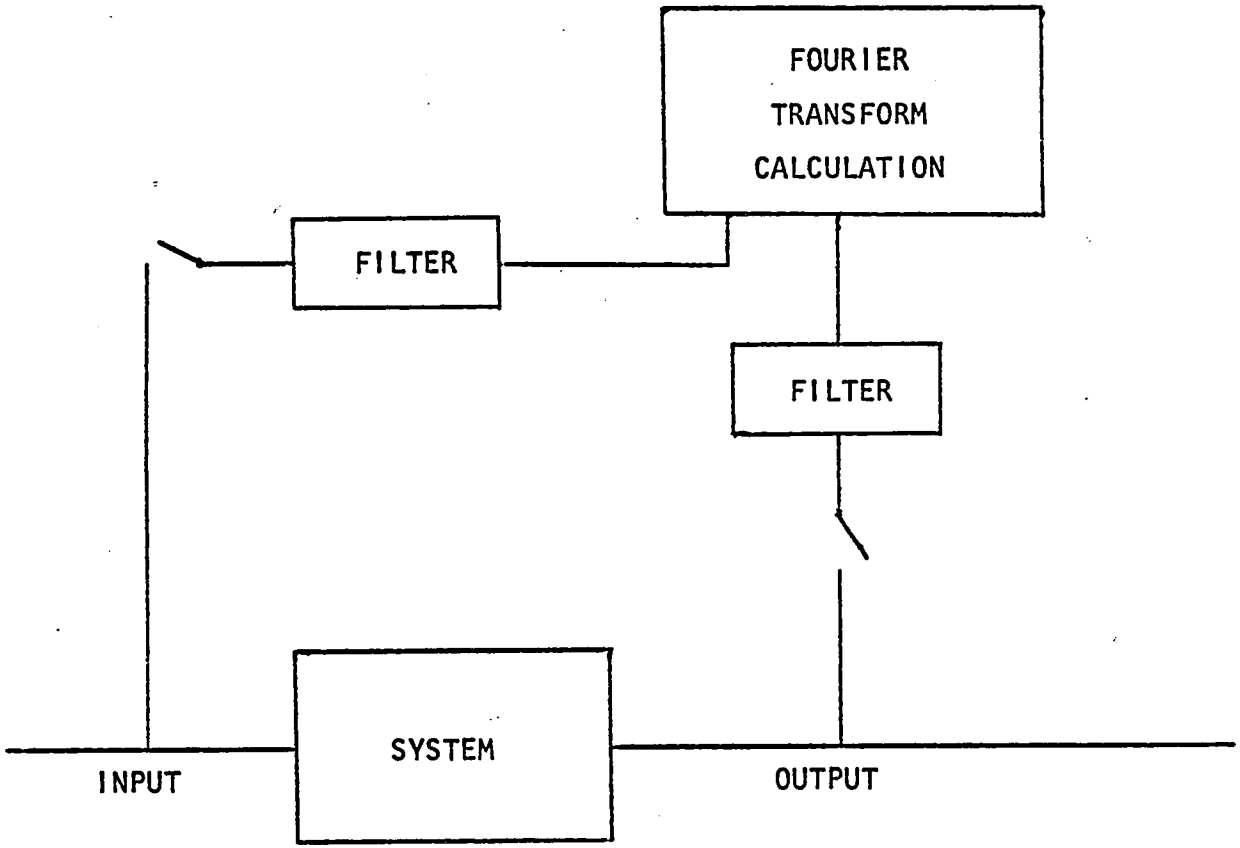

FIGURE 5-1. Post-Sample Filtering

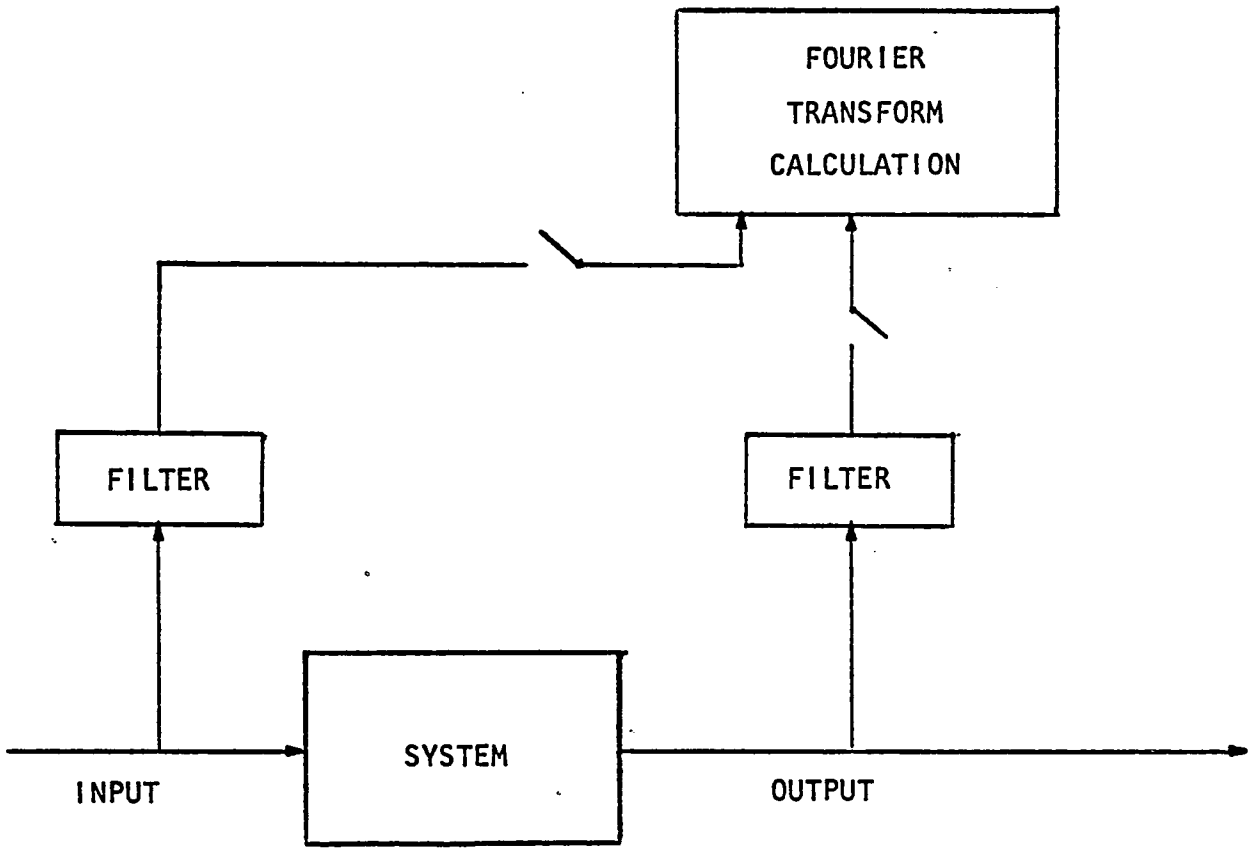

FIGURE 5-2. Pre-Sample Filtering

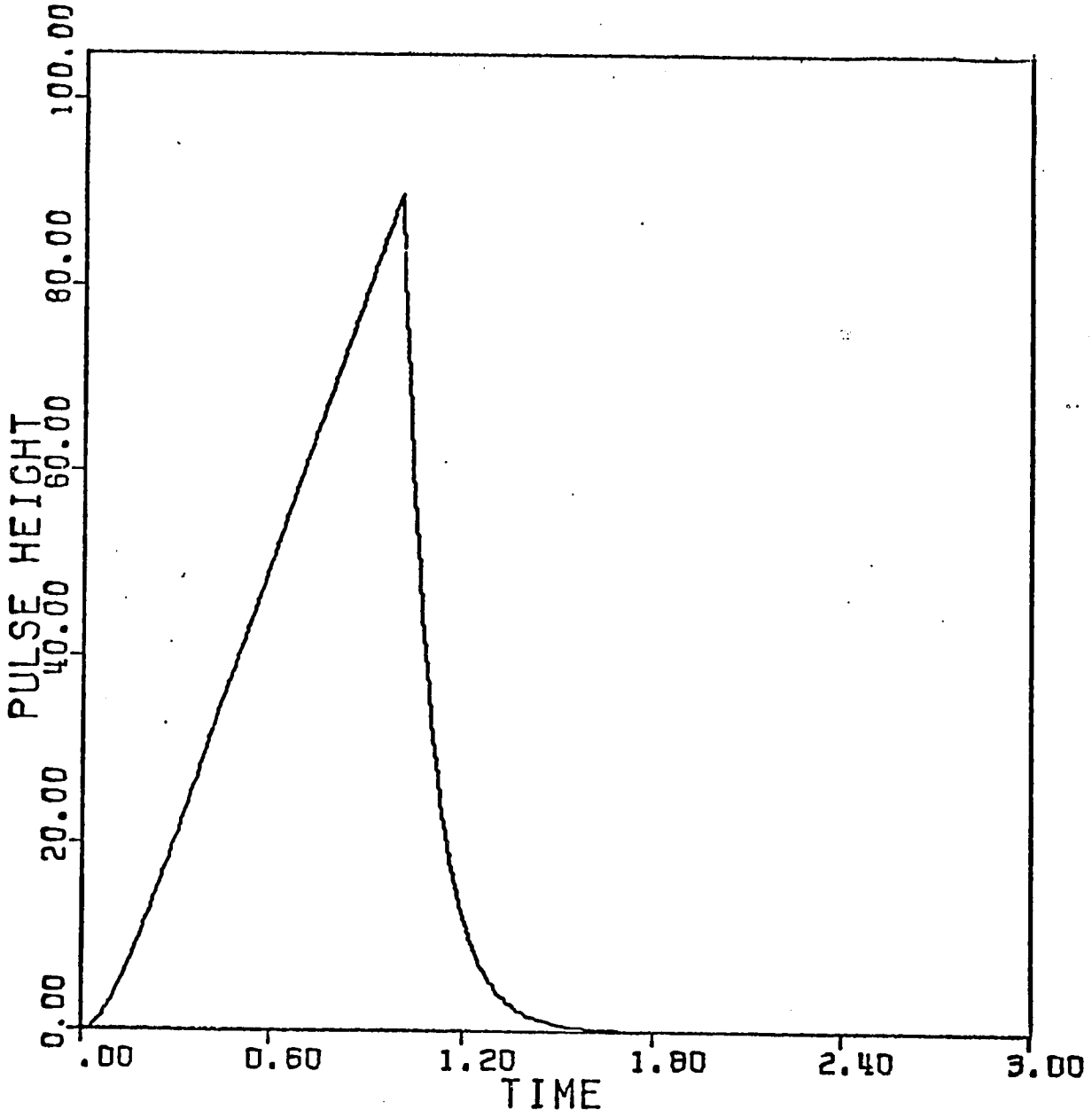

FIGURE 5-3. Lagged Ramp Input Pulse

equal to the time constant of the output filter so that the dynamics of the filters canceled in the transfer function calculation. The first order lag filter was implemented by three methods. One method used the simple numerical filtering equation

$$Y_f[(i+1)\Delta t] = Y_f[i\Delta t] + (Y[(i+1)\Delta t] - Y_f[i\Delta t]) \frac{\Delta t}{\tau_f} \quad 5.1$$

where $Y[i\Delta t]$ = unfiltered data value

$Y_f[i\Delta t]$ = filtered data value

Δt = time increment between data points

τ_f = filter time constant.

A second method used the same equation form but the Δt increment was subdivided into 100 increments and a straight line approximation was assumed between the original data points. Thus 99 pseudo data points were placed between each two original data points. The third method used the Z-transform technique to implement the first order lag filter and produced the filtering equation

$$Y_f[(i+1)\Delta t] = Y_f[i\Delta t]\, e^{-\frac{\Delta t}{\tau f}} + Y[(i+1)\Delta t]\,(1 - e^{-\frac{\Delta t}{\tau f}}) \quad 5.2$$

Table 5-1 shows the results of the filtering using the three methods for $\Delta t = 0.046$, noise RMS = 12.2 and filter time constants ranging from 1.0 to 0.1. (To put the noise value in proper perspective note that the maximum input pulse height is 90.) The maximum recoverable frequency ω_R was 3.85 for the unfiltered data points. The simple numerical filtering method gave a small

TABLE 5-1

Effect of Filter Constant on Recoverable Frequency

for Different Post-Sample Filtering Techniques

Filtering Technique:			SIMPLE NUMERICAL	100 POINT	Z TRANSFORM
ST	RMS	τ_f	ω_R	ω_R	ω_R
0.046	12.2	1.0	4.335	4.404	4.450
0.046	12.2	.9	4.335	4.406	4.453
0.046	12.2	.8	4.334	4.407	4.456
0.046	12.2	.7	4.332	4.408	4.458
0.046	12.2	.6	4.327	4.407	4.460
0.046	12.2	.5	4.318	4.405	4.460
0.046	12.2	.4	4.300	4.397	4.457
0.046	12.2	.3	4.249	4.379	4.446
0.046	12.2	.2	4.100	4.316	4.401
0.046	12.2	.1	2.411	3.902	4.045

improvement in recoverable frequency until the filter constant was decreased to a value approaching the Δt value. Then the results deteriorated as would be expected upon examining the filter equation. The 100 point method removed the $\Delta t/\tau_f$ ratio problem and increased the accuracy, but there was still only a small increase in recoverable frequency over the unfiltered case. The Z-transform technique was the better of the three methods by only a slight margin, but the increase in recoverable frequency over the unfiltered case was not significant.

With the same system and input, the noise level was lowered to an RMS of 1.22 and using the 100 point filtering technique the filter constant, τ_f, was varied from 1.0 to 0.011. The unfiltered data yielded a maximum recoverable frequency of 17.06 while Table 5-2 shows that the filtered values produced recoverable frequencies ranging from 17.07 to 17.36. The increase in recoverable frequency was even less significant than it was in the high noise-level case.

Table 5-3 presents the results of varying the filter constant using both the 100 point and Z-transform filter techniques when no noise is introduced into the system. In all cases the maximum recoverable frequency is 45.07 which is the value obtained using unfiltered data.

These results show little or no increase in recoverable frequency accruing from post-sample filtering at low noise levels and an insignificant increase for high noise levels. Consideration of the frequency spectrum of a sampled signal will provide some

TABLE 5-2

Effect of Filter Constant on Recoverable Frequency

Using the 100 Point Post-Sample Filtering Method

ω_R	τ_f	RMS	ST
17.360	1.0	1.22	0.046
17.363	.9	1.22	0.046
17.355	.8	1.22	0.046
17.332	.7	1.22	0.046
17.296	.6	1.22	0.046
17.256	.5	1.22	0.046
17.224	.4	1.22	0.046
17.204	.3	1.22	0.046
17.189	.2	1.22	0.046
17.147	.1	1.22	0.046
17.113	.0667	1.22	0.046
17.091	.05	1.22	0.046
17.079	.04	1.22	0.046
17.074	.0333	1.22	0.046
17.073	.0286	1.22	0.046
17.074	.025	1.22	0.046
17.076	.0222	1.22	0.046
17.078	.020	1.22	0.046
17.081	.0182	1.22	0.046

TABLE 5-2 CONTINUED

ω_R	τ_f	RMS	ST
17.083	.0167	1.22	0.046
17.085	.0154	1.22	0.046
17.087	.0143	1.22	0.046
17.089	.0133	1.22	0.046
17.090	.0125	1.22	0.046
17.092	.0118	1.22	0.046
17.093	.0111	1.22	0.046

TABLE 5-3

Effect of Filter Constant on the Recoverable Frequency of a Noiseless System for Two Post-Sample Filtering Techniques

SIMPLE NUMERICAL ω_R	Z TRANSFORM ω_R	τ_f	RMS	ST
45.07	45.07	.200	0.0	0.046
45.07	45.07	.100	0.0	0.046
45.07	45.07	.067	0.0	0.046
45.07	45.07	.050	0.0	0.046
45.07	45.07	.040	0.0	0.046
45.07	45.07	.033	0.0	0.046
45.07	45.07	.025	0.0	0.046
45.07	45.07	.020	0.0	0.046
45.07	45.07	.015	0.0	0.046
45.07	45.07	.012	0.0	0.046
45.07	45.07	.010	0.0	0.046

insight into the results. Figure 5-4 shows the frequency spectrum of a continuous function, $x(t)$, described by Equations 4.5 and 4.6 for a pulse duration of 0.5. In addition, plotted on Figure 5-4 is the frequency spectrum of the sampled function, $x(t)^*$, formed by sampling $x(t)$ at time increments of 0.06. The spectra of the sampled function are centered around multiples of the sampling frequency ($2\pi/.06 = 105$) and fold at 1/2 the sampling frequency ($105/2 = 52.5$). Figure 5-5 is the frequency spectrum of the unfiltered and post-sample filtered cases for a sampled signal. The filter is a first order lag with a 0.03 time constant (33 radians/time unit corner frequency). Most of the fold-over is still present. Apparently, once sampling has occurred, the high frequency components are already folded into the low frequency components and post-sample filtering cannot correct the situation. Since physical systems contain frequency components at high frequencies, this result is to be expected for all post-sample filtering.

5.2 Pre-Sample Filtering

An alternative to this is to filter the signal before sampling as shown in Figure 5-2. The effect of pre-sample filtering of the continuous signal is very apparent in the frequency domain. Figure 5-6 compares the frequency spectra of a continuous function, $x(t)$, with its sampled version, $x(t)^*$, and reveals significant fold-over in $x(t)^*$. $x(t)$ is described by Equations 4.5 and 4.6 with $T_p = 0.5$ and the sampling interval for $x(t)^*$ is 0.06. Filtering the continuous function, $x(t)$, with a first order lag having a time

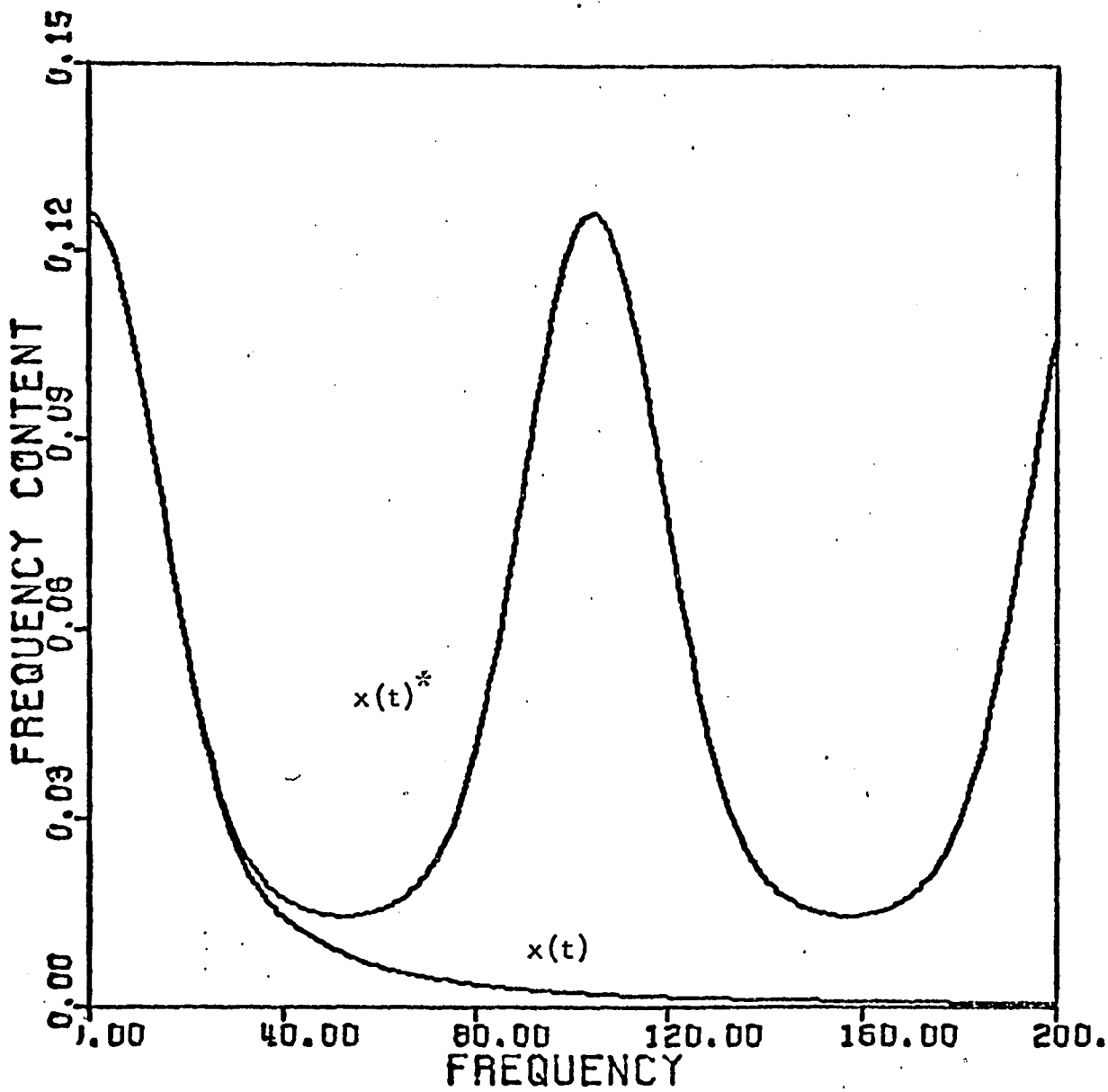

FIGURE 5-4. Comparison of the Frequency Spectra of a Continuous Function, $x(t)$, and Its Sampled Version, $x(t)^*$. Sampling Time of 0.06.

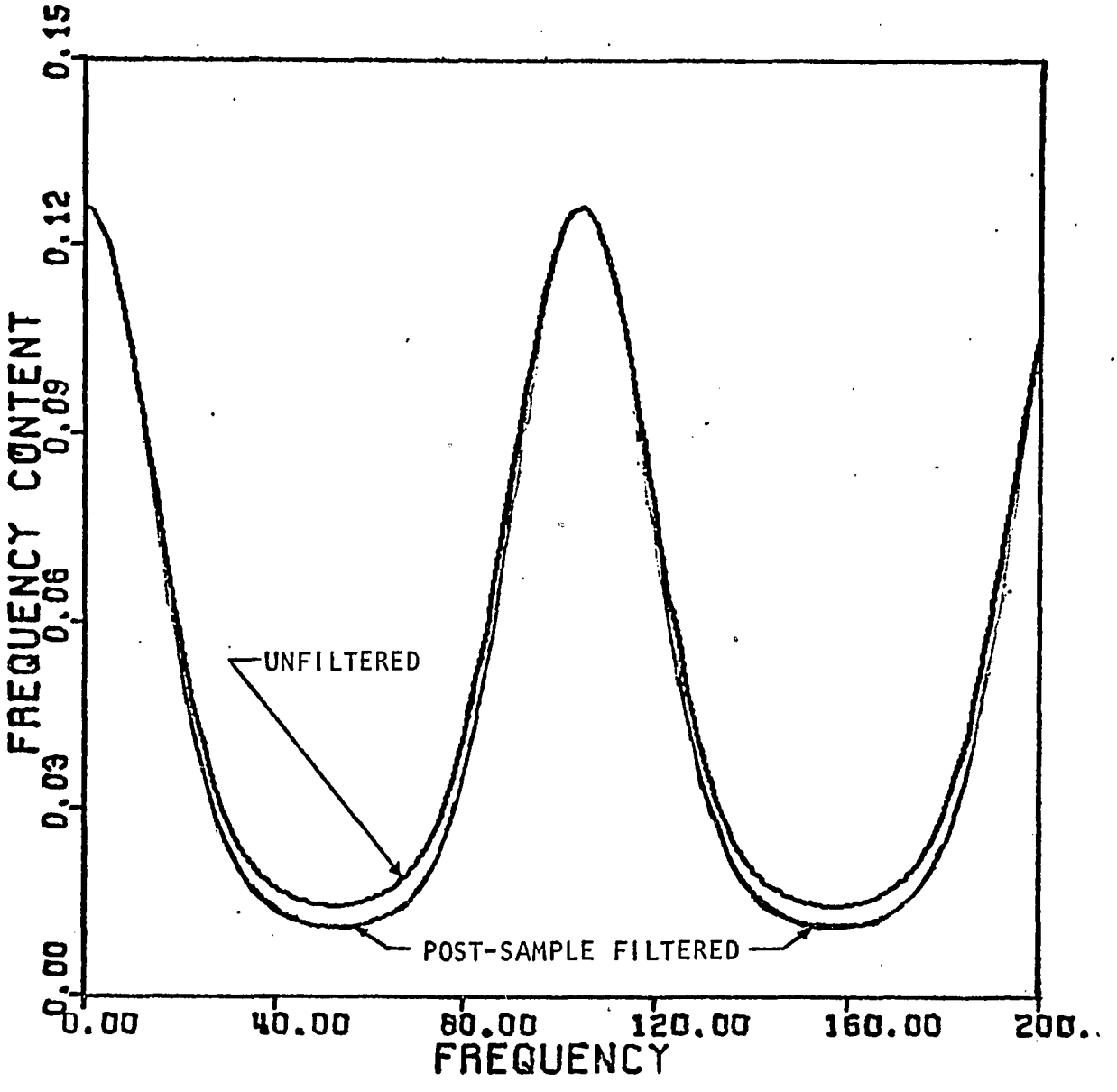

FIGURE 5-5. Comparison of the Frequency Spectra of a Sampled Function for the Unfiltered and Post-Sample Filtered Cases. Filter is a First Order Lag with a 0.03 Time Constant.

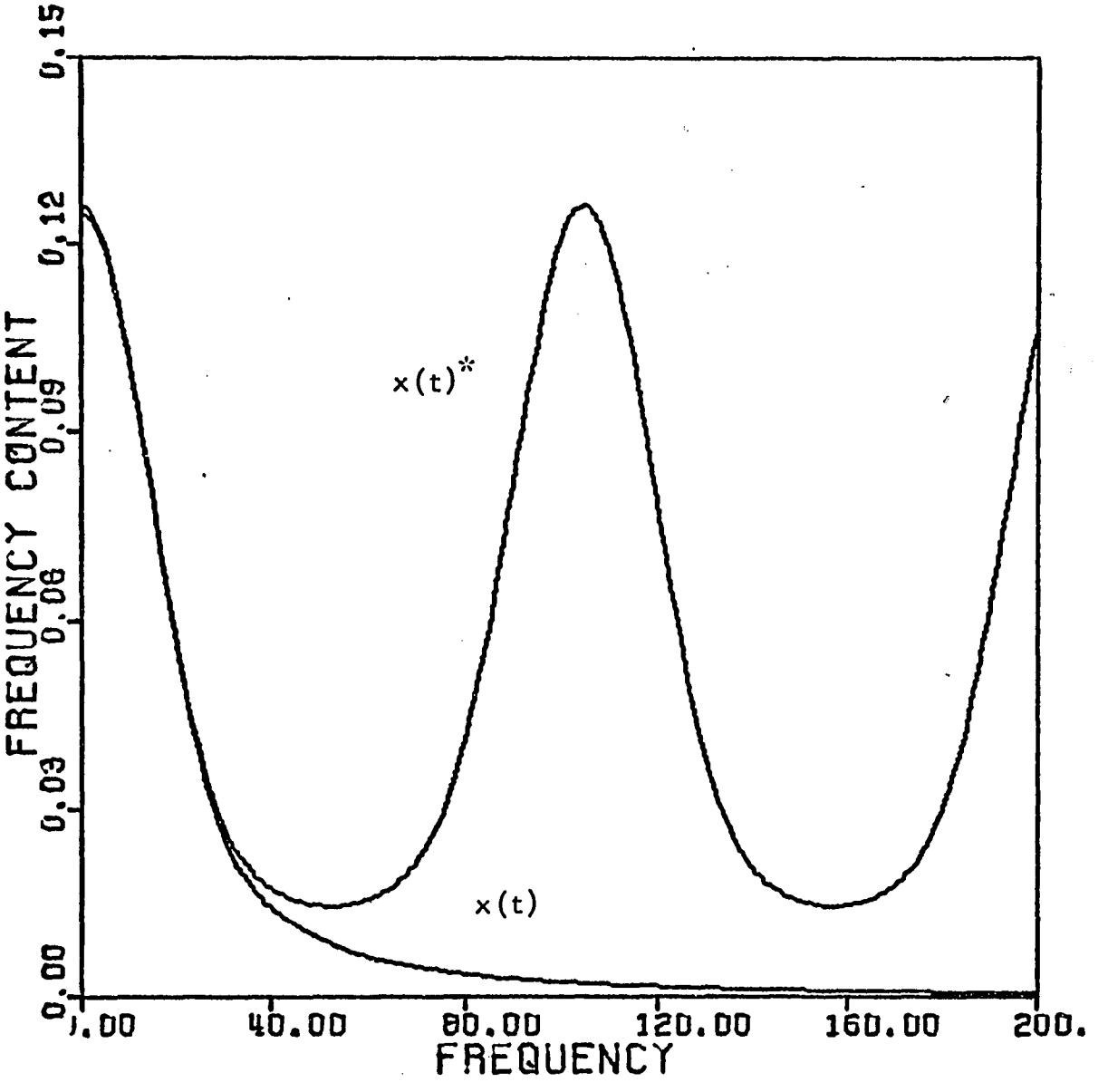

FIGURE 5-6. Effect of Sampling a Function Containing Significant High Frequency Components. Sampling Time of 0.06.

constant of 0.03 (corner frequency = 1/.03 = 33) greatly attenuates the high frequencies as shown in Figure 5-7. Sampling this filtered function at intervals of 0.06 produces practically no fold-over as shown in Figure 5-8. (Compare this with Figure 5-5.) Consequently it is to be expected that pre-sample filtering will be beneficial.

To determine the effect on the maximum recoverable frequency of filtering the continuous signal a first order lag system (time constant = 0.1) was pulsed with the input shown in Figure 5-3. Process conditions were simulated by adding white noise to the output (see Chapter 4 Section 4.2). The input and output were filtered with first order lag filters having equal time constants so that the filter dynamics canceled in the transfer function. For the test the sampling time and filter constant were held constant at 0.03 and 0.05 respectively while the noise level was varied. Then the test was repeated without filtering so that the filtering effect could be determined. The maximum recoverable frequencies calculated from this data are plotted versus noise RMS values in Figure 5-9. Filtering considerably improved the recovery, even in the noise-free (RMS = 0.0) case where the maximum recoverable frequency increased 20% from 65.7 to 81. As the improvement is quite significant at all frequencies, pre-sample filtering should be used whenever possible.

To reduce fold-over at a given sampling rate Black (1) gives one method which requires sampling at a much higher rate, filtering numerically, and subsampling at the lower rate. The high sampling frequency displaces the centers of the individual spectra enough

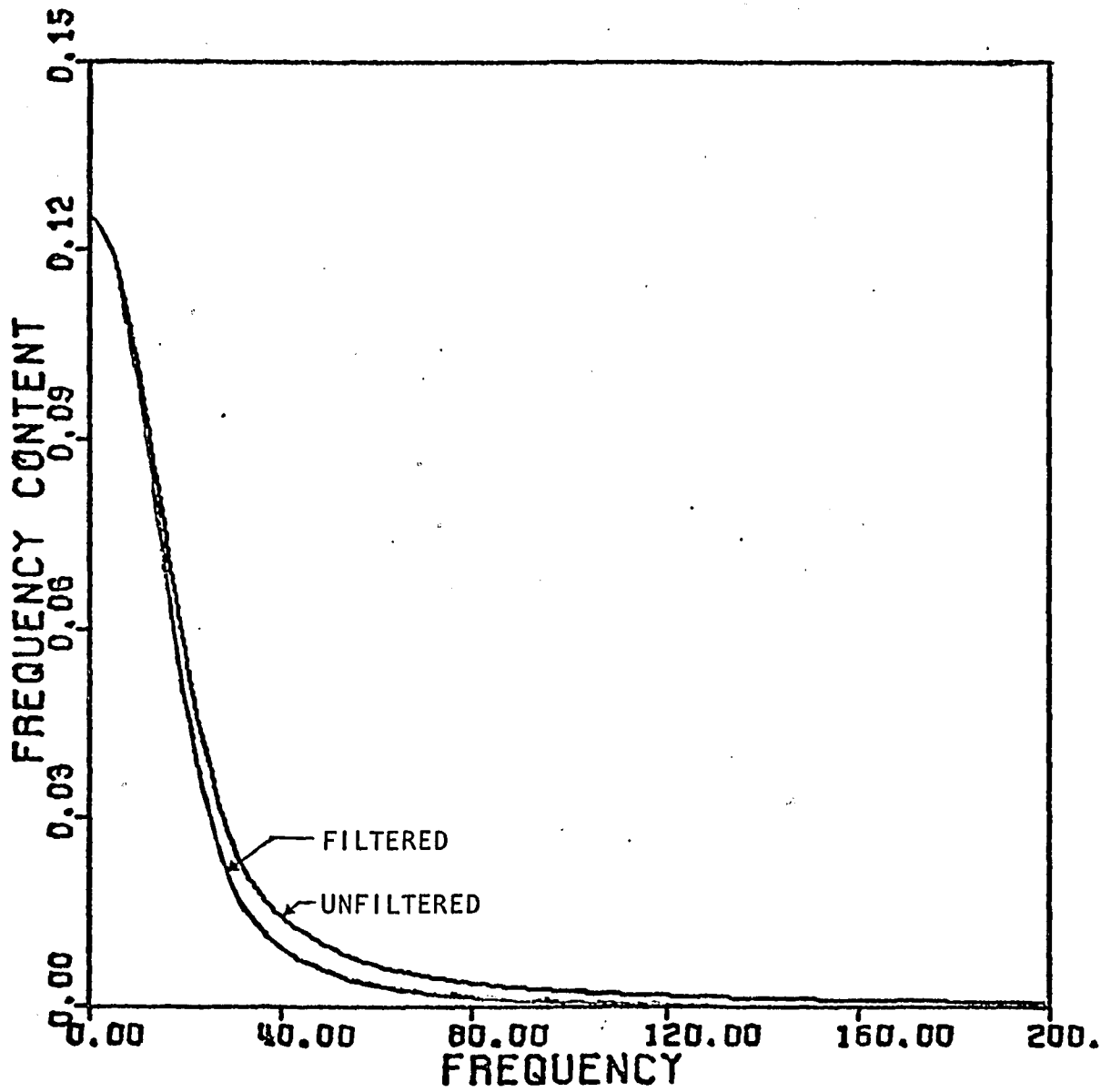

FIGURE 5-7. Effect of Filtering on the Frequency Spectrum of a Continuous Function. First Order Lag Filter with a 0.03 Time Constant.

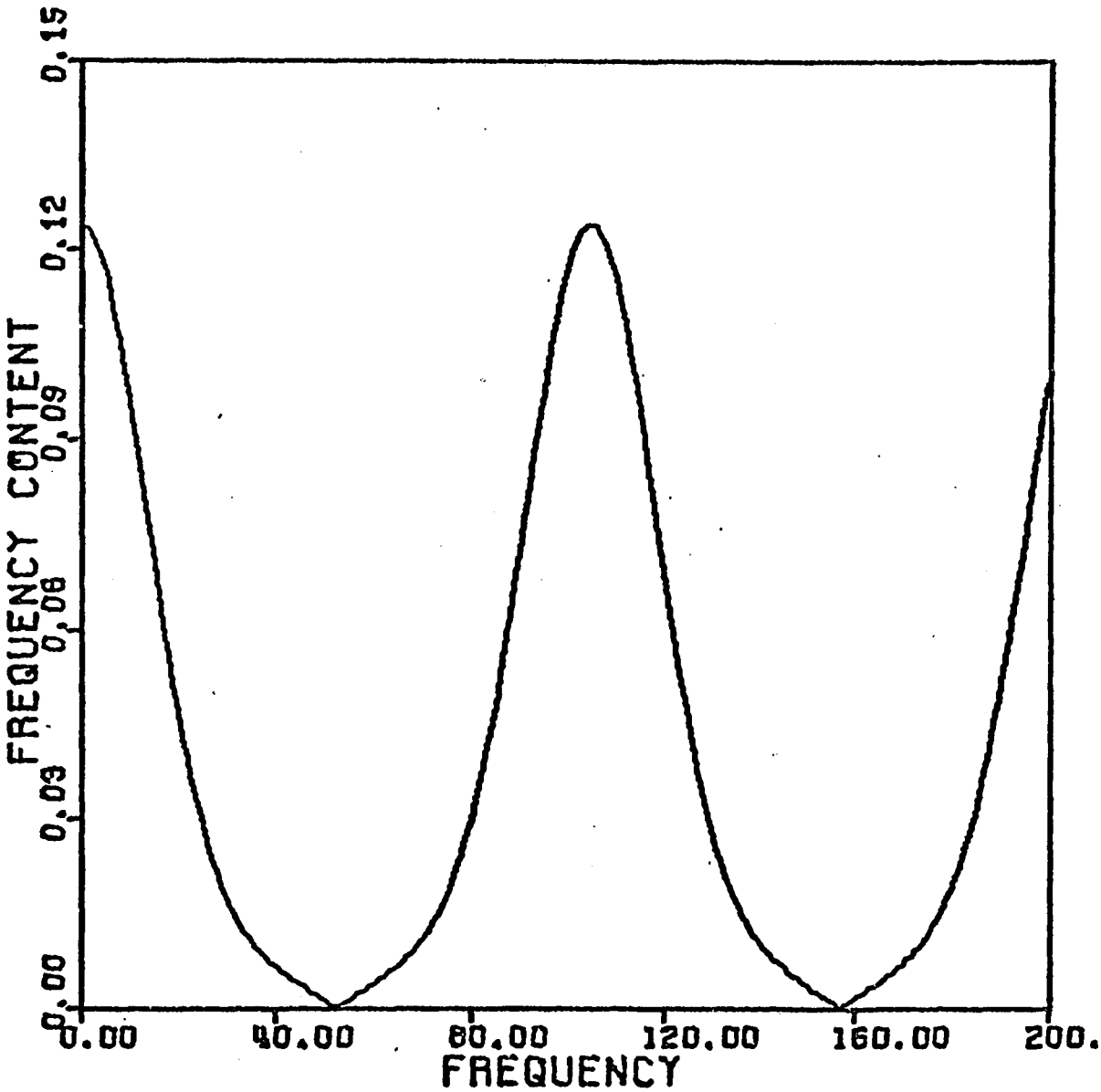

FIGURE 5-8. Frequency Spectrum of the Sampled Version of a Filtered Function. Pre-Sample Filtering Using a First Order Lag Filter with a 0.03 Time Constant. Sampling Time of 0.06.

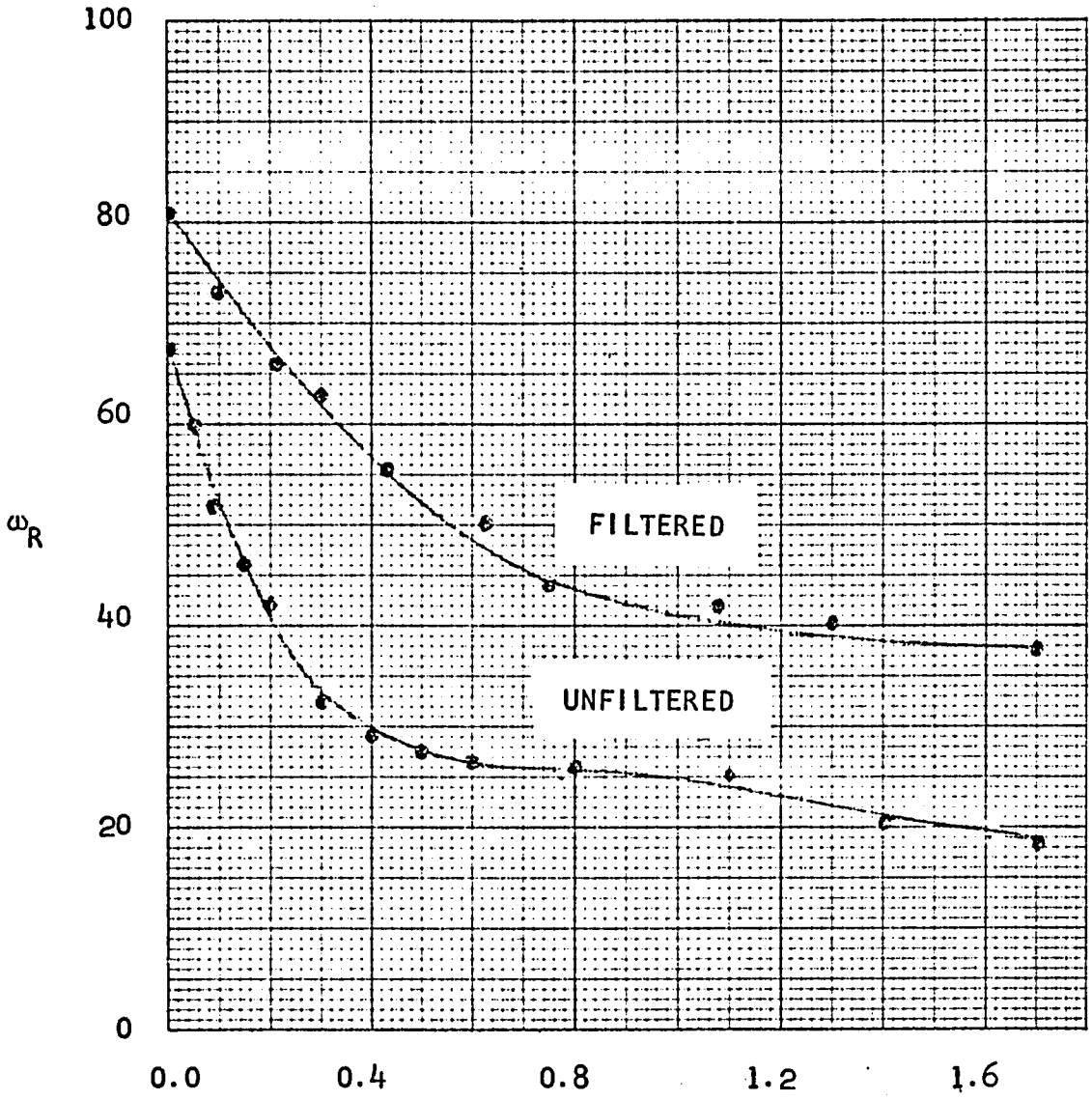

FIGURE 5-9. The Effect on the Maximum Recoverable Frequency of Pre-Sample Filtering. Sampling Time of 0.03 and Filter Constant of 0.05.

so that there is only a small amount of fold-over in the low frequencies. Filtering of this data with a low cut-off frequency filter provides data with negligible high frequency components and only a small amount of distortion in the lower frequencies. Subsampling of this data at the low sampling rate produces little fold-over in the low frequencies and consequently gives good results for the low sampling frequency. Essentially this is pre-sample filtering since the high sampling rate approximates a continuous signal. As the Fast Fourier transform imposes little penalty for additional data, in most situations this subsampling seems pointless.

5.3 Filter Time Constant

Now that filtering of the continuous signal has been shown to be very beneficial, it is appropriate to discuss how the filter constant should be chosen. The constraints can be best interpreted in terms of frequencies. When a signal is sampled, its frequency spectrum is reproduced in a chain of spectra centered around integral multiples of the sampling frequency, ω_s. If there are any components at frequencies greater than the folding frequency $(\omega_s/2)$ then these components fold back into the lower frequencies, causing distortion. To prevent this, significant attenuation should occur at all frequencies above the folding frequency. This is accomplished by specifying that the cut-off frequency of the filter be no greater than the folding frequency, or in terms of a time constant, that the time constant be no less than the reciprocal of the folding frequency, i.e. sampling time/π.

A critical upper constraint is not as obvious as the lower constraint but a reasonable guide is available. On the Bode plot significant attenuation begins at frequencies higher than the corner frequency ω_N (reciprocal of the system time constant). As it seems unreasonable for the filter to attenuate at frequencies below this value, the corner frequency of the filter should not be less than the corner frequency of the process, which now becomes an upper bound or constraint.

To evaluate the criticalness of these upper and lower constraints and the sensitivity of the maximum recoverable frequency to the filter time constant within the constraints, a test was made in which for a given input, system, and sampling time, the filter time constant was varied at various process noise levels. The input was the lagged ramp pulse shown in Figure 5-3, the system was a first order lag with a 0.1 time constant and the sampling time was 0.046. The upper filter time constant constraint is equal to the system time constant or 0.1 and the lower constraint is equal to $0.046/\pi$ = 0.0146. For the test the filter time constant was varied from 0.2 to 0.01 at noise levels of RMS = 11.2, 1.12 and 0.0. The results, presented in Table 5-4, are shown graphically in Figure 5-10 where the maximum recoverable frequency is plotted versus filter time constant with noise RMS value as a parameter. The lower constraint, which involves attenuating all frequencies above the folding frequency, is very critical. The plot shows that significant deterioration of results begins even before the lower constraint is violated. The reason for this is that the first order lag filter does not provide

TABLE 5-4

Effect of Filter Time Constant at Various Noise Levels for Pre-Sample Filtering

RMS:		11.5	1.15	0.00
ST	τ_f	ω_R	ω_R	ω_R
.046	.200	18.30	44.00	56.2
.046	.100	18.30	44.19	56.3
.046	.0667	18.35	44.33	56.3
.046	.0500	18.36	44.40	56.1
.046	.0400	18.36	44.37	55.9
.046	.0333	18.35	44.20	55.6
.046	.0286	18.33	43.82	55.2
.046	.0250	18.31	43.43	54.9
.046	.0222	18.27	43.08	54.5
.046	.0200	18.22	42.73	54.1
.046	.0182	18.18	42.41	53.6
.046	.0167	18.12	42.10	53.2
.046	.0154	18.07	41.81	52.8
.046	.0143	18.01	41.13	52.4
.046	.0133	17.96	40.57	52.1
.046	.0125	17.91	40.51	51.8
.046	.0118	17.85	39.95	51.5
.046	.0111	17.80	39.39	51.2
.046	.0105	17.75	38.83	50.9
.046	.0100	17.65	38.27	50.6

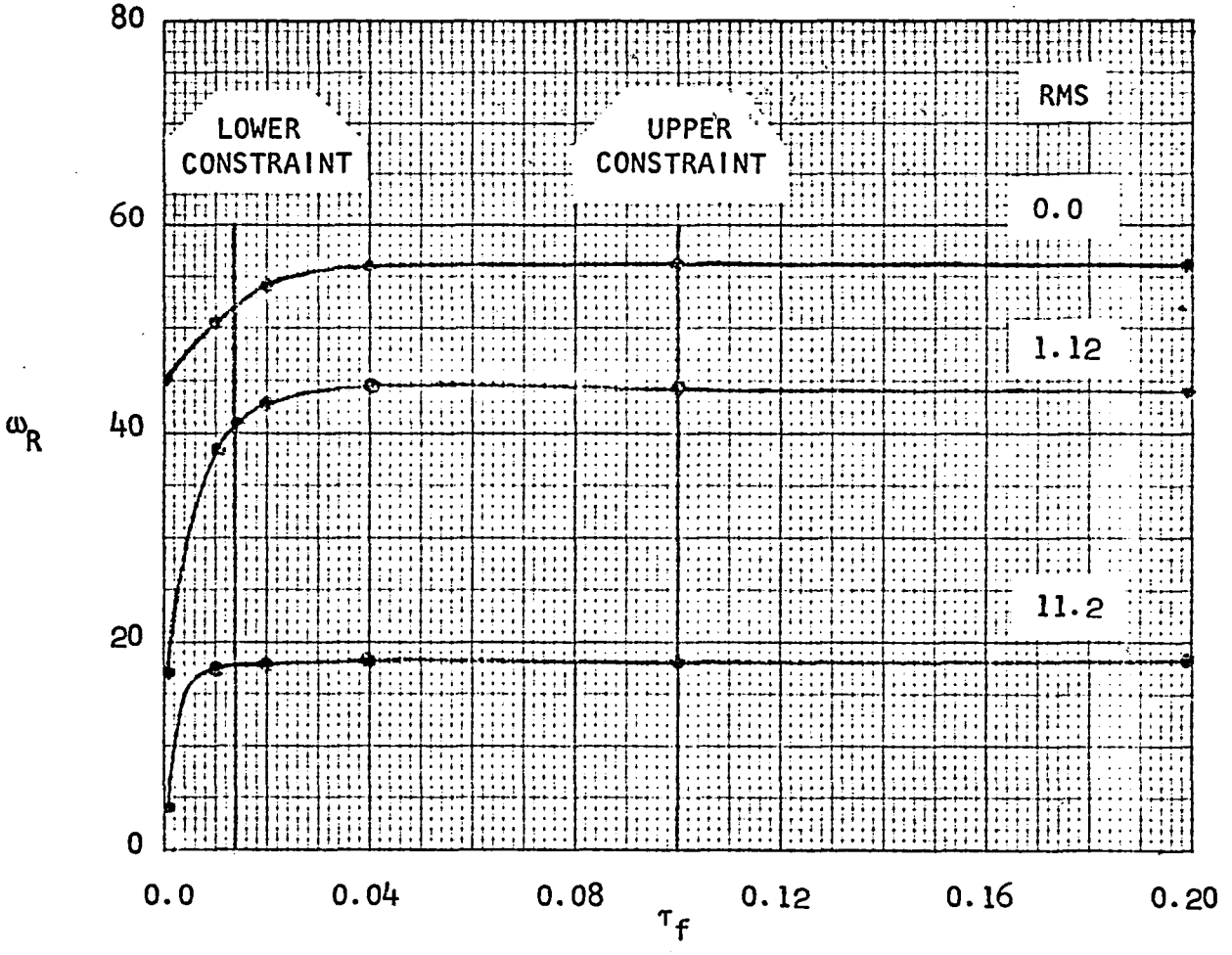

FIGURE 5-10. The Effect of the Filter Time Constant on the Maximum Recoverable Frequency. Sampling Time of 0.046.

a sharp cut-off at the corner frequency. Apparently, with no noise the optimum filter time constant is the process time constant, but as the noise level increases, the optimum constant decreases. The process time constant is a good guide to the upper bound but it is not nearly as critical as the lower bound. As long as the lower constraint is not too closely approached, time constants within the constraints will all give about the same results.

5.4 Significant Figures

The second practical aspect to be discussed in this chapter is the effect of significant figures on the maximum recoverable frequency. There are two ways in which this can enter the Fourier transform computation:

(1) through the number of significant figures or bits used by the computer's arithmetic unit,

(2) through the number of significant figures in the data, which is a function of the recording equipment.

Knowing when the computer significant figures become limiting could be critical in specifying a computer for executing Fourier transform calculations. Likewise, a correlation between data significant figures and recoverable frequency would provide a direct method of evaluating the suitability of the recording equipment. The need for defining the necessary significant figures will become more acute with the use of filtering to reduce the noise in the data. It is very likely that with the use of filtering many systems which are noise limited, as far as recovering test data, will become computer and recording equipment limited, particularly recording

equipment.

Truncating significant figures in the data has the same effect as adding noise. Recording equipment, then, may be considered as introducing noise into the data, the level of the noise increasing as fewer significant figures are provided. The noise level associated with a given number of significant figures should be amenable to mathematical analysis. Since any fraction of the maximum error should have an equal probability of occurring and assuming that enough error values are used to get a good distribution then the mean of the squared errors can be represented as the integral

$$\frac{1}{E}\int e^2\,de$$

where E = maximum span of errors

e = error value.

The maximum error which can be attributed to truncation is approximately equal to the incremental change associated with a change of one in the last significant digit. For instance, if the number 4.02 has three significant digits then the maximum error due to truncation is 0.01 (a variable with the value 4.0299^+ would be truncated to 4.02). The error is always negative or zero, therefore

$$RMS_1 = \frac{1}{E_1}\int_{-E_1}^{0} e^2\,de = \frac{E_1}{\sqrt{3}} \qquad 5.3$$

where E_1 = maximum error and maximum error span

e = value of error.

If the last significant digit is obtained by rounding the numbers up and down, then the maximum error is 1/2 of the change associated with a change of one in the last significant digit. However, both positive and negative errors are allowed and the maximum error span is the same as before. The noise RMS value is calculated as

$$RMS_2 = \frac{1}{E_2} \int_{-\frac{E_2}{2}}^{+\frac{E_2}{2}} e^2 \, de = \frac{E_2}{2\sqrt{3}} \qquad 5.4$$

where E_2 = maximum error span.

This says that if $E_1 = E_2$ then $RMS_1 = 2\ RMS_2$, or that rounding has halved the noise level.

However, it was postulated that the maximum span of the error is more important than the maximum error in determining the maximum recoverable frequency. If this is true then RMS values calculated by Equations 5.3 and 5.4 are not compatible for determining maximum recoverable frequencies. This is important because it is desired to relate data truncation noise to process noise, which has both positive and negative values. (Such a relation would provide an easy method for evaluating the suitability of recording equipment.) To see if Equation 5.4 should be used for comparing significant figures noise to process noise a test was designed and comparisons made. It should be noted that the maximum error associated with a constant number of significant digits can change with the magnitude of the variable being measured. (For example, using 2 significant digits the maximum error increases from 0.1 to 1.0 as the value of

the variable increases from 9.0 to 10. Since the largest values of the variable affect the calculation most, the maximum error most prevalent in the upper range of the values will be used for the RMS determination.

In the test, for a given system and sampling time, the data significant figures were varied from 5 to 2 for three different inputs. The system was a first order lag (time constant = 0.1), the sampling time was 0.03, and the input is described by Equations 4.5 and 4.6. The pulse durations, T_p, used were 2.0, 1.0, and 0.5. The test was repeated except that eight significant figure data was used and a white noise level predicted by Equation 5.4 for the various significant figures (from 5 to 2) was introduced into the output. Maximum recoverable frequencies were calculated from all the data and the results tabulated in Table 5-5. Listed beside each maximum recoverable frequency, ω_R, at a given number of data significant figures is the ω_R obtained with a process noise level predicted for the given number of data significant figures. Equation 5.4 appears to be an adequate approximation for converting data significant figure noise to a comparable process noise level.

Because the effect of a given noise level varies with the frequency content of the input, it is not possible to present an absolute correlation of recoverable frequency versus data significant figures. However, since each decrease in number of significant figures represents a ten-fold increase in noise level, it should still be possible to reach some conclusions about the necessary significant figures. Using a 0.1 time constant first order lag system, and the

TABLE 5-5

Comparison of the Effect of a Given Number of Data Significant Figures with the Effect of the White Noise Level Predicted for the Given Number of Data Significant Figures

PULSE DURATION	ST	DATA SIGNIFICANT FIGURES	ω_R AT GIVEN DATA SIGNIFICANT FIGURES	ω_R AT PREDICTED NOISE RMS VALUE
2.0	.03	5	72.4	72.0
2.0	.03	4	63.0	58.0
2.0	.03	3	27.0	26.8
2.0	.03	2	13.2	11.0
1.0	.03	5	67.7	67.7
1.0	.03	4	64.2	64.3
1.0	.03	3	43.2	36.0
1.0	.03	2	14.4	14.0
0.5	.03	5	72.0	72.0
0.5	.03	4	70.1	69.0
0.5	.03	3	52.8	58.0
0.5	.03	2	13.9	

pulse input described by Equations 4.5 and 4.6 for pulse durations of 2.0, 1.0 and 0.5, recoverable frequency versus data significant figures data was obtained at sampling times of 0.015, 0.03, 0.06 and 0.09. This data was plotted in Figures 5-11, 5-12, and 5-13. (The flat portions of the curves at high significant figures indicate sampling frequency limitations on the recovery.) In all cases using only 2 significant figures and in most cases even 3 significant figures severely limits the recovery. However, in most instances using 4 significant figures appears adequate; the use of 5 significant figures would almost certainly be useless because of process noise. The improvement resulting from increasing the sampling frequency at a moderate noise level (3 significant figures) is noteworthy.

Perhaps it should be mentioned that the case where the recording equipment has a minimum value of accuracy is almost directly analogous to adding random noise in the process. Equation 5.4 should be used to calculate the noise RMS value for this case also.

To study the effect of computer significant figures a subroutine was written which truncated each number in every Fourier transform calculation to the number of significant figures being used. Thus it was possible to vary the number of significant figures from 2 to 8 and simulate a computer with any specified number of significant figures. It is to be expected that limiting the number of computer significant figures will have a much more severe effect than an equal limitation on data significant figures as the computer truncates not only in the data but also in every operation in the calculation. To compare the two cases, a test was made using a

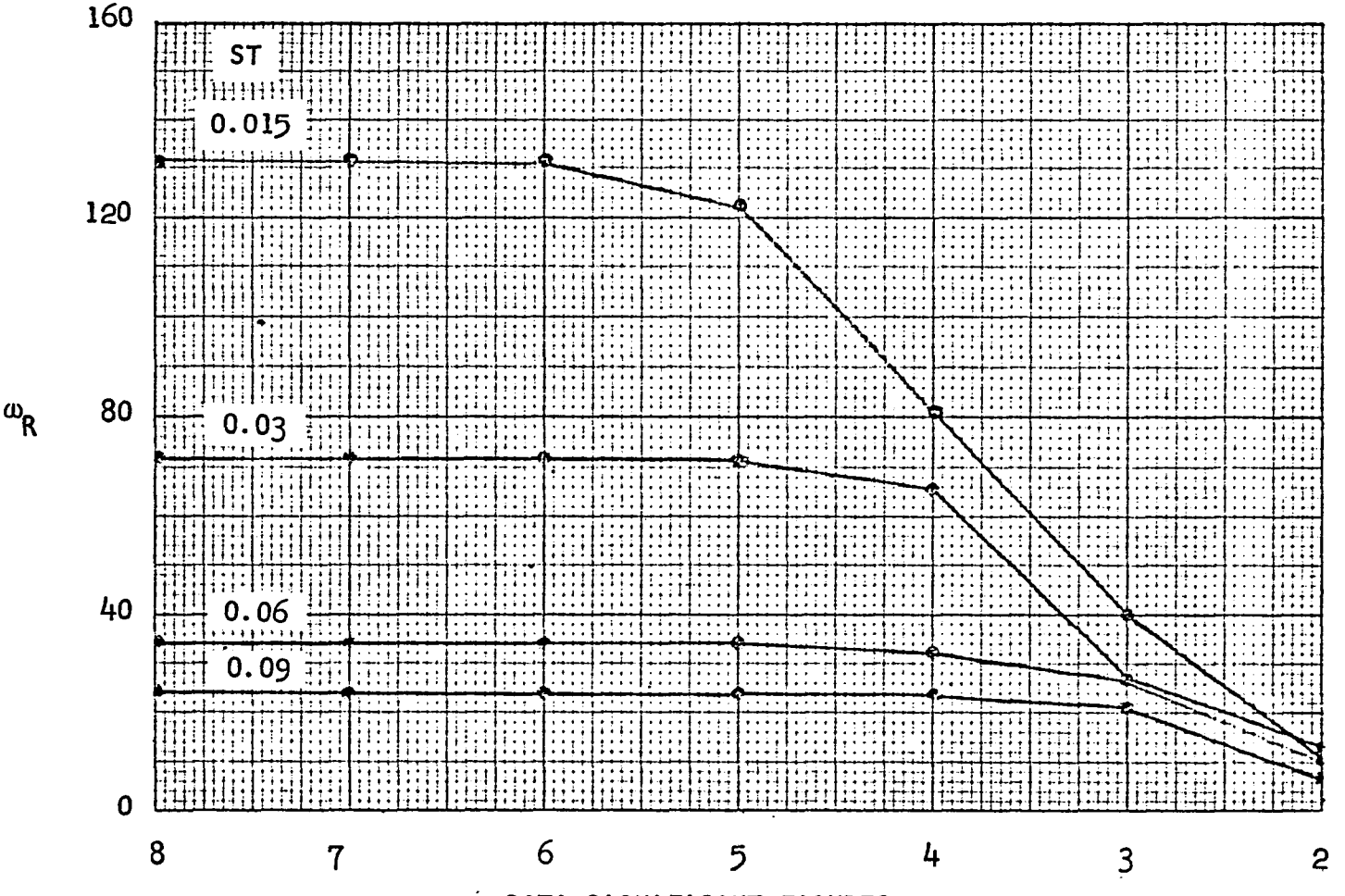

FIGURE 5-11. Effect of Data Significant Figures on the Maximum Recoverable Frequency. Pulse Duration of 2.0.

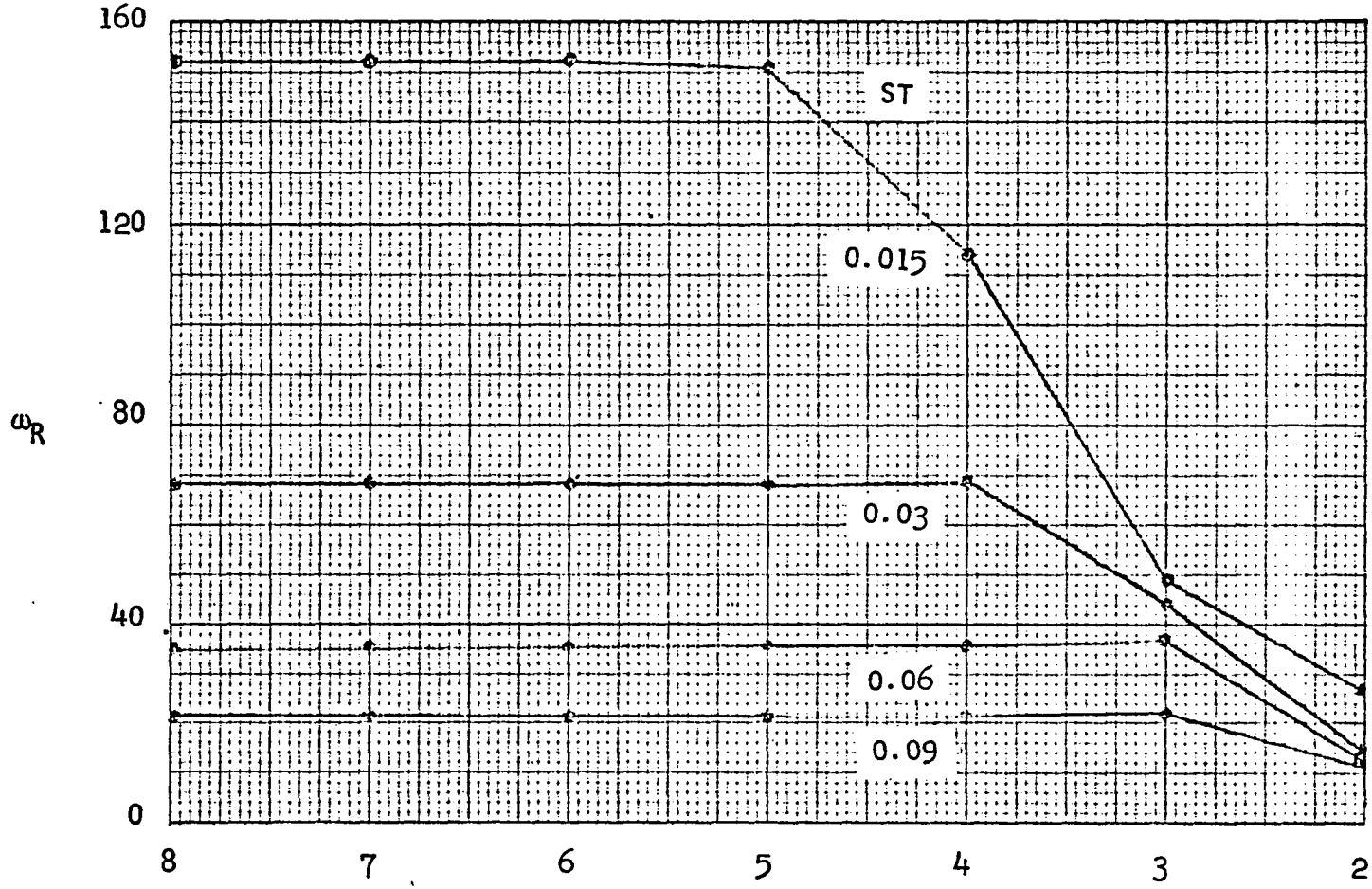

FIGURE 5-12. Effect of Data Significant Figures on the Maximum Recoverable Frequency. Pulse Duration of 1.0.

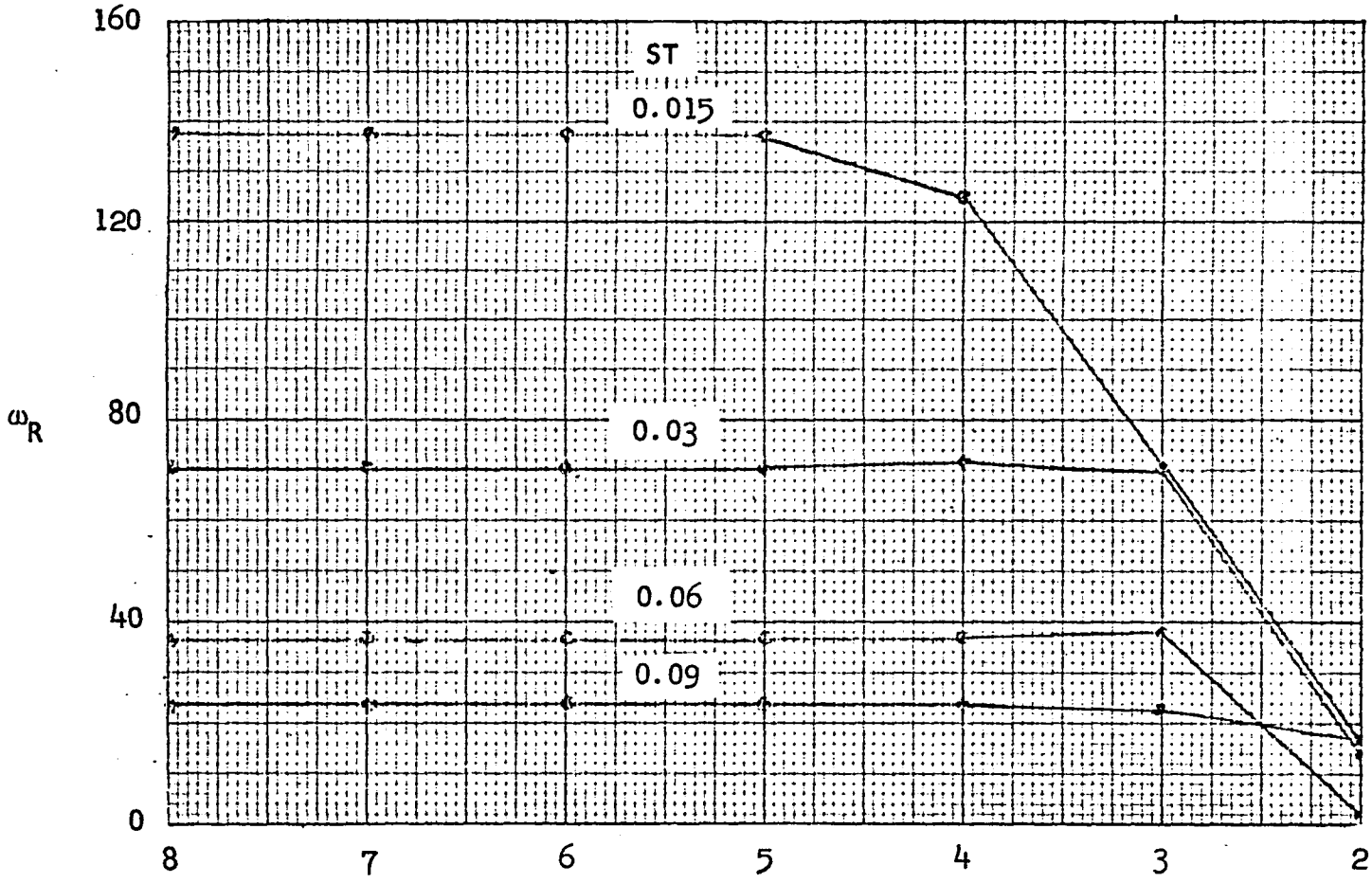

FIGURE 5-13. Effect of Data Significant Figures on the Maximum Recoverable Frequency. Pulse Duration of 0.5.

first order lag system with a 0.1 time constant and the lagged ramp input shown in Figure 5-3. The effect of computer significant figures for sampling times of 0.015, 0.03, 0.06, and 0.09 is shown in Figure 5-14. Figure 5-15 shows the effect of data significant figures for the same system, input and sampling times. The interesting observation here is that about one more significant figure is needed in the computer than is present in the data. More than 6 significant figures are not necessary in a computer for these calculations. For both data and computer significant figures increasing the sampling frequency increases the number of useful significant figures.

5.5 Conclusions

Post-sample filtering was found to be very ineffective as a means for increasing the recoverable frequency. However, pre-sample filtering or filtering of the continuous signal was very effective for increasing the recoverable frequency, even when no noise was present. A first order lag filter was used in the study and upper and lower constraints were set for determining the filter constant. The upper constraint is the system's dominant time constant while the lower constraint is the reciprocal of the folding frequency or sampling time/π. The lower constraint was found to be by far the most critical, but as long as the lower constraint is not approached too closely, there is very little difference in the results obtained with any time constant within the constraints.

Equation 5.4 was found to be adequate for calculating noise levels, resulting from limited significant figures, to compare with

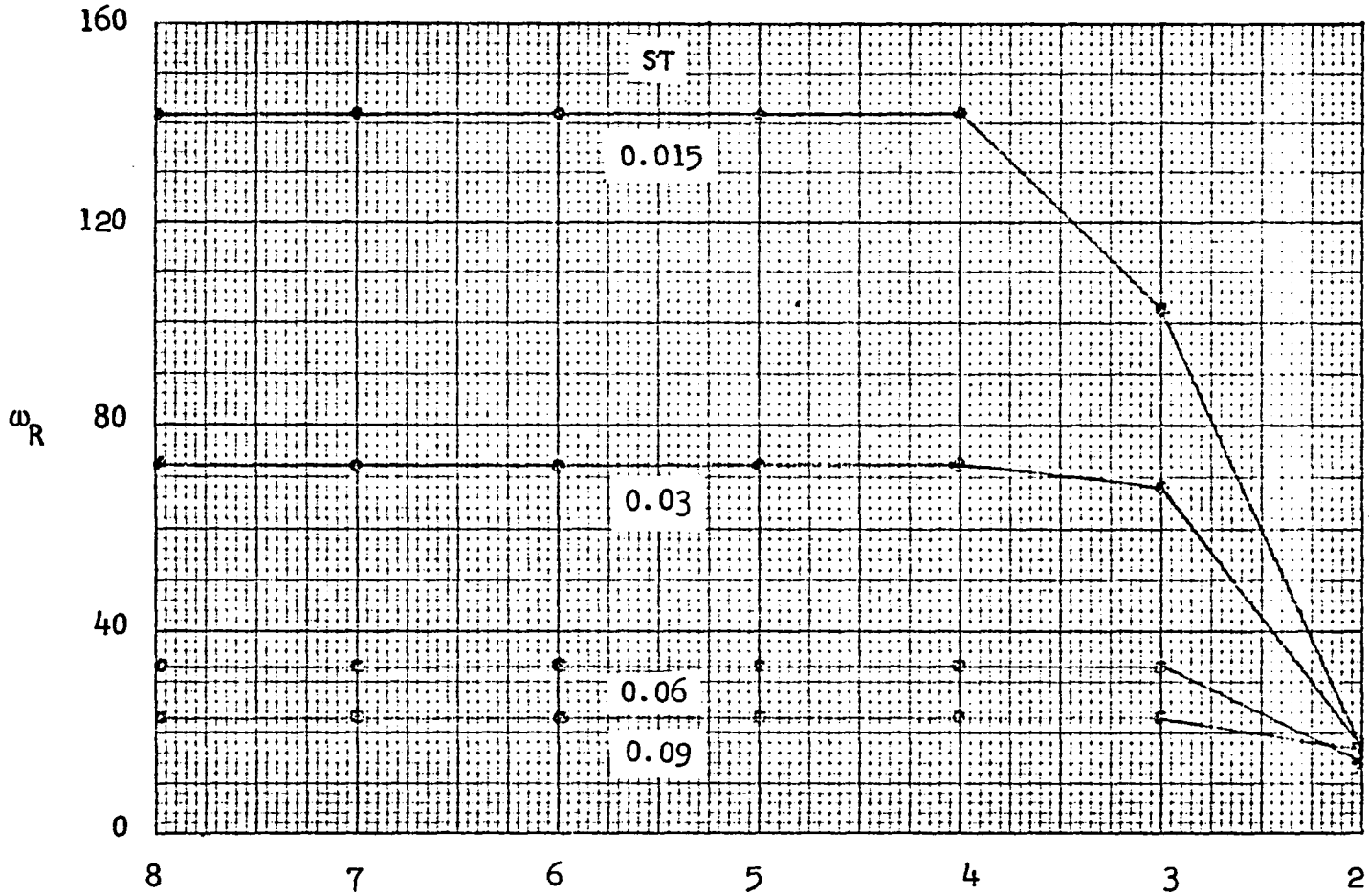

FIGURE 5-14. Effect of Data Significant Figures on the Maximum Recoverable Frequency. Filtered Ramp Input.

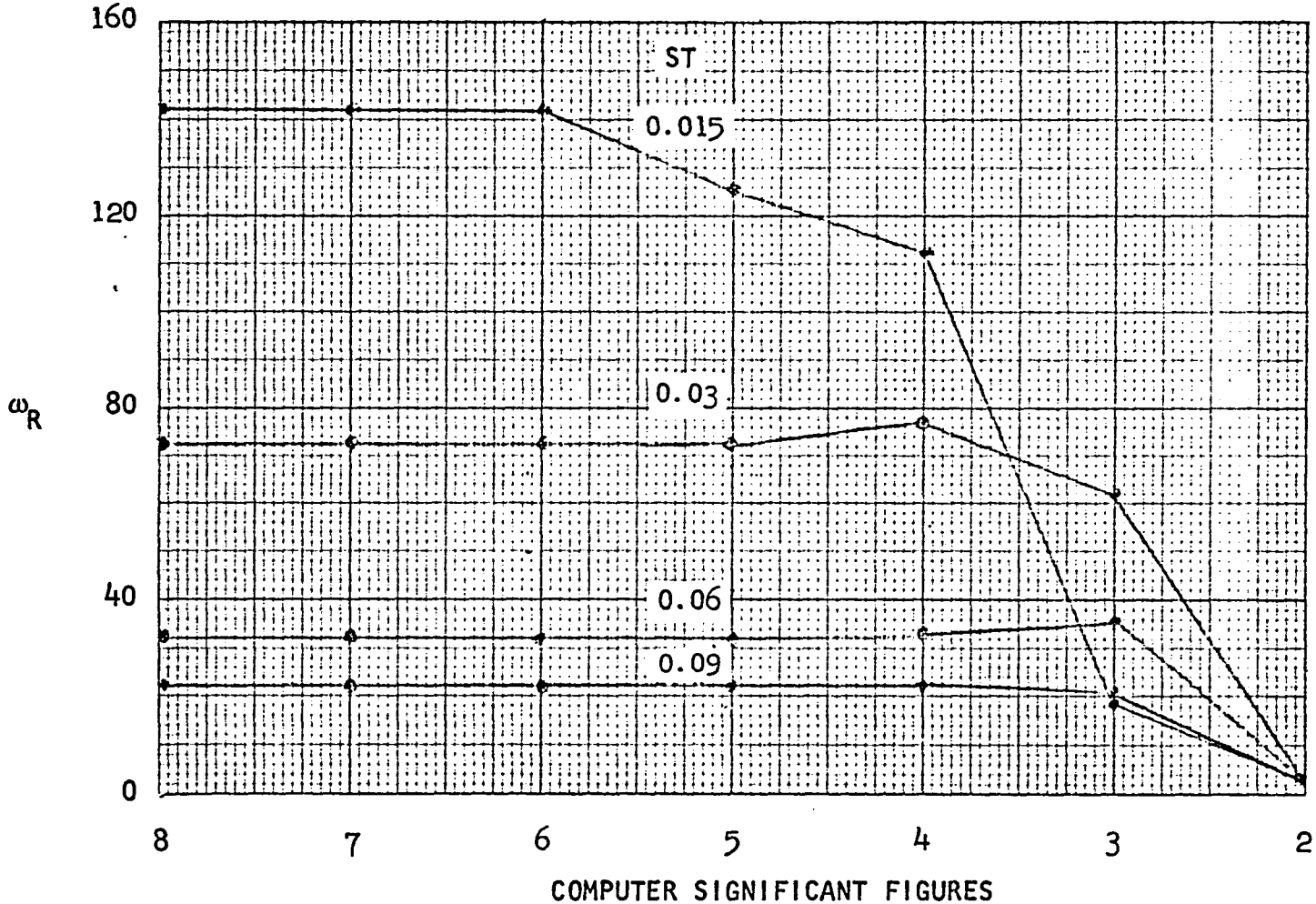

FIGURE 5-15. Effect of Computer Significant Figures on the Maximum Recoverable Frequency. Filtered Ramp Input.

process noise levels. This comparison will provide an easy method for determining the suitability of recording equipment. Four significant figure data was found to be very desirable. To avoid loss of information in calculations, it was found that the computer significant figures should be one greater than the data significant figures.

LITERATURE CITED

1. Blackman, R. B. Data Smoothing and Prediction. Dallas: Addison-Wesley Publishing Company, Inc., 1965.

2. Chang, Sheldon S. L., "Discrete Systems and Digital Computer Control," Applied Mechanics Reviews, Vol. 20, no. 5, May, 1967.

3. Clements, William C., Jr., "Pulse Testing for Dynamic Analysis," Ph.D. Dissertation, Vanderbilt University, 1963.

4. Kuo, Benjamin C. Analysis and Synthesis of Sampled-Data Control Systems. New Jersey: Prentice Hall, Inc., 1963.

5. Vincent, George C., "On the Dynamic Response of a Baffled Shell and Tube Heat Exchanger to Shell Flow Disturbances," Master's Thesis, St. Louis University, 1960.

CHAPTER 6

FAST FOURIER TRANSFORM

The "Fast Fourier Transform" is a fast efficient technique for numerically computing Fourier transforms. Several variations have been proposed but all use the same basic technique (1,2,3,6,7) in which the Fourier integral

$$\int_0^T x(t)\, e^{-j\omega t}\, dt \qquad 6.1$$

is approximated by

$$\Delta t \sum_{i=0}^{N-1} x_i\, e^{-j\omega(\frac{iT}{N})} \qquad 6.2$$

where N = number of data points

x_i = i^{th} data point obtained from curve $x(t)$

Δt = time increment between data points.

As was shown in Chapter 3 Section 3.5, mathematically this approximation is equal to much more sophisticated approximations for calculating the ratio of Fourier transforms

$$G(j\omega) = \frac{\int y(t)\, e^{-j\omega t}\, dt}{\int x(t)\, e^{-j\omega t}\, dt} \qquad 6.3$$

as long as Δt is a constant and precise arithmetic is used. Furthermore, the Fast Fourier Transform reduces the required mathematical operations by a factor of $\frac{\log_2 N}{N}$, which besides increasing the computation speed introduces a possibility of reduced round-off errors associated with the reduction in number of computations.

6.1 REFFT

One variation of the Fast Fourier Transform is the real-valued Fast Fourier Transform described in detail in Reference
The real-valued fast Fourier transform is written especially for the case where the input is restricted to real numbers and takes advantage of this to eliminate unnecessary computations. Since the data from pulse tests is always real-valued, the real-valued fast Fourier transform was utilized in writing a subroutine specifically for converting pulse response data from the time domain to the frequency domain. The subroutine, REFFT, computes the input and output transforms simultaneously and thereby effects additional economies in computation. Simultaneous computation is made possible by requiring the same Δt for the input and output pulse data. A listing and instructions for implementation are given in Appendix A.

6.2 Comparison of Integration Techniques

The speed and accuracy of REFFT was compared with three other more conventional techniques for effecting the time domain pulse data to frequency domain data transformation. REFFT benefits both in speed and accuracy by requiring that a single Δt be used for both input and output data, and since conventional techniques will also benefit in these respects from such a restriction, this

restriction was made in all cases to establish a better basis for comparison. The simple numerical integration technique of summing rectangles was used and had the calculation equation

$$G(j\omega) = \frac{\Delta t\left(\sum_{i=1}^{N}[y(i\Delta t)\cos(\omega i\Delta t)] - j\sum_{i=1}^{N}[y(i\Delta t)\sin(\omega i\Delta t)]\right)}{\Delta t\sum_{i=1}^{N}[x(i\Delta t)\cos(\omega i\Delta t)] - j\sum_{i=1}^{N}[x(i\Delta t)\sin(\omega i\Delta t)]} \qquad 6.4$$

Another technique used was the "analytical" trapezoidal approximation described in Chapter 2 Section 2.5 and Chapter 3 Section 3.5. In this technique a straight line approximation between data points is substituted into the general equation

$$G(j\omega) = \frac{\int y(t)\, e^{-j\omega t}\, dt}{\int x(t)\, e^{-j\omega t}\, dt} \qquad 6.5$$

and the integration over the Δt increment performed analytically. The total integral is formed by summing all the integrals needed to span the total pulse time, T. This results in the equation

$$G(j\omega) = \frac{\frac{1}{\omega^2}\sum_{i=1}^{N} SY\ DCO - j\sum_{i=1}^{N} SY\ DSI}{\frac{1}{\omega^2}\sum_{i=1}^{N} SX\ DCO - j\sum_{i=1}^{N} SX\ DSI} \qquad 6.6$$

where

$$SY = \frac{y[(i+1)\Delta t] - y[i\Delta t]}{\Delta t}$$

$$SX = \frac{x[(i+1)\Delta t] - x[i\Delta t]}{\Delta t}$$

$$DCO = \cos(\omega(i+1)\Delta t) - \cos(\omega i \Delta t)$$

$$DSI = \sin(\omega(i+1)\Delta t) - \sin(\omega i \Delta t) \ .$$

The third method is a variation of this latter method. In this method the trigonometric substitutions

$$DCO = 2. \ \sin[\frac{\omega\Delta t}{2}] \ \sin[\frac{\omega((i+1)\Delta t + i\Delta t)}{2}]$$

$$DSI = 2. \ \sin[\frac{\omega\Delta t}{2}] \ \cos[\frac{\omega((i+1)\Delta t + i\Delta t)}{2}]$$

are made in Equation 6.6. The substitution was made to increase the computation speed but the results show that there was also an increase in accuracy.

6.3 Accuracy Comparison

The system used in the test was a first order lag (time constant = 0.1) and the input was the pulse described by Equations 4.5 and 4.6. The accuracy of the four integration techniques was compared for input pulse durations of 2.0, 1.0, 0.5, 0.25 and 0.125; and computer significant figures ranging from 6 to 3. The maximum recoverable frequency, ω, was defined by the error

criterion equation 4.1. The results are presented in Tables 6-1 through 6-8. The subscripts used to refer to the integration techniques are: FFT (real-valued fast Fourier transform), NUM (simple numerical integration), AT (analytical trapezoid), and ATS (analytical trapezoid with the trigonometric substitution). In the tables ND refers to number of significant digits and PT refers to pulse duration. Tables 6-1 through 6-4 show that in most cases all four techniques give essentially the same results. However, the simple numerical technique (NUM) is somewhat erratic and in several instances gave noticeably poorer results than the other three methods. The difficulty seems to occur at frequencies where the frequency content of the input is very low. At two significant figures the AT method is the poorest with the ATS method considerably better. However, the NUM method is slightly better than the ATS method at two significant figures and the FFT method is much better than any of the other three methods. For three or more significant figures there is very little to choose between FFT, ATS and AT as far as accuracy. Tables 6-5 through 6-8 show the results for computer significant figures ranging from 6 to 3. An additional characteristic revealed here is that the AT and ATS methods at low significant figures give poor results for very low frequencies. If the error accumulated in these low frequencies is discarded, then in several instances the error integral predicts a relatively high recoverable frequency. In the tables this is shown as, for example, $70.0^{*}_{2.0}$ which means that the error criterion predicts a maximum recoverable frequency of

TABLE 6-1

Integration Technique Comparison for Limited Data

Significant Figures. Sampling Time of 0.015.

ω_{FFT}	ω_{AS}	ω_{A}	ω_{NUM}	ND	PT
132.14	131.34	132.34	100.05	6	2.0
123.12	122.51	122.89	64.52	5	2.0
81.75	81.30	81.44	69.37	4	2.0
41.22	40.42	20.55	40.51	3	2.0
15.75	11.49	0.00	13.88	2	2.0
143.01	142.66	143.01	133.89	6	1.0
140.84	140.90	140.84	104.47	5	1.0
114.73	114.63	114.61	114.72	4	1.0
49.48	49.31	40.59	49.50	3	1.0
22.04	26.55	0.00	15.34	2	1.0
137.48	137.72	137.34	132.20	6	.5
136.92	137.26	136.97	124.34	5	.5
125.18	125.16	125.17	124.80	4	.5
70.46	71.21	74.06	71.54	3	.5
40.42	16.42	0.00	23.14	2	.5

TABLE 6-1 CONTINUED

ω_{FFT}	ω_{AS}	ω_{A}	ω_{NUM}	ND	PT
140.20	140.19	140.32	139.74	6	.25
140.60	141.20	141.17	146.37	5	.25
141.43	143.84	136.34	73.53	4	.25
98.84	102.26	98.00	42.05	3	.25
38.61	0.00	0.00	8.17	2	.25
148.20	148.13	148.13	147.87	6	.125
148.22	147.90	148.05	152.91	5	.125
147.79	146.29	147.77	105.93	4	.125
111.25	106.59	103.00	46.77	3	.125
34.96	1.48	0.00	7.34	2	.125

TABLE 6-2

Integration Technique Comparison for Limited Data

Significant Figures. Sampling Time of 0.03.

ω_{FFT}	ω_{AS}	ω_{A}	ω_{NUM}	ND	PT
71.89	71.77	71.85	66.58	6	2.0
71.79	71.39	71.79	56.51	5	2.0
65.58	65.45	65.39	60.62	4	2.0
28.33	26.77	27.66	25.25	3	2.0
18.60	13.15	0.00	14.42	2	2.0
68.54	68.52	68.53	68.40	6	1.0
68.31	68.21	68.34	66.13	5	1.0
69.24	69.30	69.30	69.28	4	1.0
44.19	44.16	44.17	44.17	3	1.0
21.55	14.42	0.00	14.22	2	1.0
70.33	70.44	70.51	70.78	6	.50
70.37	70.43	70.55	69.40	5	.50
71.52	71.66	71.64	71.53	4	.50
69.65	69.76	69.75	69.71	3	.50
38.48	13.85	0.00	18.30	2	.50
74.03	74.17	74.17	74.30	6	.25
74.04	74.22	74.09	73.08	5	.25
73.66	73.52	63.39	66.15	4	.25
69.51	70.98	59.00	30.75	3	.25
45.97	0.00	0.00	9.22	2	.25

TABLE 6-3

Integration Technique Comparison for Limited Data

Significant Figures. Sampling Time of 0.06.

ω_{FFT}	ω_{AS}	ω_{A}	ω_{NUM}	ND	PT
34.04	34.09	34.07	33.62	6	2.0
33.92	34.03	33.89	31.96	5	2.0
32.68	32.70	32.67	32.75	4	2.0
26.90	26.59	26.83	25.07	3	2.0
10.10	10.32	0.00	9.10	2	2.0
35.44	35.49	35.49	35.51	6	1.0
35.45	35.53	35.50	35.29	5	1.0
35.70	35.73	35.73	35.73	4	1.0
38.65	38.75	38.75	38.78	3	1.0
19.82	12.42	0.00	12.68	2	1.0
36.86	37.03	37.03	37.04	6	.50
36.87	37.01	37.03	36.89	5	.50
36.79	36.94	36.94	36.95	4	.50
38.10	38.14	38.14	38.14	3	.50
26.32	2.36	1.65	13.38	2	.50

TABLE 6-4

Integration Technique Comparison for Limited Data Significant Figures. Sampling Time of 0.09.

ω_{FFT}	ω_{AS}	ω_{A}	ω_{NUM}	ND	PT
24.16	24.18	24.19	24.30	6	2.0
24.19	24.23	24.24	24.41	5	2.0
24.00	23.99	23.99	23.89	4	2.0
21.22	21.33	21.20	21.30	3	2.0
12.00	6.35	11.17	8.84	2	2.0
21.59	21.63	21.63	21.62	6	1.0
21.57	21.61	21.61	21.66	5	1.0
21.75	21.76	21.76	21.77	4	1.0
22.09	22.21	22.21	22.22	3	1.0
21.95	11.52	1.56	9.93	2	1.0
23.92	23.94	23.94	23.94	6	0.5
23.91	23.92	23.93	23.97	5	0.5
23.90	23.91	23.91	23.92	4	0.5
23.24	23.34	23.34	23.34	3	0.5
24.61	17.00	0.00	14.43	2	0.5

TABLE 6-5

Integration Technique Comparison for Limited Computer Significant Figures. Sampling Time of 0.015.

ω_{FFT}	ω_{ATS}	ω_{AT}	ω_{NUM}	ND	PT
132.62	131.86	132.62	99.43	6	2.0
116.98	123.10	123.49	64.41	5	2.0
46.84	71.52	70.41	36.12	4	2.0
17.97	0.00	0.00	1.87	3	2.0
142.98	142.79	143.07	133.24	6	1.0
140.37	141.42	141.19	102.56	5	1.0
74.82	110.00 * 2	112.00 * 2	47.00	4	1.0
28.57	20.00 * 5	22.00 * 5	12.04	3	1.0
137.43	137.65	137.26	131.91	6	.50
134.92	135.66	135.27	121.09	5	.50
110.55	118.00 * 4	109.00 * 4	64.20	4	.50
45.98	0.00	0.00	9.20	3	.50
140.01	140.24	140.29	139.35	6	.25
139.77	141.46	140.29	144.18	5	.25
121.74	136.00 * 4	137.00 * 4	69.53	4	.25
45.66	0.00	0.00	2.38	3	.25

TABLE 6-5 CONTINUED

ω_{FFT}	ω_{ATS}	ω_{AT}	ω_{NUM}	ND	PT
148.19	148.24	148.19	147.81	6	.125
147.49	147.33	145.76	152.30	5	.125
144.65	144.00 * 4.0	142.00 * 4	66.83	4	.125
15.38	0.00	0.00	1.30	3	.125

TABLE 6-6

Integration Technique Comparison for Limited Computer Significant Figures. Sampling Time of 0.03.

ω_{FFT}	ω_{AS}	ω_{A}	ω_{NUM}	ND	PT
72.06	71.80	71.90	66.57	6	2.0
72.73	71.47	72.12	55.51	5	2.0
45.44	65.86	65.73	34.02	4	2.0
21.33	1.29	1.14	9.05	3	2.0
68.52	68.56	68.57	68.31	6	1.0
67.06	68.53	68.67	65.23	5	1.0
56.95	69.37	69.58	44.96	4	1.0
27.88	23.00	* 29.00 3.5	12.67	3	1.0
70.36	70.43	70.50	70.69	6	.50
70.37	70.22	70.32	68.14	5	.50
67.22	65.22	62.41	56.22	4	.50
40.74	0.00	0.00	8.32	3	.50
74.00	74.19	74.18	74.30	6	.25
73.80	74.39	74.02	73.11	5	.25
71.05	65.11	* 70.00 2.0	62.50	4	.25
33.25	* 60.00 11	0.00	2.77	3	.25

TABLE 6-7

Integration Technique Comparison for Limited Computer Significant Figures. Sampling Time of 0.06.

ω_{FFT}	ω_{AS}	ω_{A}	ω_{NUM}	ND	PT
34.04	34.10	34.07	33.61	6	2.0
33.89	34.06	33.93	31.83	5	2.0
30.25	33.29	33.50	26.47	4	2.0
16.26	27.00 * 4	29.30 * 4	9.53	3	2.0
35.46	35.49	35.49	35.50	6	1.0
35.56	35.57	35.53	35.09	5	1.0
36.80	35.83	35.73	31.58	4	1.0
28.05	36.00 * 4	36.00 * 3	12.55	3	1.0
36.85	37.02	37.04	37.04	6	.50
36.83	37.05	37.07	36.86	5	.50
36.69	34.98	34.99	37.09	4	.50
29.50	27.00 * 3.5	27.00 * 3.5	7.09	3	.50

TABLE 6-8

Integration Technique Comparison for Limited Computer Significant Figures. Sampling Time of 0.09.

ω_{FFT}	ω_{AS}	ω_{A}	ω_{NUM}	ND	PT
24.15	24.18	24.19	24.32	6	2.0
24.13	24.21	24.24	24.54	5	2.0
23.27	23.93	23.86	24.07	4	2.0
15.61	21.00* 4	21.00* 4	10.38	3	2.0
21.60	21.63	21.63	21.62	6	1.0
21.64	21.60	21.61	21.63	5	1.0
22.01	21.81	21.70	21.49	4	1.0
22.32	21.80* 3	22.50* 3	11.92	3	1.0
23.93	23.93	23.94	23.94	6	.50
23.94	23.88	23.90	23.96	5	.50
24.19	22.40	22.93	23.95	4	.50
26.94	19.00* 4	20.50* 4	4.78	3	.50

70.0 if the error accumulated up to a frequency of 2.0 is discarded. Figure 6-1 is a log magnitude ratio versus log frequency plot which exhibits this instability at low frequencies. The same trends observed in Tables 6-1 to 6-4 are present in these tables. Therefore, these results show FFT to be the preferred integration technique.

6.4 Speed Comparison

To compare calculation speeds a test was set up using the same four integration techniques. Unlike FFT, the number of output frequencies of the ATS, AT, and NUM techniques is independent of the number of data points. However, to establish a basis for comparison $G(j\omega)$ was calculated at the same number of frequencies for all the techniques as the number given by FFT. Table 6-9 presents the effect on the calculation time of varying the number of data points for the four techniques. FFT is by far the fastest method and the speed advantage increases quickly with increases in the number of data points. REFFT is written so that a number of data points falling between two powers of 2 will require the calculation time of the higher power of two, but the speed of the method is such that this has little effect.

6.5 Conclusions

Comparison of the REFFT subroutine with more conventional calculation techniques reveals that REFFT is superior in both speed and accuracy. At very low significant figures its accuracy was noticeably superior and at higher significant figures its accuracy was equal to any of the other techniques. With respect to speed none of the other techniques was comparable.

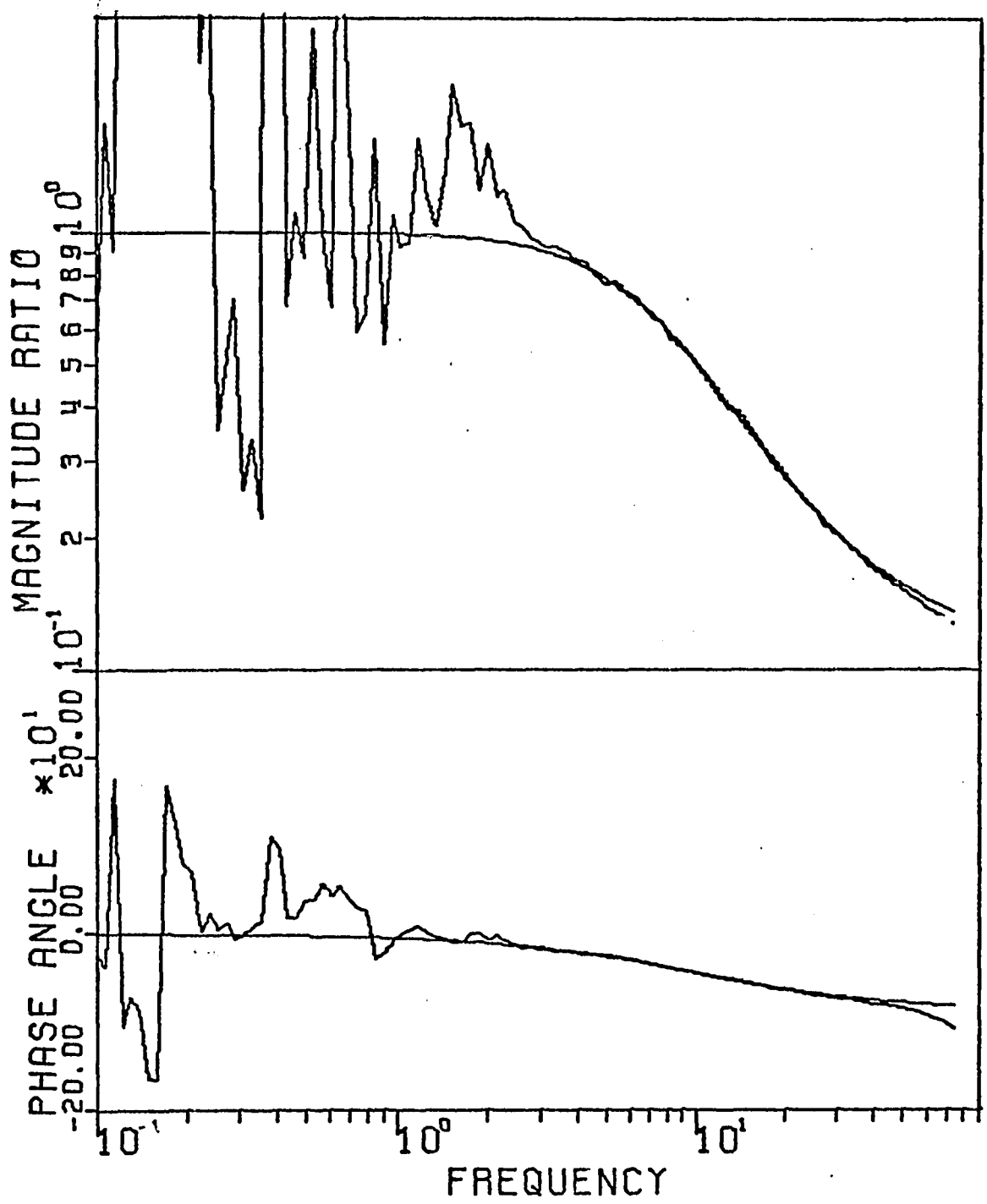

FIGURE 6-1. Bode Plot Exhibiting Instability at Low Frequencies.

TABLE 6-9

Speed Comparison of Integration Techniques

NUMBER OF DATA POINTS	CALCULATION TIME, SEC*				RATIO OF CALC. TIME TO FFT CALC. TIME		
	FFT	ATS	AT	NUM	ATS	AT	NUM
32	0.02	0.14	0.24	0.13	7.0	12.0	6.5
64	0.03	0.52	0.93	0.50	17.3	31.0	16.7
128	0.05	2.05	3.65	1.92	41.0	73.0	38.4
256	0.14	8.13	14.48	7.61	58.1	103.4	54.3

* SDS Sigma 5 Computer

LITERATURE CITED

1. Bergland, G. D., "A Fast Fourier Transform Algorithm for Real-Valued Series," Communications of the A. C. M., Vol. 11, no. 10, pp. 703-710, October, 1968.

2. _____, "A Fast Fourier Transform Algorithm Using Base 8 Iterations," Mathematics of Computation, Vol. 22, no. 102, pp. 275-279, April, 1968.

3. _____, "The Fast Fourier Transform Recursive Equations for Arbitrary Length Records," Mathematics of Computation, Vol. 21, pp. 236-238, April, 1967.

4. Cochran, W. T., Cooley, Favin, and others, "What is the Fast Fourier Transform?" I.E.E.E. Trans. on Audio and Electroacoustics, Vol. AU-15, no. 2, pp. 45-55, June, 1967.

5. Cooley, James W., Lewis, Welch. "Application of the Fast Fourier Transform to Computation of Fourier Integrals, Fourier Series, and Convolution Integrals," I.E.E.E. Trans. on Audio and Electroacoustics, Vol. AU-15, no. 2, pp. 79-84, June, 1967.

6. Cooley, J. W. and J. W. Turkey. "An Algorithm for the Machine Calculation of Complex Fourier Series," Mathematics of Computation, Vol. 19, pp. 297-301, April, 1965.

7. Gentleman, W. M. and G. Sands. "Fast Fourier Transforms for Fun and Profits," 1966 Fall Joint Computer Conf., AFIPS Proc., Vol. 29, Washington, D.C.: Spartan, 1966, pp. 563-578.

CHAPTER 7

SUMMARY

In order to make a definitive study of the maximum recoverable frequency from Fourier analysis and develop correlations with the factors influencing it, a criterion is needed to define the maximum recoverable frequency mathematically. Accordingly, twelve different criteria were evaluated in Chapter 2 and the integral of the squared fractional complex point error

$$\int \left(\frac{e_{cp}}{M_{cp}}\right)^2 dL\omega$$

was selected as the best criterion.

This error criterion was applied in Chapter 3 to determine what effect the fold-over from sampling has on the maximum recoverable frequency. For a noiseless system the maximum recoverable frequency was found to be a function of the sampling frequency where the sampling frequencies for the input and output pulses were equal. Defining a "theoretical" maximum recoverable frequency as 1/2 the sampling frequency, the percentage of this theoretical value which could be recovered was found to be approximately constant and equal to 66% for first order systems and a 0.01 error criterion value. The percentage recovery for noiseless second order systems was somewhat higher than for first order systems.

Investigation in Chapter 4 into the effect of noise showed that noise causes significant reductions in the maximum recoverable frequency for high sampling frequencies but has a much less severe effect at lower sampling frequencies. This is explained by the shape of the frequency content curve and the existence of a relationship between noise level and the frequency content at the maximum recoverable frequency. This relationship is shown graphically in Figures 4-9, 10, 11, and 12. For a given sampling frequency it was found that the RMS value of the noise was related to the frequency content of the output pulse (FCO) by the following equation:

$$\log \text{RMS} = b \log \text{FCO} + \log a \qquad 7.1$$

While the constant "b" changed very little with sampling frequency, the constant "a" did vary with sampling frequency. This correlation defines the noise constraint on the maximum recoverable frequency and coupled with the sampling frequency constraint developed in Chapter 3 adequately predicts the maximum recoverable frequency. As shown by Equation 7.1, increasing the frequency content in the presence of noise is beneficial. Although this is frequently accomplished by shortening the input pulse duration, it was shown that it is possible for this action to have the opposite effect and decrease the frequency content at the frequencies of interest.

Both pre- and post-sample filtering as a means of increasing the recoverable frequency were investigated in Chapter 5. Although post-sample filtering proved ineffective, pre-sample filtering

(filtering of the continuous signal) was very effective in increasing the recoverable frequency, even when no noise was present. Upper and lower constraints were defined for the time constant of the first order lag filter used in the study. The upper constraint is the system's dominant time constant while the lower constraint is the reciprocal of the folding frequency or sampling time/π. The lower constraint was found to be by far the most critical of the two constraints, but unless the lower constraint was approached too closely, very little difference in the results was noted for any time constant within the constraints.

Chapter 5 also considers the effect of significant figures on the Fourier transform calculation. Equation 5.4 was found to be adequate for relating noise derived from limited data significant figures to the normal process noise. This should prove useful in determining the suitability of recording equipment. This study found that four significant figure data was very desirable and that the number of computer significant figures should be one greater than the number of data significant figures.

In Chapter 6 a version of the Fast Fourier Transform is applied to the pulse data to frequency domain transformation problem. A special subroutine, REFFT, which uses the real-valued fast Fourier transform in a very efficient manner, is introduced to perform the calculations. The speed and accuracy of this method was compared with more conventional calculation methods and demonstrated to be superior. At very low significant figures it

proved more accurate and at higher significant figures it was equal to any of the other techniques. The speed comparison revealed the REFFT subroutine to be extremely fast compared to the other methods.

APPENDIX A

The following is a description of the implementation and use of subroutine REFFT.

Purpose

REFFT is a subroutine which will quickly convert pulse response time data to frequency response data.

Description

This subroutine uses the real-valued Fast Fourier Transform for converting pulse response data from the time domain to the frequency domain. The ratio of the time required for calculating Fourier transforms via the Fast Fourier Transform to the time required by conventional techniques is approximately $\frac{\log_2 N}{N}$, where N is the number of data points. As N increases, the reduction in time required quickly becomes very large. The real-valued Fast Fourier Transform is a Fast Fourier Transform technique written especially for the case where the input is restricted to real numbers and it takes advantage of this to eleminate unnecessary calculations. The technique is described in detail in "A Fast Fourier Transform Algorithm for Real-Valued Series," by G. D. Bergland in Communications of the ACM, Vol. 11, no. 10, pp. 703-710, October, 1968.

Subroutine REFFT has been written specifically for converting pulse response data and computes the input and output pulse transforms

simultaneously, thereby effecting additional economics in calculation. The accuracy of REFFT is at least as good as that of conventional techniques and in some cases it is better than conventional techniques. The printed output provided by REFFT is phase angles, amplitude ratios and associated frequencies.

Implementation

REFFT assumes that the same constant time increment, ST, between data points is used for both the input and output pulses. REFFT must be provided with NX, NY, ST, X, Y from the main program where

NX = number of data points in X array

NY = number of data points in Y array

ST = time increment between data points

X = input pulse data array

Y = output pulse data array.

These values enter REFFT through a COMMON statement. From this data REFFT calculates and prints out phase angles, amplitude ratios and the associated frequencies. The frequencies will range between 0.0 and 1/2 the sampling frequency (sampling frequency = $2\pi/ST$). The number of frequencies will be equal to one plus the smallest power of 2 which is greater than or equal to NY. REFFT is designed to accomodate an NY of up to 1024.

Modifications

Changing the maximum NY which the program will handle is relatively simple. Let MN equal the maximum NY. Note that MN must be a power of 2 ($1024 = 2^{10}$) which is greater than or equal to any

NY desired. The memory allocations in DIMENSION and COMMON must be as follows

DIMENSION KE($\frac{MN}{4}$), WC($\frac{MN}{4}$), WS($\frac{MN}{4}$), PHA($\frac{MN}{2}$ + 1), G($\frac{MN}{2}$ + 1)

COMMON NX, NY, X(MN), Y(MN)

In addition in subroutine REFFT the statement

DO 7 M =1,10

must be changed to

DO 7 M = 1,P

where 2^P = MN.

Increasing the frequency resolution involves only two changes. The program searches to find NN, the smallest power of 2 greater than or equal to NY, and outputs a number of frequencies equal to NN + 1. To increase the resolution, then, in REFFT, statement 1 can be changed to read, for example,

1 NN = 2 * I

If still greater resolution is desired then multiply I by a larger power of 2. When this modification is made the following statement should be added immediately following statement 1

M = M + K

where 2^K = the power of 2 multiplied times I in statement 1.

Should the real and imaginary values of the complex point represented by the amplitude ratio G and the phase angle PHA be desired, they are readily available. The complex point G(jω) is calculated as

G(jω) = AR + j AI

where AR = real value of $G(j\omega)$

AI = imaginary value of $G(j\omega)$.

AR and AI are available in the program and can be outputted as desired.

Example

Given data points for the input pulse, X(t), and the output pulse, Y(t), from a pulse response test on a system it is desired to convert this data to frequency response data, i.e. phase angles, amplitude ratios, and frequencies. The data, X(t) and Y(t), could be read into the program from data cards, but in this example the data will be generated in Subroutine DATA. For this case NX = NY but this is not necessary and involved no changes in REFFT. The pulse input used has the equations

$$X(t) = \frac{8t^3}{T_P} \qquad \text{for} \qquad 0 \leq t \leq \frac{T_P}{2}$$

$$X(t) = 8\left(1 - \frac{t}{T_P}^3\right) \qquad \text{for} \qquad \frac{T_P}{2} < t \leq T_P$$

where T_P = pulse duration.

The system is a first order lag with a time constant of 0.1.

Program

APPENDIX A

DESCRIPTION AND IMPLEMENTATION OF REFFT

```
C*************************************************************************
C     EXAMPLE PROGRAM ILLUSTRATING THE USE OF REFFT
C*************************************************************************
C
C     ST = TIME INTERVAL BETWEEN DATA POINTS
      COMMON NX,NY,ST,X(1024),Y(1024)
      READ 8,ST
    8 FORMAT(F6.4)
      CALL DATA
      CALL REFFT
      STOP
      END
C*************************************************************************
      SUBROUTINE REFFT
C
C     SUBROUTINE FOR CONVERTING PULSE RESPONSE
C     TIME DATA TO FREQUENCY RESPONSE DATA
C     VIA THE REAL-VALUED FAST FOURIER TRANSFORM
C*************************************************************************
C
C     THIS PROGRAM EVALUATES THE COMPLEX POINT G(JW) = AR + J AI
C     AND PRINTS THE MAGNITUDE,G, PHASE ANGLE,PHA, AND FREQ,W
C     AR = REAL PART OF G(JW)
C     AI = IMAGINARY PART OF G(JW)
C
C     INPUT TO SUBROUTINE ENTERED THROUGH COMMON STATEMENT
C               (NOTES:
C                     1.  THE VALUE OF ST SHOULD BE IN
C                     THE TIME UNITS DESIRED FOR THE
C                     FREQUENCY VALUES, I.E. ST IN
C                     SECONDS IF FREQUENCY VALUES IN
```

```
C                       RADIANS/SEC. DESIRED.
C                       2.  THE ST OF X IS ASSUMED EQUAL
C                       TO THAT OF Y.
C
C     INPUT:
C           NX...NUMBER OF DATA POINTS IN ARRAY X
C           NY...NUMBER OF DATA POINTS IN ARRAY Y
C           ST...TIME INCREMENT BETWEEN DATA POINTS
C           X...ARRAY OF INPUT PULSE VALUES
C           Y...ARRAY OF OUTPUT PULSE VALUES
C
C     OUTPUT:
C           W.....FREQUENCY ASSOCIATED WITH G AND PHA, RADIANS/TIME UNIT
C           G.....AMPLITUDE RATIO
C           PHA...PHASE ANGLE, DEGREES
C
      DIMENSION KE(512),WC(512),WS(512),PHA(512),G(512)
      DIMENSION AR(512),AI(512),W(512)
      COMMON NX,NY,ST,X(1024),Y(1024)
C
C      DETERMINE SMALLEST POWER OF 2 ENCOMPASSING NY AND
C      FILL IN MISSING POINTS OF X AND Y WITH ZEROES
      I=2
      DO 7 M=1,10
      IF(NY.LE.I) GO TO 1
    7 I=I*2
      GO TO 90
    1 NN=I
      NYP1 = NY + 1
      NXP1 = NX + 1
      DO 8 I=NYP1,NN
```

```
    8   Y(I) = 0.0
        DO 4 I=NXP1,NN
    4   X(I) = 0.0
        MM2 = M-2
        MM3 = M - 3
        NMM2 = 2**MM2
        ANN = NN
        SCALE = 6.2831853/ANN
C
C       CALCULATE EXPONENT TABLE
        KMD = 4
        KE(1) = 0
        KE(2) = 1
        DO 203 J=1,MM2
        IF(J.NE.MM2) GO TO 205
        DO 204 JE=2,NMM2
        AKE = KE(JE)
        OMEGA = SCALE*AKE
        WS(JE) = SIN(OMEGA)
        WC(JE) = COS(OMEGA)
  204   CONTINUE
  205   KD = KMD - 3
        IM = KMD/2
        DO 202 I=1,KD,2
        I1 = KMD - I
        KE(I1) = KE(IM)
  202   IM = IM - 1
        KE(2) = 2*KE(2)
        IN = 2*KE(2)
        DO 201 K1 = 4,KMD,2
        IM1 = K1 - 1
```

```
  201   KE(K1) = IN - KF(IM1)
  203   KMD = KMD*2
C
C       CALCULATE TRANSFORM
        MXX = 1
        MX = NN/4
        MM1 = M - 1
        DO 100 I=1,MM1
        IC1 = 1
        DO 101 J=1,MXX
        IC2 = IC1 + MX
        IC3 = IC2 + MX
        IC4 = IC3 + MX
        IF(J.EQ.1) GO TO 9
        C1 = WC(J)
        S1 = WS(J)
    9   DO 102 K=1,MX
        XIC1 = X(IC1)
        XIC2 = X(IC2)
        XIC3 = X(IC3)
        XIC4 = X(IC4)
        YIC1 = Y(IC1)
        YIC2 = Y(IC2)
        YIC3 = Y(IC3)
        YIC4 = Y(IC4)
        IF(J.EQ.1) GO TO 5
        WXR = C1*XIC2 + S1*XIC4
        WXI = -S1*XIC2 + C1*XIC4
        WYR = C1*YIC2 + S1*YIC4
        WYI = -S1*YIC2 + C1*YIC4
        X(IC1) = XIC1 + WXR
```

```
      Y(IC1) = YIC1 + WYR
      X(IC2) = XIC3 + WXI
      Y(IC2) = YIC3 + WYI
      X(IC3) = XIC1 - WXR
      Y(IC3) = YIC1 - WYR
      X(IC4) = -XIC3 + WXI
      Y(IC4) = -YIC3 + WYI
      GO TO 6
    5 X(IC1) = XIC1 + XIC3
      Y(IC1) = YIC1 + YIC3
      X(IC2) = XIC2 + XIC4
      Y(IC2) = YIC2 + YIC4
      X(IC3) = XIC1 - XIC3
      Y(IC3) = YIC1 - YIC3
      X(IC4) = -XIC2 + XIC4
      Y(IC4) = -YIC2 + YIC4
    6 IC1 = IC1 + 1
      IC2 = IC2 + 1
      IC3 = IC3 + 1
  102 IC4 = IC4 + 1
  101 IC1 = IC4
      MXX = MXX*2
  100 MX = MX/2
C
C       UNSCRAMBLE POINTS
      K1 = 1
      DO 504 J = 3,NN,2
      K1 = K1 + 1
      J1 = J + 1
      K = KF(K1) + 1
      XR = X(J)
```

```
      XI = X(J1)
      YR = Y(J)
      YI = Y(J1)
      DC = XI*XI + XR*XR
      AR(K) = (YR*XR + YI*XI)/DC
      AI(K) = (YI*XR - YR*XI)/DC
      AIK = AI(K)
      ARK = AR(K)
      PHA(K) = ATAN2(AIK,ARK)*57.29578
  504 G(K) = SQRT((YR*YR+YI*YI)/(XR*XR+XI*XI))
      NN2 = NN/2
      N2P1 = NN2 + 1
      A2 = 1.
      DO 506 I=1,N2P1,NN2
      IF(I.GT.1)A2=-1.
      XR = X(1) + A2*X(2)
      YR = Y(1) + A2*Y(2)
      AR(I) = YR/XR
      AI(I) = 0.0
      AII = 0.0
      ARI = AR(I)
      PHA(I) = ATAN2(AII,ARI)*57.29578
  506 G(I) = ARI
C
C     PRINT OUTPUT
      PRINT 200
  200 FORMAT(6X4HFREQ,11X1HG,12X5HANGLE//)
      F1 = SCALE/ST
      DO 400 I=1,N2P1
      I1 = I-1
      F2 = I1
```

```
      FREQ = F1*F2
      W(I) = FREQ
      PRINT 401,W(I),G(I),PHA(I)
 401  FORMAT(1XF10.4,2F15.7)
 400  CONTINUE
 90   RETURN
      END
C
C*****************************************************************************
      SUBROUTINE DATA
C*****************************************************************************
C
C     GENERATES THE X ARRAY, Y ARRAY, NX, AND NY
      COMMON NX,NY,ST,X(1024),Y(1024)
      I=0
      PULSE=0.0
      Y2=0.0
C
C     FIRST ORDER LAG SYSTEM TIME CONSTANT
      TC = 0.1
C
C     PULSE DURATION
      PT = 1.0
C
      PTD = PT*PT*PT
      PT2 = PT/2.
      TS = 0.0
      L = 2000
      ICORE = (ST/.0005)*(2./PT) + .5
      CORE = ICORE
      H = ST/CORE
```

```
  2    TS = TS + H
C
C      CALCULATE CUBED TRIANGULAR PULSE
       IF(TS.GT.PT2) GO TO 3
       PSD = 8.*TS*TS*TS/PTD
       GO TO 4
  3    IF(TS.GT.PT) GO TO 5
       PSD = 8.*(1.-TS/PT)*(1.-TS/PT)*(1.-TS/PT)
       GO TO 4
  5    PSD = 0.0
  4    PULSE = PSD
       Y2 = Y2 + (PULSE - Y2)*H/TC
       I = I + 1
       IF(I.LT.ICARF) GO TO 2
       I = 0
       J = J + 1
       Y(J) = Y2
       X(J) = PULSE
       IF ( TS.LT.PT2) GO TO 2
       IF(Y2.GT.0.00001) GO TO 2
C
C      FOR THIS EXAMPLE NX=NY BUT THIS IS NOT NECESSARY
       NX = J
       NY = J
       RETURN
       END
```

APPENDIX B

PROGRAM FOR EVALUATING THE EFFECT ON THE ACCURACY OF REFFT OF LIMITING THE NUMBER OF COMPUTER SIGNIFICANT FIGURES

```
C
C*************************************************************************
C      PROGRAM FOR EVALUATING THE EFFECT ON THE ACCURACY
C      OF REFFT OF LIMITING THE COMPUTER SIGNIFICANT FIGURES
C*************************************************************************
C
C
C     ND = NUMBER OF SIGNIFICANT FIGURES
C     CHOP = DATA TIME LENGTH
C
       COMMON CHOP
       COMMON ND
       COMMON NX,NY,ST,X(512),Y(512)
C
C      INPUT:
C      ST = TIME INTERVAL BETWEEN DATA POINTS
C      PT = PULSE DURATION; READ IN TWICE THE DESIRED VALUE
C      TC = FIRST ORDER LAG SYSTEM TIME CONSTANT
C
       READ 100,ST,PT,TC
  100  FORMAT(3F10.5)
C
C      DO LOOP TO GENERATE FIVE DIFFERENT PULSE TIMES
       DO 31 K4=1,5
       PT=PT/2.
       IF(K4.EQ.1) CHOP=3.0
       IF(K4.EQ.2) CHOP=2.2
       IF(K4.EQ.3) CHOP=1.85
       IF(K4.EQ.4) CHOP=1.65
       IF(K4.EQ.5) CHOP=1.5
C
```

```
C       DO LOOP VARIES NUMBER OF SIGNIFICANT FIGURES
        ND=7
        DO 88 JT=1,5
        ND=ND-1
        PRINT 87
        PRINT 86,ND,ST,PT
   86   FORMAT(1HO,20HSIGNIFICANT DIGITS =,I3,5X4HST =,F6.3,5X4HPT =,F6.3)
        PRINT 87
   87   FORMAT(1HO)
        CALL DATA(PT,TC)
        CALL REFFT
   88   CONTINUE
    89  CONTINUE
  31    CONTINUE
        STOP
        END
C
C*******************************************************************************
      SUBROUTINE REFFT
C*******************************************************************************
C
C       SUBROUTINE FOR CONVERTING PULSE RESPONSE
C       TIME DATA TO FREQUENCY RESPONSE DATA
C       VIA THE REAL-VALUED FAST FOURIER TRANSFORM
C
C       THIS PROGRAM EVALUATES THE COMPLEX POINT G(JW) = AR + J AI
C       AND PRINTS THE MAGNITUDE,G, PHASE ANGLE,PHA, AND FREQ,W
C       AR = REAL PART OF G(JW)
C       AI = IMAGINARY PART OF G(JW)
C
C       INPUT TO SUBROUTINE ENTERED THROUGH COMMON STATEMENT
```

```
      COMMON ND
      COMMON NX,NY,ST,X(1024),Y(1024)
C
C      DETERMINE SMALLEST POWER OF 2 ENCOMPASSING NY AND
C      FILL IN MISSING POINTS OF X AND Y WITH ZEROES
      NN = 2
      DO 7 M=1,10
```

```
      IF(NY.LE.NN) GO TO 1
    7 NN = NN*2
      GO TO 90
    1 NYP1 = NY + 1
      NXP1 = NX + 1
      DO 8 I=NYP1,NN
    8 Y(I) = 0.0
      DO 9 I=NXP1,NN
    9 X(I)=0.0
      MM2 = M-2
      MM3 = M - 3
      NMM2 = 2**MM2
      ANN = NN
      SCALE = 6.2831853/ANN
C
C       CALCULATE EXPONENT TABLE
      KMD = 4
      KE(1) = 0
      KE(2) = 1
      DO 203 J=1,MM2
      IF(J.NE.MM2) GO TO 205
      DO 204 JE=2,NMM2
      AKE = KE(JE)
      OMEGA = SCALE*AKE
      WS(JE) = SIN(OMEGA)
      WC(JE) = COS(OMEGA)
  204 CONTINUE
  205 KD = KMD - 3
      IM = KMD/2
      DO 202 I=1,KD,2
      I1 = KMD - I
```

```
      KE(I1) = KF(IM)
  202 IM = IM - 1
      KE(2) = 2*KE(2)
      IN = 2*KE(2)
      DO 201 K1 = 4,KMD,2
      IM1 = K1 - 1
  201 KE(K1) = IN - KF(IM1)
  203 KMD = KMD*2
C
C       CALCULATE TRANSFORM
      MXX = 1
      MX = NN/4
      MM1 = M - 1
      DO 100 I=1,MM1
      IC1 = 1
      DO 101 J=1,MXX
      IC2 = IC1 + MX
      IC3 = IC2 + MX
      IC4 = IC3 + MX
      IF(J.EQ.1) GO TO 9
      C1 = WC(J)
      S1 = WS(J)
      C1=PREC(C1)
      S1=PREC(S1)
    9 DO 102 K=1,MX
      XIC1 = X(IC1)
      XIC2 = X(IC2)
      XIC3 = X(IC3)
      XIC4 = X(IC4)
      YIC1 = Y(IC1)
      YIC2 = Y(IC2)
```

```
      YIC3 = Y(IC3)
      YIC4 = Y(IC4)
      XIC1=PREC(XIC1)
      XIC2=PREC(XIC2)
      XIC3=PREC(XIC3)
      XIC4=PREC(XIC4)
      YIC1=PREC(YIC1)
      YIC2=PREC(YIC2)
      YIC3=PREC(YIC3)
      YIC4=PREC(YIC4)
      IF(J.EQ.1) GO TO 5
      WXR=PREC(PREC(C1*XIC2)+PREC(S1*XIC4))
      WXI=PREC(PREC(-S1*XIC2)+PREC(C1*XIC4))
      WYR=PREC(PREC(C1*YIC2)+PREC(S1*YIC4))
      WYI=PREC(PREC(-S1*YIC2)+PREC(C1*YIC4))
      X(IC1) = XIC1 + WXR
      Y(IC1) = YIC1 + WYR
      X(IC2) = XIC3 + WXI
      Y(IC2) = YIC3 + WYI
      X(IC3) = XIC1 - WXR
      Y(IC3) = YIC1 - WYR
      X(IC4) = -XIC3 + WXI
      Y(IC4) = -YIC3 + WYI
      GO TO 6
5     X(IC1) = XIC1 + XIC3
      Y(IC1) = YIC1 + YIC3
      X(IC2) = XIC2 + XIC4
      Y(IC2) = YIC2 + YIC4
      X(IC3) = XIC1 - XIC3
      Y(IC3) = YIC1 - YIC3
      X(IC4) = -XIC2 + XIC4
```

```
      Y(IC4) = -YIC2 + YIC4
    6 IC1 = IC1 + 1
      IC2 = IC2 + 1
      IC3 = IC3 + 1
  102 IC4 = IC4 + 1
  101 IC1 = IC4
      MXX = MXX*2
  100 MX = MX/2
C
C       UNSCRAMBLE POINTS, CALCULATE G AND PHA
      K1 = 1
      DO 504 J = 3,NN,2
      K1 = K1 + 1
      J1 = J + 1
      K = KF(K1) + 1
      XR = X(J)
      XI = X(J1)
      YR = Y(J)
      YI = Y(J1)
      XR=PREC(XR)
      XI=PREC(XI)
      YR=PREC(YR)
      YI=PREC(YI)
      DC=PREC(PREC(XI*XI)+PREC(XR*XR))
      AR(K)=PREC(PREC(PREC(YR*XR)+PREC(YI*XI))/DC)
      AI(K)=PREC(PREC(PREC(YI*XR)-PREC(YR*XI))/DC)
      AIK = AI(K)
      ARK = AR(K)
      PHA(K) = ATAN2(AIK,ARK)*57.29578
      DS=PREC(PREC(XR*XR)+PREC(XI*XI))
  504 G(K)=PREC(SQRT(PREC(PREC(PREC(YR*YR)+PREC(YI*YI))/DS)))
```

```
      NN2 = NN/2
      N2P1 = NN2 + 1
      A2 = 1.
      X1=X(1)
      X2=X(2)
      Y1=Y(1)
      Y2=Y(2)
      DO 506 I=1,N2P1,NN2
      IF(I.GT.1)A2=-1.
      XR=PREC(PREC(X1)+PREC(A2*X2))
      YR=PREC(PREC(Y1)+PREC(A2*Y2))
      AR(I)=PREC(YR/XR)
      AI(I) = 0.0
      AII = 0.0
      ARI = AR(I)
      PHA(I) = ATAN2(AII,ARI)*57.29578
  506 G(I) = ARI
      PRINT 200
  200 FORMAT(6X4HFREQ,11X1HG,12X5HANGLE//)
      F1 = SCALE/ST
C
C     INTEGRATE THE ERROR
C     CER= INTEGRAL OF THE NORMALIZED, SQUARED COMPLEX POINT ERROR
      ER(1) = 0.0
      CER(1) = 0.0
      CER(2) = 0.0
      DO 400 I=2,N2P1
      I1 = I-1
      F2 = I1
      FREQ = F1*F2
      W(I) = FREQ
```

```
C
C       CALCULATE TRUE COMPLEX POINT,GA,PHA
C       CALCULATE TRUE COMPLEX POINT, GA, PHA
C       GA = TRUE AMPLITUDE RATIO
C       PA = TRUE PHASE ANGLE
        D = 1. + .01*FREQ*FREQ
        AA = 1./D
        BA = - .1*(FREQ/D)
        GA = 1./SQRT(D)
        PA = ATAN2(BA,AA)*57.29578
        E1 = AR(I) - AA
        E2 = AI(I) - BA
        D1 = AA*AA + BA*BA
        ER(I) = SQRT((E1*E1 + E2*E2)/D1)
        IF(I.EQ.2) GO TO 400
        E3 = I-2
        DLW = ALOG10(F2/F3)
        CER(I) = CER(I1) +    ((ER(I)+ER(I1))*(ER(I)+ER(I1))*DLW)/4.
C
C       OUTPUT
        PRINT 600, FREQ,CER(I),G(I),GA,PHA(I),PA
  600   FORMAT(1XF10.4,F13.8,5XF10.8,5XF10.8,5XF10.5,5XF10.5)
  400   CONTINUE
C
C       SEARCH FOR FREQ AT CER=0.01, W01
        IF(CER(N2P1).LT..01) GO TO 90
        DO 36 I5=1,N2P1
        I4=N2P1-I5
        IF(CER(I4).GT..01) GO TO 36
        I6=I4+1
        WR = (.01-CER(I4))/(CER(I6)-CER(I4))
```

```
      W01 = W(I4) + (W(I6) - W(I4))*WR
      GO TO 37
   36 CONTINUE
      GO TO 90
   37 PRINT 38, W01
   38 FORMAT(1X6HW01 = ,F10.4)
   90 RETURN
      END
C
C*************************************************************************
      SUBROUTINE DATA(PT,TC)
C*************************************************************************
C
C     GENERATES THE X, Y ARRAYS
C
      COMMON CHAP
      COMMON ND
      COMMON NX,NY,ST,X(512),Y(512)
      I = 0
      PULSE = 0.0
      Y2 = 0.0
      PTD = PT*PT*PT
      PT2 = PT/2.
      TS = 0.0
      L = 2000
      ICORE = (ST/.0005)*(2./PT) + .5
      CORE = ICORE
      H = ST/CORE
    2 TS = TS + H
C
C     CALCULATE CUBED TRIANGULAR PULSE
```

```
      IF(TS.GT.PT2) GO TO 3
      PSD = 8.*TS*TS*TS/PTD
      GO TO 4
    3 IF(TS.GT.PT) GO TO 5
      PSD = 8.*(1.-TS/PT)*(1.-TS/PT)*(1.-TS/PT)
      GO TO 4
    5 PSD = 0.0
    4 PULSE = PSD
      Y2 = Y2 + (PULSE - Y2)*H/TC
      L = L + 1
      IF(L.LT.ICARF) GO TO 2
      L = 0
      I = I + 1
      Y(I) = Y2
      X(I) = PULSE
      IF(TS.LT.CHAP) GO TO 2
      NX = I
      NY = I
      RETURN
      END
C
C*******************************************************************************
      FUNCTION PREC(XX)
C*******************************************************************************
C
C     FUNCTION PREC TRUNCATES THE ARGUMENT AT PREC TO
C     ND SIGNIFICANT FIGURES.
C
      DIMENSION IDIG(6)
      COMMON CHAP
      COMMON ND
```

```
      IF(XX.NE.0.) GO TO 4
      PREC = 0.
      GO TO 9
4     Y=ABS(XX)
      J=ALOG10(Y)
      X=XX/(10.**J)
      DO7 I=1,ND
      IDIG(I)=X
7     X=(X-FLOAT(IDIG(I)))*10.
      X=0.
      DO 8 I=1,ND
8     X=X+FLOAT(IDIG(I))*10.**(-I+1)
      PREC=X*10.**J
9     RETURN
      END
```

APPENDIX C

PROGRAM FOR EVALUATING THE EFFECT ON THE ACCURACY OF THE ANALYTICAL TRAPEZOID INTEGRATION TECHNIQUE OF LIMITING THE NUMBER OF COMPUTER SIGNIFICANT FIGURES

```
C*************************************************************************
C     PROGRAM FOR EVALUATING THE EFFECT ON THE ACCURACY OF THE
C     ANALYTICAL TRAPEZOID INTEGRATION TECHNIQUE OF LIMITING THE
C     NUMBER OF COMPUTER SIGNIFICANT FIGURES
C*************************************************************************
C
C     G = AMPLITUDE RATIO
C     PHA = PHASE ANGLE
C     X = INPUT PULSE DATA ARRAY
C     Y = OUTPUT PULSE DATA ARRAY
      COMMON CHOP
      COMMON ND
      COMMON STX,STY,X(500),Y(500),TX(500),TY(500),NX,NY
C
C     INPUT:
C           STX = TIME INCREMENT BETWEEN X DATA POINTS
C           STY = TIME INCREMENT BETWEEN Y DATA POINTS
C           PT = PULSE DURATION
C           TC = FIRST ORDER LAG SYSTEM TIME CONSTANT
C           W1 = LOWER FREQUENCY INVESTIGATED
C           W2 = UPPER FREQUENCY INVESTIGATED
   10 READ 20, STX,STY,PT,TC,W1,W2
   20 FORMAT(6F10.4)
      TF=0.03
C
C     DO LOOP TO VARY THE INPUT PULSE DURATION
      DO 89 K4=1,5
      PT=PT/2.
C
C     CHOP DETERMINES THE TRUNCATION POINT OF THE PULSE DATA
      IF(K4.EQ.1) CHOP=3.0
```

```
      IF(K4.EQ.2) CHAP=2.2
      IF(K4.EQ.3) CHAP=1.85
      IF(K4.EQ.4) CHAP=1.65
      IF(K4.EQ.5) CHAP=1.5
      ND=7
C
      DO 100P TO VARY THE NUMBER OF SIGNIFICANT DIGITS
      DO 88 JT=1,5
      PRINT 87
      PRINT 86,ND,STX,PT
   86 FORMAT(1HO,20HSIGNIFICANT DIGITS =,I3,5X4HST =,F6.3,5X4HPT =,F6.3)
      PRINT 87
   87 FORMAT(1HO)
      CALL DATAY(PT,TC,TF)
      CALL CALC(PT,W1,W2)
   88 CONTINUE
   89 CONTINUE
      GO TO 10
   13 STOP
      END
C
C*******************************************************************************
      SUBROUTINE CALC(TP,W1,W2)
C*******************************************************************************
C
C     SUBROUTINE TO PERFORM INTEGRATION
      DIMENSION FR(300), CFR(300), W(203)
      DIMENSION PA(203),GA(203)
      DIMENSION G(203)
      DIMENSION PHA(203)
      COMMON CHAP
```

```
      COMMON ND
      COMMON STX,STY,X(500),Y(500),TX(500),TY(500),NX,NY
      TC=0.1
      JEN=100
      DO70 I =1,NY
      YL=Y(I )
      Y(I )=PREC(YL)
      XL=X(I )
      X(I )=PREC(XL)
      TL=TY(I )
      TY(I )=PREC(TL)
70    TX(I )=TY(I )
      DO 2 ID=2,102
      ER(1)=0.0
      CER(1)=0.0
      UC=0.0
      UR = 0.0
      XC=0.0
      XR=0.0
      WJ=ID-2
      M=ID-1
      I=M
      I1=I-1
      WLL=ALOG(W1)
      WUL=ALOG(W2)
      WE=(WUL-WLL )*WJ/100. + WLL
      W(M)=EXP(WE)
      WI=W(M)
      DO 190 K=2,NY
      K1=K-1
      AN1=PREC(WI*TY(K))
```

```
      AN2=PREC(WI*TY(K1))
      DSI=PREC(PREC(SIN(AN1))-PREC(SIN(AN2)))
      DCB=PREC(PREC(CBS(AN1))-PREC(CBS(AN2)))
      SC=PREC(PREC(Y(K)-Y(K1))/STX)
      SR=PREC(PREC(X(K)-X(K1))/STX)
      XC=XC+PREC(SC*DSI)
      XC=PREC(XC)
      XR=XR+PREC(SR*DSI)
      XR=PREC(XR)
      UC=UC+PREC(SC*DCB)
      UC=PREC(UC)
      UR=UR+PREC(SR*DCB)
      UR=PREC(UR)
  190 CONTINUE
      DS1=UR*UR+XR*XR
      DS2=UC*UR+XC*XR
      DS3=UC*XR-UR*XC
      G(M)=SQRT((UC*UC+XC*XC)/DS1)
      DR=DS2/DS1
      DI=DS3/DS1
      PHA(I)=ATAN2(DI,DR)*57.29578
      D=1.+.01*WI*WI
      GA(I)=1./SQRT(D)
      AA = 1./D
      BA=-.1*(WI/D)
      PA(I)=ATAN2(BA,AA)*57.29578
      D1 = AA*AA + BA*BA
      E2=DI-BA
      E1=DR-AA
      ER(I) = SQRT((E1*E1 + E2*E2)/D1)
      IF(I.EQ.1) GB TB 2
```

```
      WMD=W(I1)
      DLW=ALOG10(WI/WMD)
      CER(I) = CER(I1) +    ((ER(I)+ER(I1))*(ER(I)+ER(I1))*DLW)/4.
      PRINT 338,W(I),CER(I)
  338 FORMAT(1X2F15.7)
  2   CONTINUE
      IF(CER(JEN).LT..01) GO TO 90
      DO 36 I5=1,100
      I4=100-I5
      IF(CER(I4).GT..01) GO TO 36
      I6=I4+1
      WR = (.01-CER(I4))/(CER(I6)-CER(I4))
      W01 = W(I4) + (W(I6) - W(I4))*WR
      GO TO 37
  36  CONTINUE
      GO TO 90
  37  PRINT 38, W01
  38  FORMAT(1X6HW01 = ,F10.4)
   90 CONTINUE
      STX=STY
      RETURN
      END
C
C*******************************************************************************
      SUBROUTINE DATAY(PT,TC,TF)
C*******************************************************************************
C
C     GENERATES X,Y DATA
      COMMON CHAP
      COMMON ND
      COMMON STX,STY,X(500),Y(500),TX(500),TY(500),NX,NY
```

```
      DD = 0.0
      IX=3791359
      I=0
      PULSE = 0.0
      Y2=0.0
      PTD = PT*PT*PT
      PT2 = PT/2.
      TS = 0.0
      L = 2000
      ICARF = (STY/.0005)*(2./PT) + .5
      CARF = ICARF
      H = STY/CARF
    2 TS = TS + H
      TS10 = 10.*TS
      TSM = TS10 - 10.
      IF(TS.GT.PT2) GO TO 3
      PSD = 8.*TS*TS*TS/PTD
      GO TO 4
    3 IF(TS.GT.PT) GO TO 5
      PSD = 8.*(1.-TS/PT)*(1.-TS/PT)*(1.-TS/PT)
      GO TO 4
    5 PSD = 0.0
    4 PULSE = PSD
      Y2 = Y2 + (PULSE - Y2)*H/TC
      L = L + 1
      IF(L.LT.ICARF) GO TO 2
      L = 0
      I = I + 1
      Y(I) = Y2
      X(I) = PULSE
      TY(I) = TS
```

```
      IF(TS.LT.PT2) GO TO 2
      IF(TS.LT.CHOP) GO TO 2
      NY = 1
      NX = 1
      AN = NY
      RMS=SQRT(DD/AN)
      PRINT 8, RMS
    8 FORMAT(1X6HRMS = ,F15.7)
      RETURN
      END
C
C*************************************************************************
      FUNCTION PREC(XX)
C*************************************************************************
C
C     FUNCTION PREC TRUNCATES THE ARGUMENT OF PREC TO ND
C     SIGNIFICANT DIGITS
      DIMENSION IDIG(6)
      COMMON CHOP
      COMMON ND
      IF(XX.NE.0.) GO TO 4
      PREC=0.0
      GO TO 9
    4 Y=ABS(XX)
      J=ALOG10(Y)
      X=XX/(10.**J)
      DO7 I=1,ND
      IDIG(I)=X
    7 X=(X-FLOAT(IDIG(I)))*10.
      X=0.
      DO 8 I=1,ND
```

```
8     X=X+FLOAT(IDIG(I))*10.**(-I+1)
      PREC=X*10.**J
9     RETURN
      END
```

APPENDIX D

PROGRAM TO DETERMINE THE EFFECT OF USING DIFFERENT SAMPLING TIMES FOR THE INPUT PULSE AND THE OUTPUT PULSE. INTEGRATION TECHNIQUE IS THE ANALYTICAL TRAPEZOID WITH THE TRIGONOMETRIC SUBSTITUTION.

```
C*************************************************************************
C      PROGRAM TO DETERMINE THE EFFECT OF USING DIFFERENT SAMPLING
C      TIMES FOR THE INPUT PULSE AND THE OUTPUT PULSE.  INTEGRATION
C      TECHNIQUE IS THE ANALYTICAL TRAPEZOID WITH THE TRIGNOMETRIC
C      SUBSTITUTION
C*************************************************************************
C
C      INPUT:
C            STX = SAMPLING INTERVAL FOR INPUT PULSE
C            STY = SAMPLING INTERVAL FOR OUTPUT PULSE
C            PT = INPUT PULSE DURATION
C            TC = FIRST ORDER LAG SYSTEM TIME CONSTANT
C
C      G = AMPLITUDE RATIO
C      PHA = PHASE ANGLE
       COMMON STX,STY,X(500),Y(500),TX(500),TY(500),NX,NY
   10  READ 20, STX,STY,PT,TC
   20  FORMAT(4F10.4)
       TF=0.03
       CALL DATAX(PT,TC,TF)
       CALL DATAY(PT,TC,TF)
       CALL CALC(PT,TC)
       GO TO 10
   13  STOP
       END
C
C*************************************************************************
       SUBROUTINE CALC(PT,TC)
C*************************************************************************
C
       IMPLICIT REAL*8 (A-H,O-Z)
```

```
      REAL*4 W,FCO,FCI
      REAL*4 WP,ACO,ACI
      DIMENSION ACO(203), ACI(203), WP(203)
      DIMENSION FR(300), CER(300), W(203)
      DIMENSION FCI(203), FCO(203)
      DIMENSION BUF(5000)
      DIMENSION AB(2),ARD(3)
      COMMON STX,STY,X(500),Y(500),TX(500),TY(500),NX,NY
      DATA AB/9HFREQUENCY/,ARD/17HFREQUENCY CONTENT/
      TC = .1
      DO 2 I=1,150
      CER(1)=0.0
      UC=0.0
      UR = 0.0
      XC=0.0
      XR=0.0
      I1 = I-1
      WI = I
      W(I) = WI
C
C     INTEGRATION
      A1 = WI/2.
      A2X=A1*STX
      A2Y = A1*STY
      AX=2.*DSIN(A2X)
      AY=2.*DSIN(A2Y)
  100 DO 190 K2=2,NX
      K1=K2-1
      SX = (X(K2) - X(K1))/STX
      B = (A1*(TX(K2) + TX(K1)))
      DSTX=AX*DCOS(B)
```

```
      DCBX=-DSIN(B)*AX
      XR = XR + SX*DSIX
      UR = UR + SX*DCBX
  190 CONTINUE
      DO 191 K2=2,NY
      K1=K2-1
      SY=(Y(K2) - Y(K1))/STY
      B = (A1*(TY(K2) + TY(K1)))
      DSIY=AY*DCOS(B)
      DCBY=-DSIN(B)*AY
      XC = XC + SY*DSIY
      UC = UC + SY*DCBY
  191 CONTINUE
      WSQ = WI*WI
      UC = UC/WSQ
      XC = XC/WSQ
      XR = XR/WSQ
      UR = UR/WSQ
C
C     CALCULATE INPUT, FCI, AND OUTPUT,FCO, FREQUENCY CONTENT
      FCI(I) = DSQRT(UR*UR + XR*XR)
      FCO(I) = DSQRT(UC*UC + XC*XC)
C
      DS1 = UR*UR + XR*XR
      DS2 = UC*UR + XC*XR
      DS3= UC*XR - UR*XC
      G=DSQRT((UC*UC+XC*XC)/DS1)
      DR = DS2/DS1
      DI = DS3/DS1
      PHA=DATAN2(DI,DR)*57.29578
      D=1.+TC*TC*WI*WI
```

```
      AA = 1./D
      BA = -TC*(WT/D)
      GA=1./DSQRT(D)
      PA=DATAN2(BA,AA)*57.29578
      E1 = DR-AA
      E2 = DI-BA
      D1 = AA*AA + BA*BA
      ER(I)=DSQRT((E1*E1 + E2*E2)/D1)
      IF(I.EQ.1) GOTO2
      AW = W(I)
      BW = W(I1)
      DW = DLOG10(AW) - DLOG10(BW)
      DLW = DABS(DW)
      CER(I) = CER(I1) +    ((ER(I)+ER(I1))*(ER(I)+ER(I1))*DLW)/4.
  600 FORMAT(1XF10.4,F13.8,5XF10.8,5XF10.8,5XF10.5,5XF10.5)
    2 CONTINUE
C
C     SEARCH FOR FREQ AT ERROR CRITERION VALUE OF 0.01
      IF(CER(100).LT..01) GO TO 90
      DO 36 I5=1,100
      I4 = 100-I5
      IF(CER(I4).GT..01) GO TO 36
      I6=I4+1
      WR = (.01-CER(I4))/(CER(I6)-CER(I4))
      W01 = W(I4) + (W(I6) - W(I4))*WR
      GO TO 37
   36 CONTINUE
      GO TO 90
   37 PRINT 38, W01
   38 FORMAT(1X6HW01 = ,F10.4)
   90 CONTINUE
```

```
C
C       CALCULATE ANALYTICAL INPUT, ACI, AND OUTPUT, ACO, FREQ CONTENT
        STORE = .25*TP
        I=1
        AFCI = STORE
        AFCO = AFCI
        WP(1)=0.0
        ACI(1)=AFCI
        ACO(1)=AFCO
        DO 5 K=1,151
        F=K-1
        WT=F*TP
        WT2=WT/2.
        W2T=WT*F
        W4T3=W2T*WT*WT
        A=12./W2T - 96./W4T3
        B=48./W4T3
        UC = A*DCOS(WT2) + B*(1. + DCOS(WT))
        XC = - A*DSIN(WT2) - B*DSIN(WT)
        AFCI = DSQRT(UC*UC + XC*XC)
        AFCO =AFCI/DSQRT(1. + .01*F*F)
        J=K
        ACO(J)=AFCO
        ACI(J)=AFCI
        WP(J)=F
    5   CONTINUE
        DO 39 J=1,150
        J1=152-J
        K=J1-1
        FCI(J1)=FCI(K)
   39   W(J1)=W(K)
```

```
      W(1)=0.0
C
C     PLOT COMPARISON OF FCI-ACI AND FC0-AC0
      CALL PLOTS(BUF,5000)
      CALL PLOT(0.,0.,-3)
      CALL SCALE(FCI,5.,151,1)
      CALL SCALE(FC0,5.,151,1)
      ACI(152)=FCI(152)
      ACI(153)=FCI(153)
      AC0(152)=FC0(152)
      AC0(153)=FC0(153)
      W(152)=0.0
      W(153)=30.
      CALL AXIS(0.,0.,AB,-9,5.,0.,W(152),W(153))
      CALL AXIS(0.,0.,BRD,+17,5.,90.,FCI(152),FCI(153))
      CALL LINE(W,FCI,151,1,0,0)
      CALL LINE(W,ACI,151,1,0,0)
      CALL PLOT(0.,10.,-3)
      CALL AXIS(0.,0.,BRD,+17,5.,90.,FC0(152),FC0(153))
      CALL AXIS(0.,0.,AB,-9,5.,0.,W(152),W(153))
      CALL LINE(W,FC0,151,1,0,0)
      CALL LINE(W,AC0,151,1,0,0)
      CALL PLOT(0.,0.,-3)
      CALL PLOT(0.,0.,999)
      RETURN
      END
C
C*****************************************************************************
      SUBROUTINE DATAX(PT,TC,TF)
C*****************************************************************************
C
```

```
C       GENERATE X ARRAY
        IMPLICIT REAL*8 (A-H,O-Z)
        COMMON STX,STY,X(500),Y(500),TX(500),TY(500),NX,NY
        I=0
        PULSE = 0.0
        Y2=0.0
        PTD = PT*PT*PT
        PT2 = PT/2.
        TS = 0.0
        L = 2000
        ICORF = (STX/.0005)*(2./PT) + .5
        CORF = ICORF
        H = STX/CORF
    2   TS = TS + H
C
C       LAGGED RAMP INPUT
        TS10 = 10.*TS
        TSM = TS10 - 10.
        IF(TS.GT.PT2) GO TO 3
        PSD = 100.*TS + 10./DEXP(TS10) - 10.
        GO TO 4
    3   PSD = (90. + 10./DEXP(10.D0))/DEXP(TSM)
        GO TO 4
    5   PSD = 0.0
    4   PULSE = PSD
        Y2 = Y2 + (PULSE - Y2)*H/TC
        L = L + 1
        IF(L.LT.ICORF) GO TO 2
        L = 0
        I = I + 1
        X(I) = PULSE
```

```
      TX(I) = TS
      IF(TS.LT.PT2) GO TO 2
      IF(X(I).GT.0.001) GO TO 2
      NX = I
    7 FORMAT(1X2F15.7)
      XPON=STX/TF
      A1=1./DEXP(XPON)
      A2=1.-A1
      DUM = 0.0
      RETURN
      END
C
C*******************************************************************************
      SUBROUTINE DATAY(PT,TC,TF)
C*******************************************************************************
C
C     GENERATE Y ARRAY
      IMPLICIT REAL*8 (A-H,O-Z)
      COMMON STX,STY,X(500),Y(500),TX(500),TY(500),NX,NY
      DD = 0.0
      IX=3791359
      I=0
      PULSE = 0.0
      Y2=0.0
      PTD = PT*PT*PT
      PT2 = PT/2.
      TS = 0.0
      L = 2000
      ICORF = (STY/.0005)*(2./PT) + .5
      CORF = ICORF
      H = STY/CORF
```

```
  2    TS = TS + H
C
C      LAGGED RAMP INPUT
       TS10 = 10.*TS
       TSM = TS10 - 10.
       IF(TS.GT.PT2) GO TO 3
       PSD = 100.*TS + 10./DEXP(TS10) - 10.
       GO TO 4
  3    PSD = (90. + 10./DEXP(10.D0))/DEXP(TSM)
       GO TO 4
  5    PSD = 0.0
  4    PULSE = PSD
       Y2 = Y2 + (PULSE - Y2)*H/TC
       I = I + 1
       IF(I.LT.ICARE) GO TO 2
       I = 0
       I = I + 1
       Y(I) = Y2
       TY(I) = TS
       IF(TS.LT.PT2) GO TO 2
       IF(Y(I).GT.0.001) GO TO 2
       NY = I
       AN = NY
       RMS = DSQRT(DD/AN)
       PRINT 8, RMS
  8    FORMAT(1X6HRMS = ,F15.7)
  7    FORMAT(1X2F15.7)
       XPON=STY/TF
       A1=1./DEXP(XPON)
       A2=1.-A1
       DUM = 0.0
```

```
      RETURN
      END
C
C*************************************************************************
      SUBROUTINE RN(IX,IY,YFL)
C*************************************************************************
C
C     CALCULATES RANDOM NUMBER
      IMPLICIT REAL*8 (A-H,O-Z)
      IY=IX*65539
      IF(IY)5,6,6
    5 IY=IY+2147483647+1
    6 YFL=IY
      YFL=YFL*.4656613E-9
      IX=IY
      RETURN
      END
```

APPENDIX E

PROGRAM TO CALCULATE AND PLOT COMPARISONS OF THE ANALYTICAL FREQUENCY CONTENT AND NORMALIZED FREQUENCY CONTENT OF TWO CUBED TRIANGULAR PULSES

```
C*************************************************************************
C      PROGRAM TO CALCULATE AND PLOT COMPARISONS OF THE
C      ANALYTICAL FREQUENCY CONTENT AND NORMALIZED FREQUENCY
C      CONTENT OF TWO CUBED TRIANGULAR PULSES
C*************************************************************************
C
C      TP = PULSE DURATION
C      WP = FREQUENCY
C      KT = DETERMINES WHICH PULSE IS BEING CALCULATED
C      ACI = FREQUENCY CONTENT OF FIRST PULSE
C      ACO = NORMALIZED FREQUENCY CONTENT OF FIRST PULSE
C      FCI = FREQUENCY CONTENT OF SECOND PULSE
C      FCO = NORMALIZED FREQUENCY CONTENT OF SECOND PULSE
C
       IMPLICIT REAL*8 (A-H,O-Z)
       REAL*4 WP,ACI,ACO,FCI,FCO
       DIMENSION FCI(203),FCO(203),ACI(203),ACO(203),WP(203),BUF(5000)
       KT=1
       DO 44 JF=1,2
       KT=KT+1
C
C      INPUT
       READ 3,TP
   3   FORMAT(F10.2)
C
       STORE = .25*TP
       I =1
       AFCI = STORE
       AFCO=AFCI/STORE
       WP(1)=0.0
       IF(KT.EQ.3) GO TO 99
```

```
      ACI(1)=AFCI
      ACO(1)=AFCO
      GO TO 98
   99 FCI(1)=AFCI
      FCO(1)=AFCO
   98 CONTINUE
      DO5 K=1,200
      J = K + 1
      F=K
      WT=F*TP
      WT2=WT/2.
      W2T=WT*F
      W4T3=W2T*WT*WT
      A=12./W2T - 96./W4T3
      B=48./W4T3
      UC = A*DCOS(WT2) + B*(1. + DCOS(WT))
      XC = - A*DSIN(WT2) - B*DSIN(WT)
      AFCI = DSQRT(UC*UC + XC*XC)
      AFCO=AFCI/STORE
      IF(KT.EQ.3) GO TO 33
      ACO(J)=AFCO
      ACI(J)=AFCI
      GO TO 8
   33 FCI(J)=AFCI
      FCO(J)=AFCO
    8 CONTINUE
      WP(J)=F
    5 CONTINUE
   44 CONTINUE
      CALL PLOTS(BUF,5000)
      CALL PLOT(0.,0.,-3)
```

```
C
C       SCALE FACTORS
        WP(202)=0.0
        WP(203)=40.0
        ACI(202)=0.0
        ACI(203)=0.025
        FCI(202)=ACI(202)
        FCI(203)=ACI(203)
        ACB(202)=0.0
        ACB(203)=0.2
        FCB(202)=ACB(202)
        FCB(203)=ACB(203)
C
        CALL AXIS(0.,0.,9HFREQUENCY,-9,5.,0.,WP(202),WP(203))
        CALL AXIS(0.,0.,17HFREQUENCY CONTENT,+17,5.,90.,ACI(202),ACI(203))
        CALL LINE(WP,ACI,201,1,0,0)
        CALL LINE(WP,FCI,201,1,0,0)
        CALL PLOT(20.,0.,-3)
        CALL AXIS(0.,0.,1H ,-1,5.,0.,WP(202),WP(203))
        CALL AXIS(0.,0.,1H ,+1,5.,90.,ACB(202),ACB(203))
        CALL LINE(WP,ACB,201,1,0,0)
        CALL LINE(WP,FCB,201,1,0,0)
        CALL PLOT(0.,0.,-3)
        CALL PLOT(0.,0.,999)
        STOP
        END
```

VITA

The author was born in Magee, Mississippi on February 15, 1943. His first two years of public school were spent at Vivian Elementary School in Vivian, Louisiana, followed by 2 1/2 years at Pearl Elementary School near Jackson, Mississippi. Further education was obtained in the public schools of Magee, Mississippi where he graduated from Magee High School in 1961. In June 1965 he graduated cum laude with the degree of Bachelor of Science in Chemical Engineering from the University of Mississippi. The Master of Science degree in Chemical Engineering was received in January 1967 from Louisiana State University.

On August 20, 1966 he was married to the former Janice Page of Baytown, Texas, and on February 27, 1969 he became the father of a daughter, Christy Lynn.

At the present time he is a candidate for the degree of Doctor of Philosophy in Chemical Engineering. After completing the requirements for this degree he will assume the position of Assistant Professor of Chemical Engineering at the Virginia Polytechnic Institute.

EXAMINATION AND THESIS REPORT

Candidate: Carlos Ray Dollar

Major Field: Chemical Engineering

Title of Thesis: Fourier Transforms for System Identification

Approved:

Paul W. Murrill
Major Professor and Chairman

Max Goodrich
Dean of the Graduate School

EXAMINING COMMITTEE:

Ralph W. Pike

Johnny R. Johnson

Frank R. Groves Jr.

Cecil L. Smith

Date of Examination:

July 2, 1969